Further investigation into the "Thorium anomaly" from isotopic fission fragment yields of ^{232}Th produced in inverse-kinematics

Zakopane 2026

e849 experiment collaboration

Alex Cobo Zarzuelo
04/09/2026

The fission process

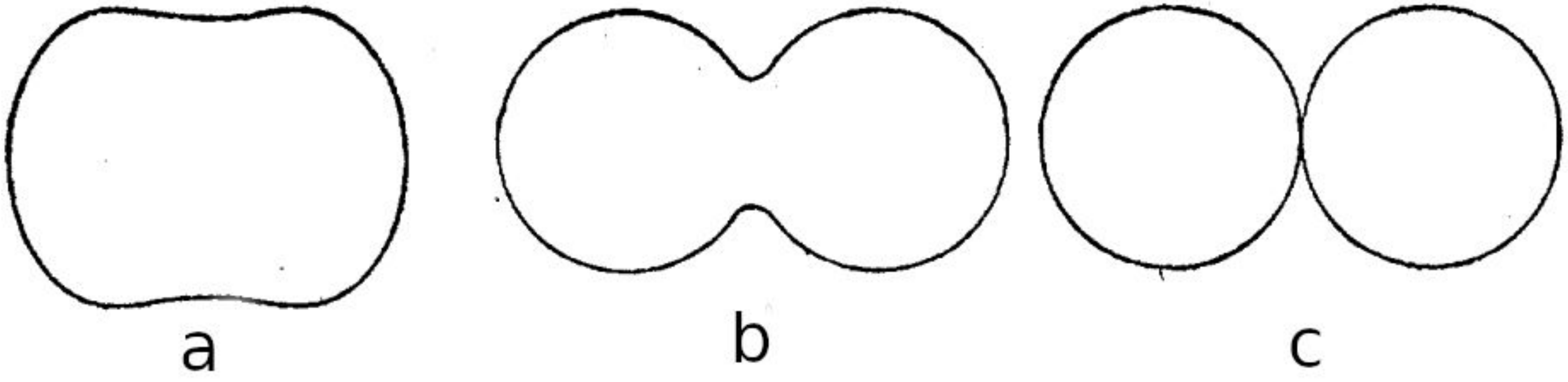

Unestable competition between surface tension (Nuclear force) and repulsion (Coulomb) leads to **deformation** and **split** of a heavy nucleus into **2 fragments**

Bohr, N., & Wheeler, J. A. (1939). The mechanism of nuclear fission. Physical Review, 56(5), 426.

The fission process

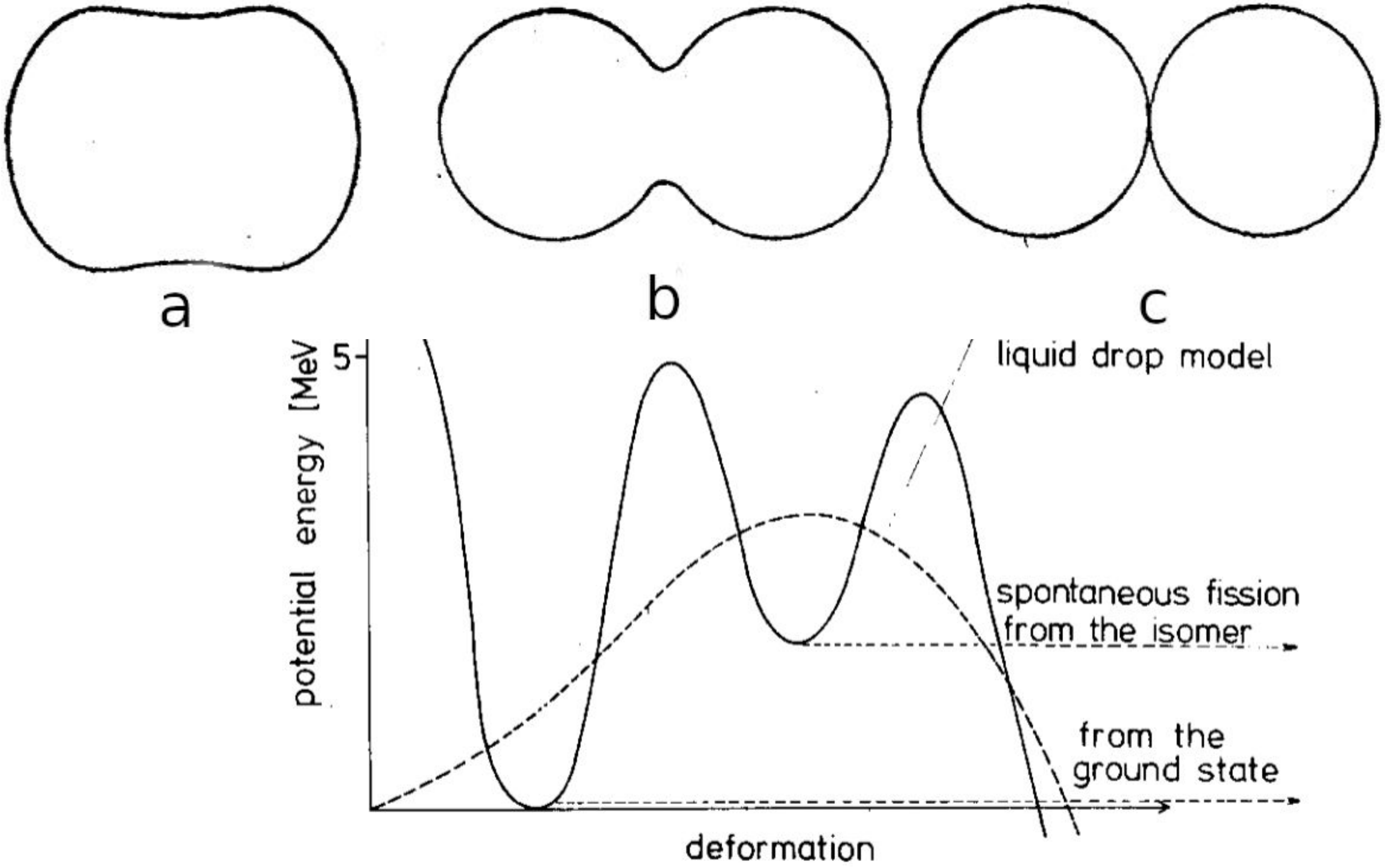

Metag, V., Habs, D., & Specht, H. J. (1980). Spectroscopic properties of fission isomers. Physics Reports, 65(1), 1-41.

Unestable competition between surface tension (Nuclear force) and repulsion (Coulomb) leads to deformation and split of a heavy nucleus into 2 fragments

The **potential energy surface (PES)** represents the **energy of the system** at a given **deformation**

The fission process

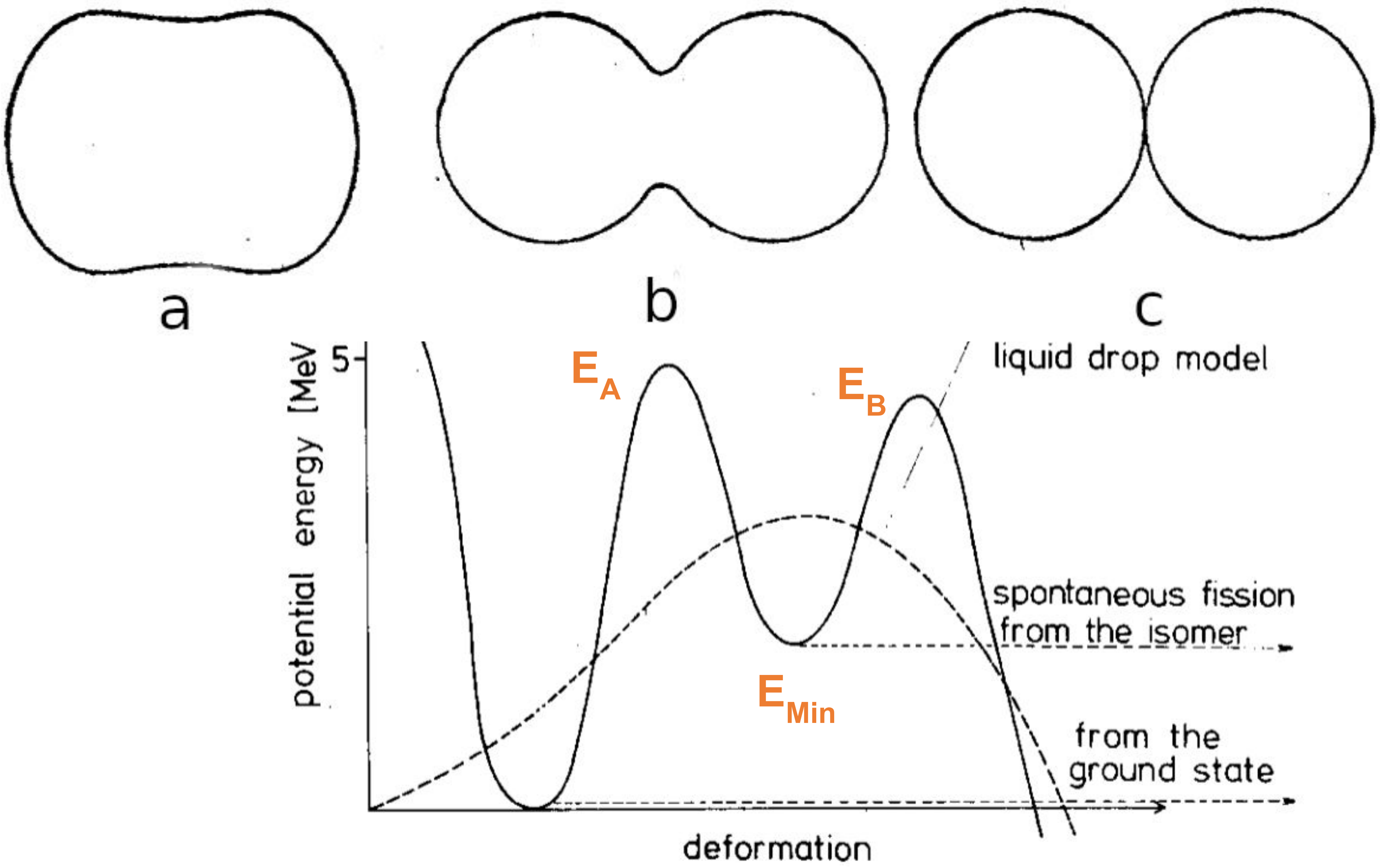

Unestable competition between surface tension (Nuclear force) and repulsion (Coulomb) leads to deformation and split of a heavy nucleus into 2 fragments

The potential energy surface (PES) represents the energy of the system at a given deformation

Including **nuclear structure** permits to pass from **single hump (dotted)** to **double humped PES (solid)**

Metag, V., Habs, D., & Specht, H. J. (1980). Spectroscopic properties of fission isomers. Physics Reports, 65(1), 1-41.

The fission process

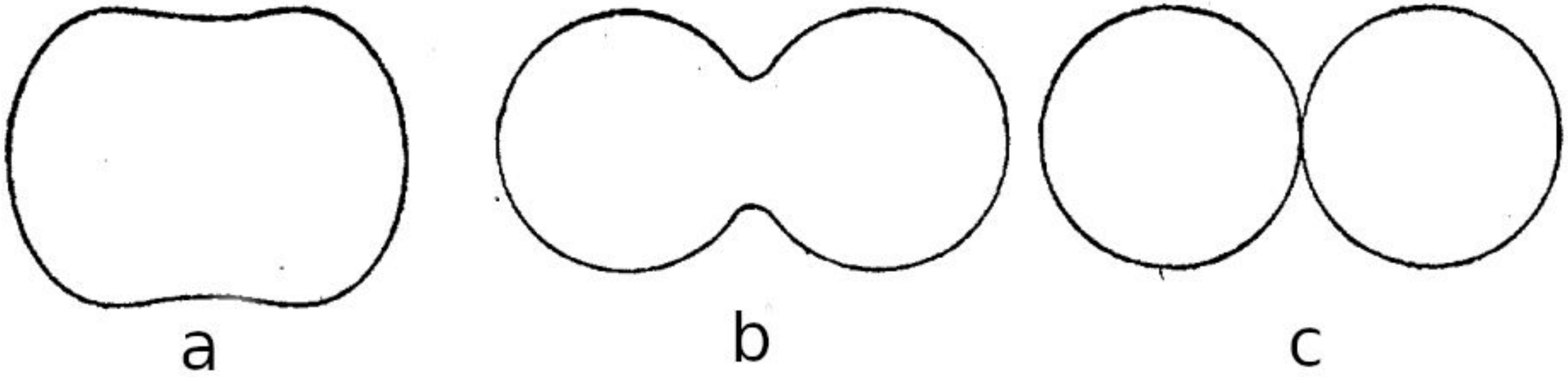

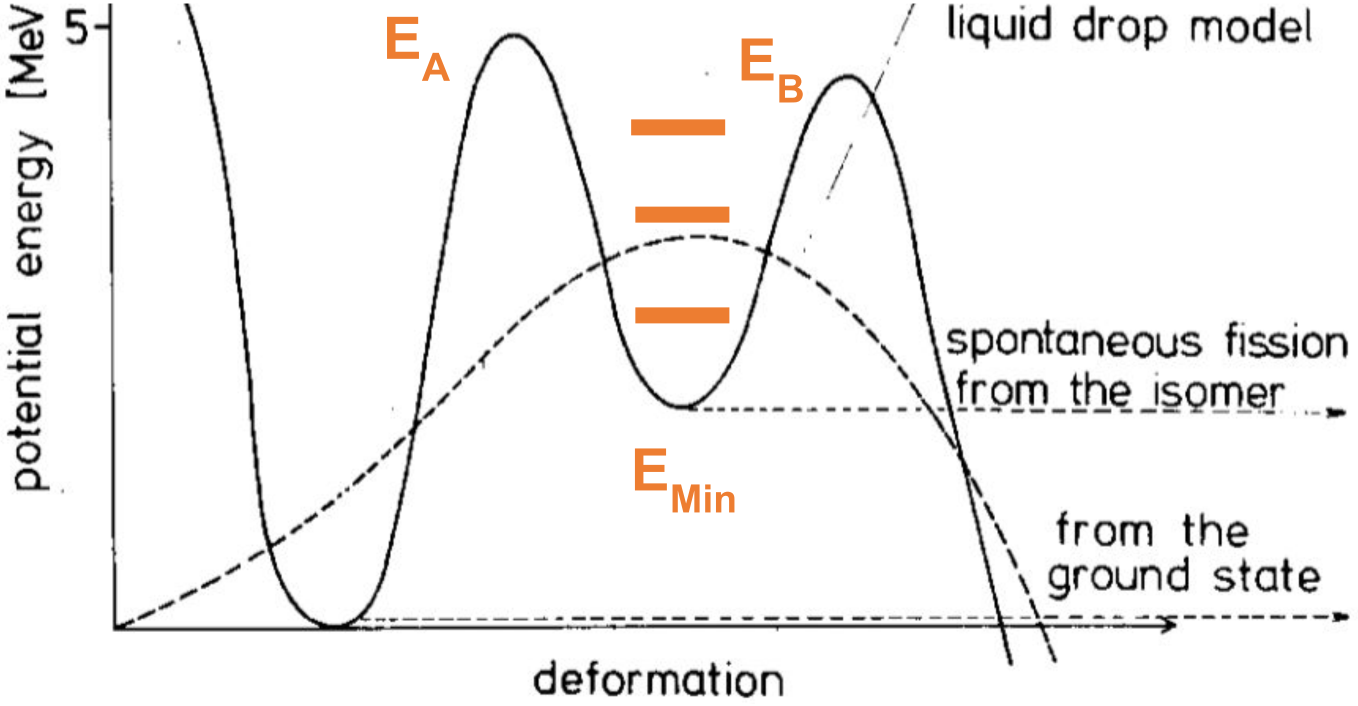

Metag, V., Habs, D., & Specht, H. J. (1980). Spectroscopic properties of fission isomers. Physics Reports, 65(1), 1-41.

Unestable competition between surface tension (Nuclear force) and repulsion (Coulomb) leads to deformation and split of a heavy nucleus into 2 fragments

The potential energy surface (PES) represents the energy of the system at a given deformation

Including nuclear structure permits to pass from single hump (dotted) to double humped PES (solid)

↓

- Explain **asymmetric fission in actinides**
- Presence of new **discrete energy levels**

Fission observables

The **PES** can**not** be directly **measured** => **observables related** to it

Fission observables: fission probability

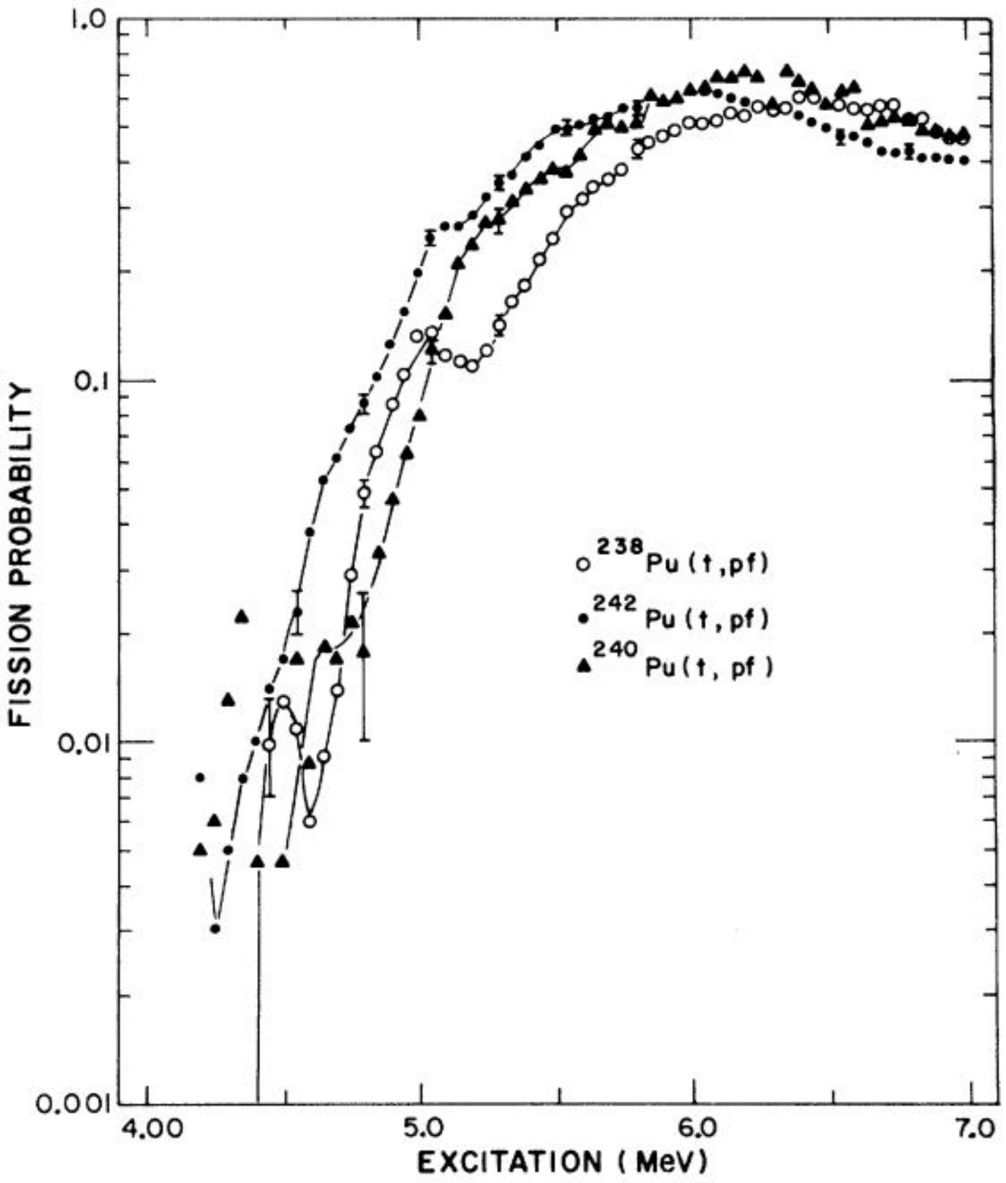

The PES cannot be directly measured => observables related to it

After forming a **fissioning system**, the nucleus can **decay through various channels**: n-, γ- emission, **fission**, …

- **No fission** probability **below** the fission **barrier**
- The **peaks** represent **resonances in** the **PES pocket**

Cramer, J. D., & Britt, H. C. (1970). Fission studies of thorium, uranium, and plutonium isotopes with (t, pf) reactions. Physical Review C, 2(6), 2350.

Fission observables: fission probability

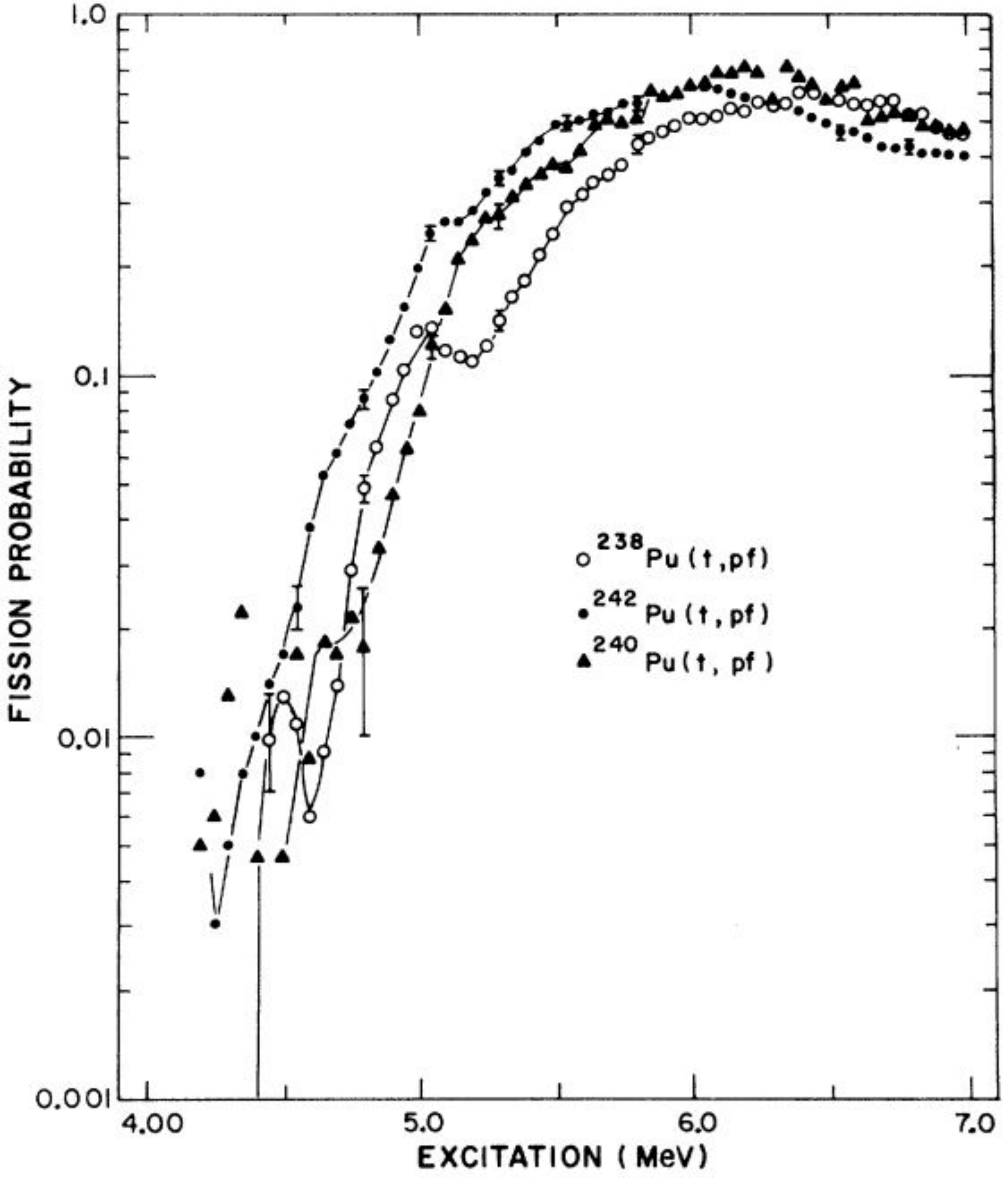

The PES cannot be directly measured => observables related to it

After forming a fissioning system, the nucleus can decay through various channels: n-, γ- emission, fission, …

- No fission probability below the fission barrier
- The peaks represent resonances in the PES pocket

The **PES** shapes and **barrier penetrability** calculations are used to **extract barrier heights**:

Nucleus	Ref	E_A MeV	$\hbar\omega_A$ MeV	E_{IS} MeV	E_{Min} MeV	$\hbar\omega_{Min}$ MeV	E_B MeV	$\hbar\omega_B$ MeV	E_B-E_A MeV
Theory:									
^{240}Pu	a	6.3	-	2.5	-	-	5.3	-	-1.0
	e	5.8	-	2.7	-	-	5.6	-	-0.20
	c	5.2	-	2.3	1.8	-	5.5	-	0.30
Experiment:									
^{240}Pu	f	6.05	1.00	2.95	2.35	1.20	5.55	0.70	-0.50

Cramer, J. D., & Britt, H. C. (1970). Fission studies of thorium, uranium, and plutonium isotopes with (t, pf) reactions. Physical Review C, 2(6), 2350.

Fission observables: fission probability

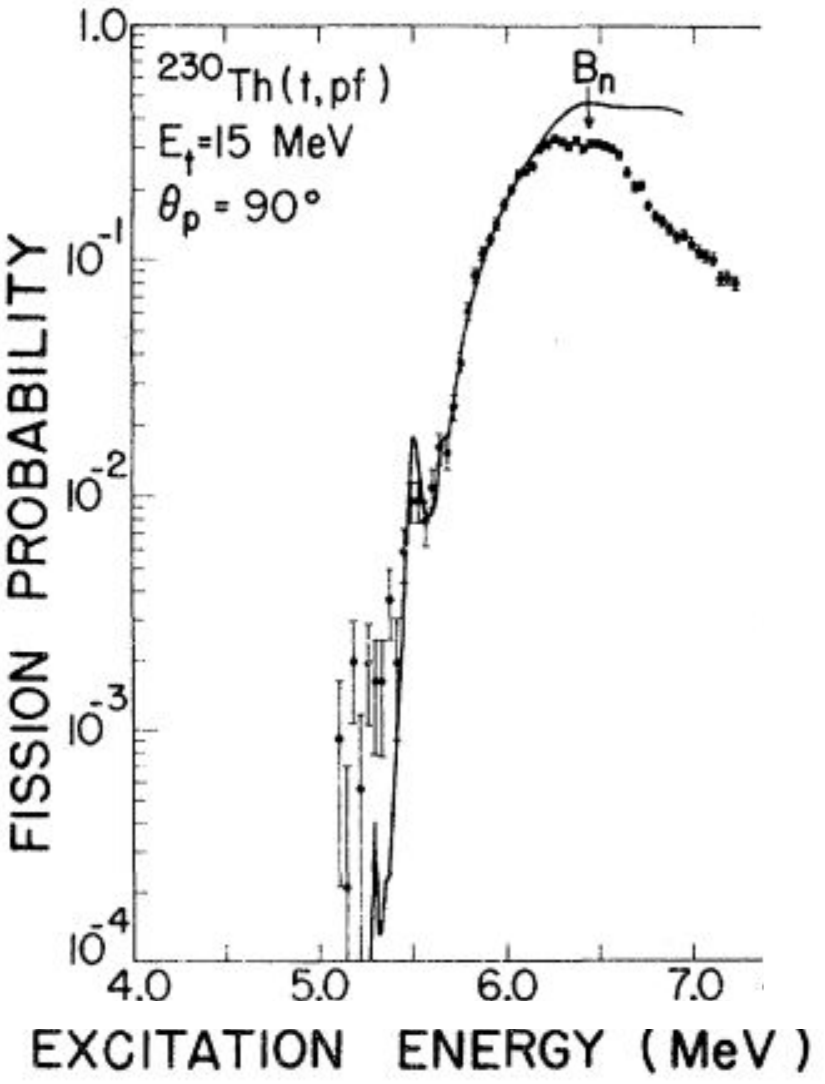

Nucleus	Ref	E_A MeV	$\hbar\omega_A$ MeV	E_{IS} MeV	E_{Min} MeV	$\hbar\omega_{Min}$ MeV	E_B MeV	$\hbar\omega_B$ MeV	$E_B - E_A$ MeV
Theory:									
^{232}Th	a	4.8	-	2.8	-	-	7.3	-	2.5
	b	4.3	-	1.9	1.4	-	8.6	-	4.3
	c	3.4	-	2.3	1.8	-	6.6	-	3.2
Experiment:									
^{232}Th	Present	5.50	0.90	4.43	4.25	0.36	6.18	0.47	0.68

The **theoretical models** can**not reproduce** the **observations** for the **Thorium isotopes**

THORIUM ANOMALY (1)

Back, B. B., Britt, H. C., Garrett, J. D., & Hansen, O. (1972). Subbarrier fission resonances in Th isotopes. Physical Review Letters, 28(26), 1707.

Fission observables: yields

The **probability of producing a fission fragment** with a given A, Z, N, etc. :

$$Y(Z,A) = 200 \cdot \frac{N(Z,A)}{\sum_{Z,A} N(Z,A)}$$

Fission observables: yields

The probability of producing a fission fragment with a given A, Z, N, etc. :

$$Y(Z,A) = 200 \cdot \frac{N(Z,A)}{\sum_{Z,A} N(Z,A)}$$

Two groups of **asymmetric fission** driven by **octupolar deformation**

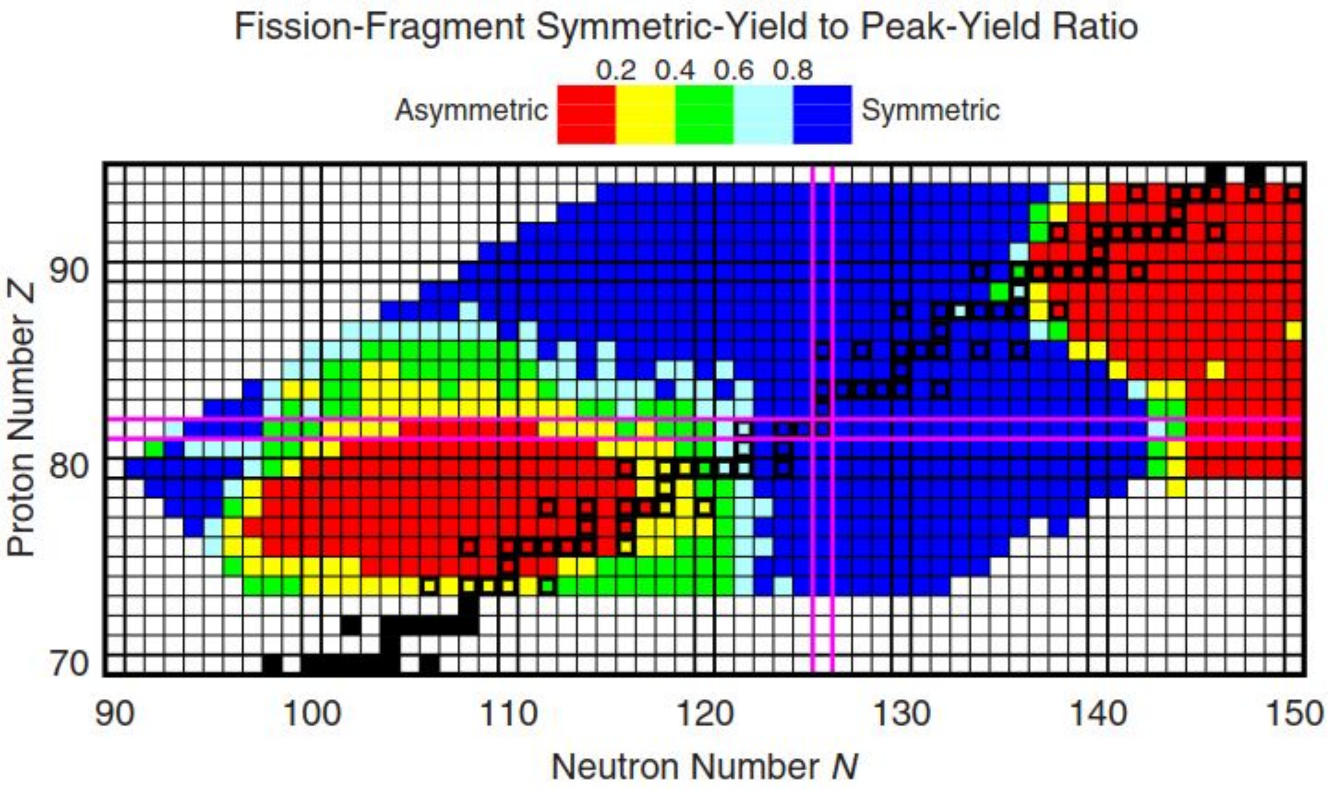

Möller, P., & Randrup, J. (2015). Calculated fission-fragment yield systematics in the region 74≤ Z≤ 94 and 90≤ N≤ 150. Physical Review C, 91(4), 044316.

Fission observables: yields

The probability of producing a fission fragment with a given A, Z, N, etc. :

$$Y(Z, A) = 200 \cdot \frac{N(Z, A)}{\sum_{Z,A} N(Z, A)}$$

Two groups of **asymmetric fission**:

1) n-deficient sub-Pb -> **governed by Z_L~36**

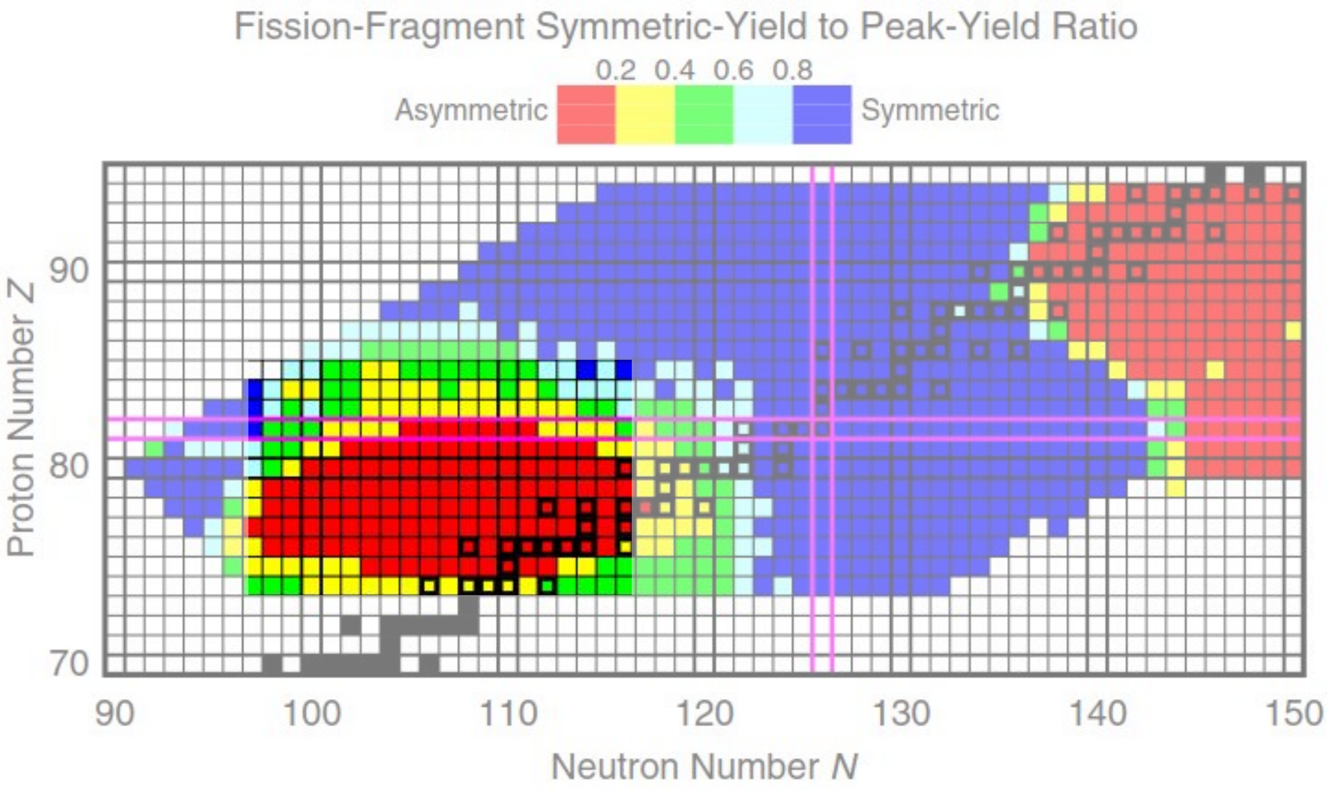

Möller, P., & Randrup, J. (2015). Calculated fission-fragment yield systematics in the region 74≤ Z≤ 94 and 90≤ N≤ 150. Physical Review C, 91(4), 044316.

Fission observables: yields

The probability of producing a fission fragment with a given A, Z, N, etc. :

$$Y(Z,A) = 200 \cdot \frac{N(Z,A)}{\sum_{Z,A} N(Z,A)}$$

Two groups of **asymmetric fission**:
2) Around ^{238}U -> **driven by Z_H~54**

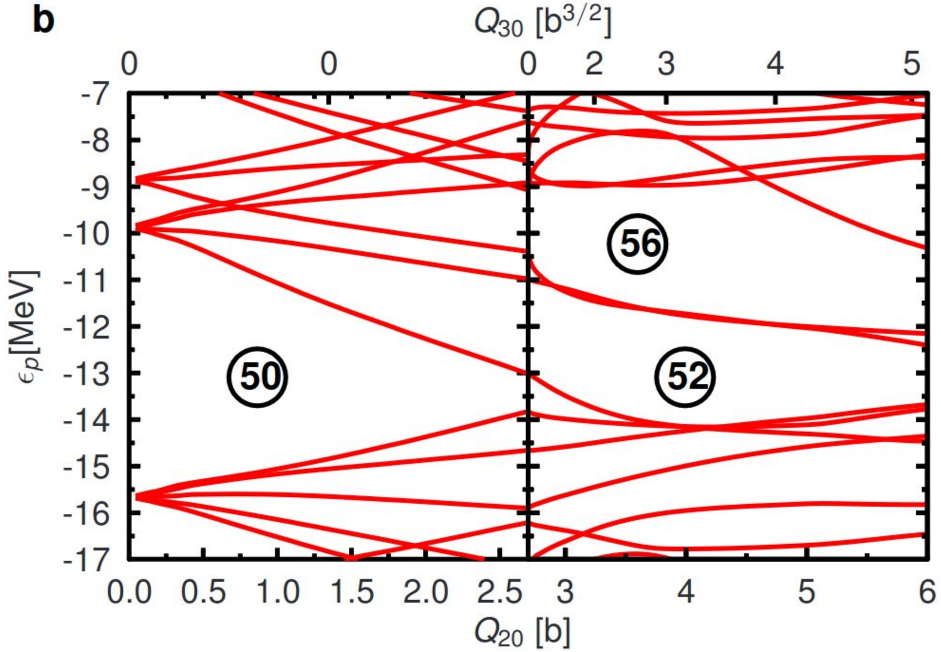

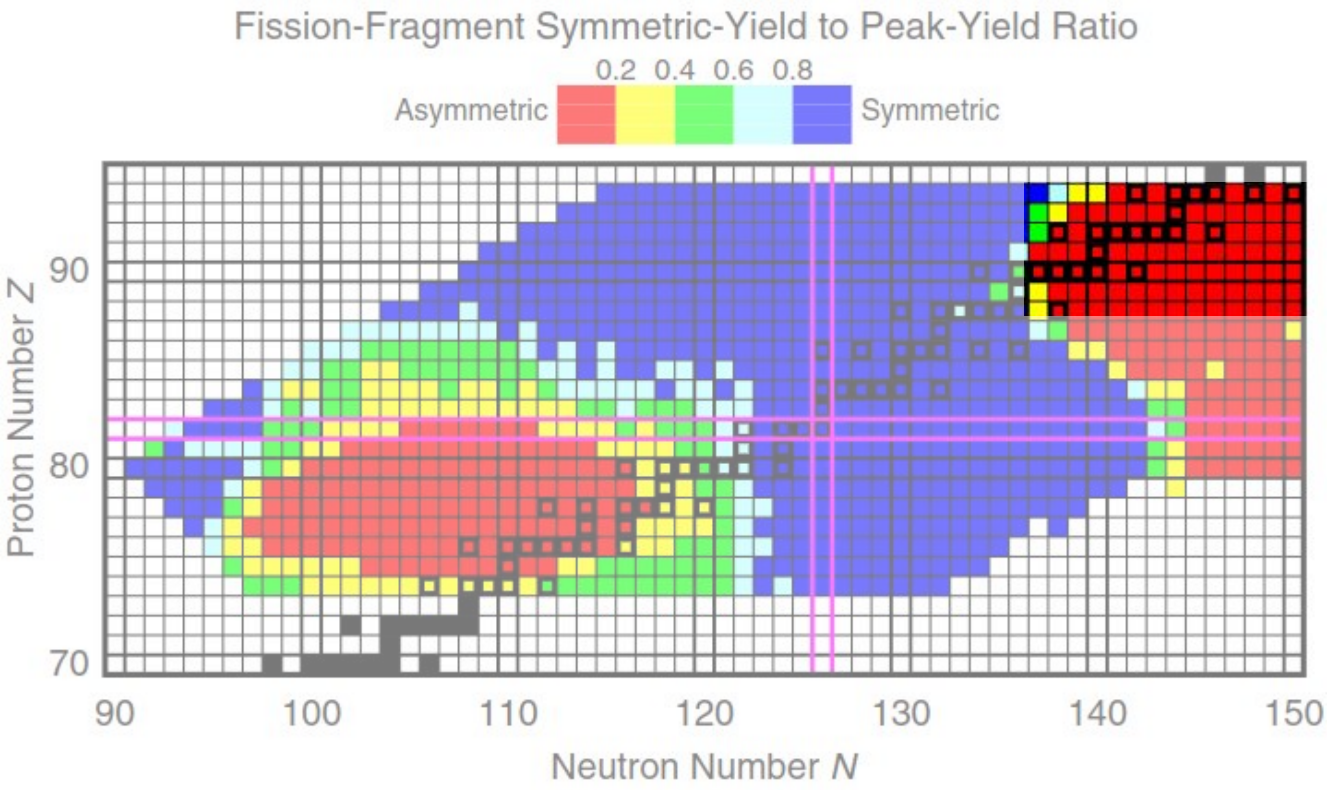

Scamps, G., & Simenel, C. (2018). Impact of pear-shaped fission fragments on mass-asymmetric fission in actinides. Nature, 564(7736), 382-385.

Möller, P., & Randrup, J. (2015). Calculated fission-fragment yield systematics in the region 74≤ Z≤ 94 and 90≤ N≤ 150. Physical Review C, 91(4), 044316.

Fission observables: yields

The probability of producing a fission fragment with a given A, Z, N, etc. :

$$Y(Z,A) = 200 \cdot \frac{N(Z,A)}{\sum_{Z,A} N(Z,A)}$$

Two groups of **asymmetric fission**:
2) Around ^{238}U -> **driven by Z_H~54**

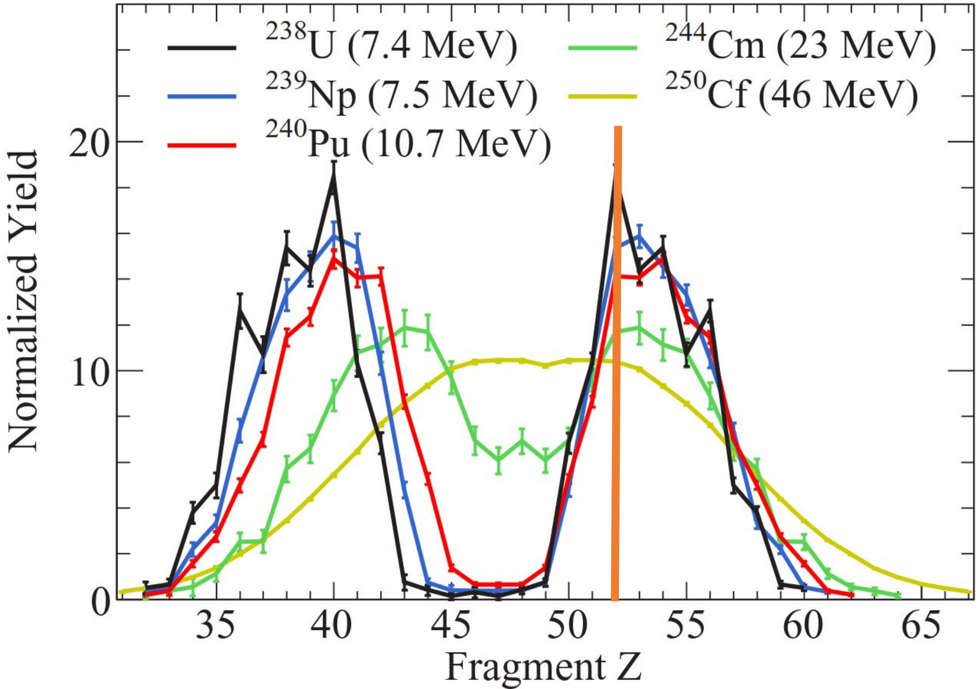

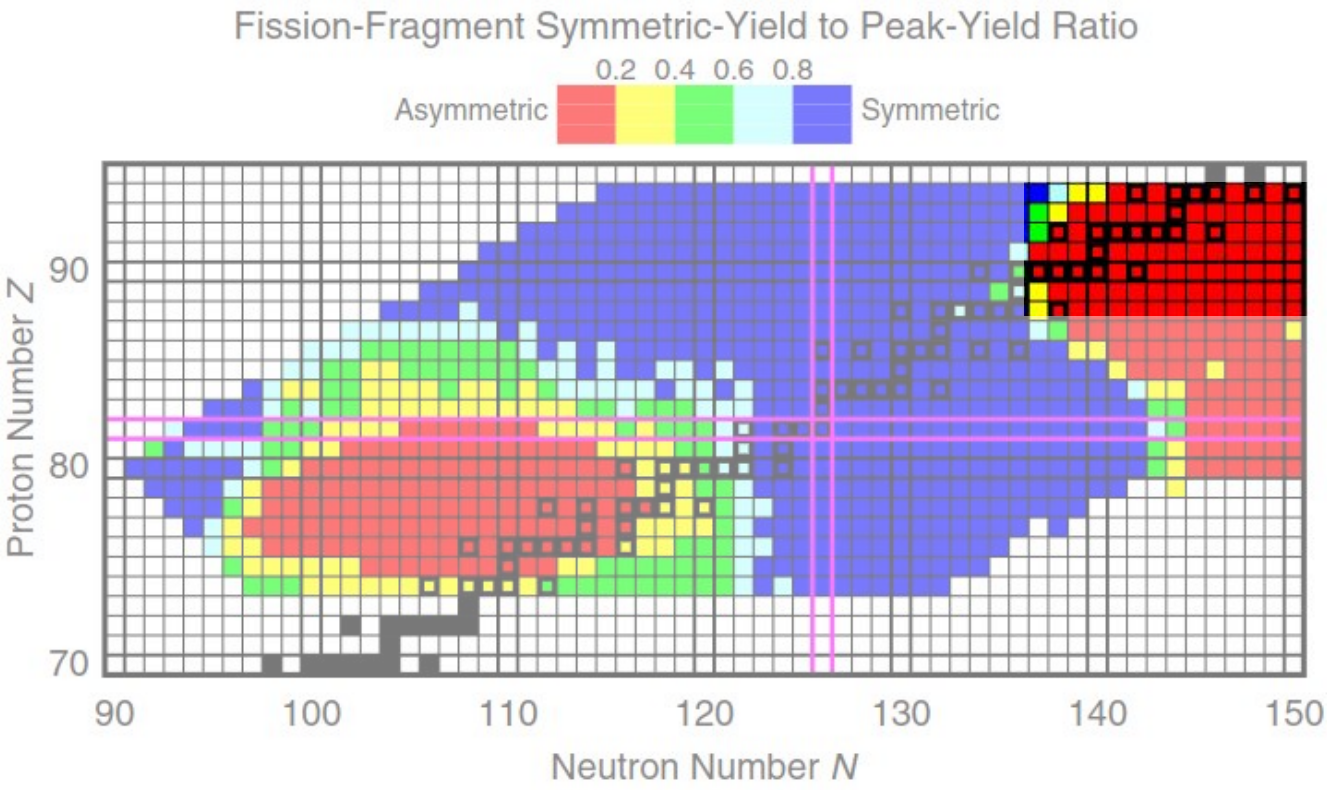

Ramos, D., Caamaño, M., Farget, F., Rodríguez-Tajes, C., Audouin, L., Benlliure, J., ... & Schmitt, C. (2018). Isotopic fission-fragment distributions of U 238, Np 239, Pu 240, Cm 244, and Cf 250 produced through inelastic scattering, transfer, and fusion reactions in inverse kinematics. Physical review C, 97(5), 054612.

Möller, P., & Randrup, J. (2015). Calculated fission-fragment yield systematics in the region 74≤ Z≤ 94 and 90≤ N≤ 150. Physical Review C, 91(4), 044316.

Fission observables: yields

The probability of producing a fission fragment with a given A, Z, N, etc. :

$$Y(Z, A) = 200 \cdot \frac{N(Z, A)}{\sum_{Z,A} N(Z, A)}$$

^{232}Th mass yields exhibit **more asymmetric** fission than ^{236}U **at low excitation energy** (6.64 MeV)

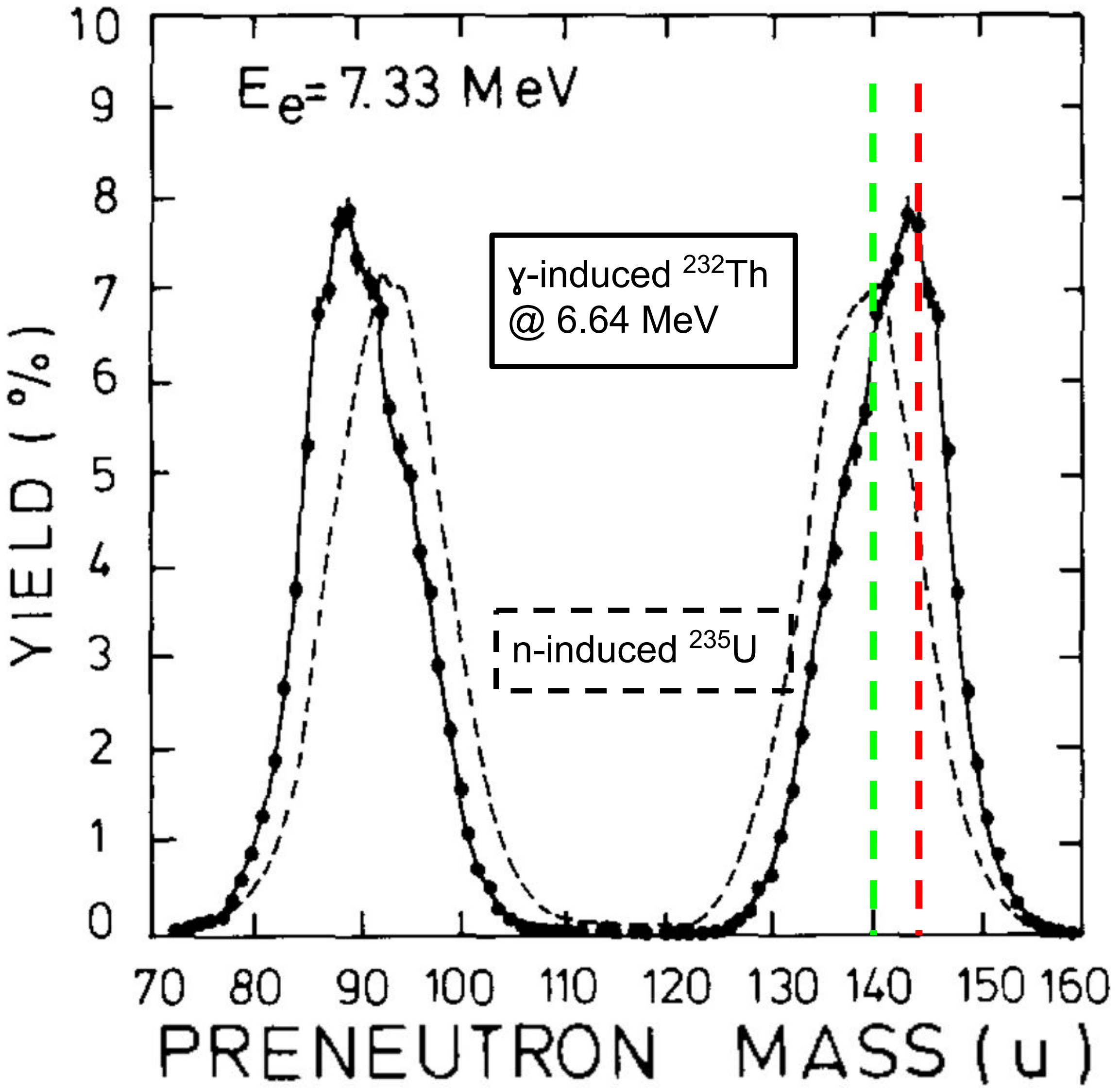

Piessens, M., Jacobs, E., Pommé, S., & De Frenne, D. (1993). Mass and kinetic energy distributions for the photofission of 232Th with 6.44 to 13.15 MeV bremsstrahlung. Nuclear Physics A, 556(1), 88-106.

Fission observables: yields

GANIL

The **probability of producing a fission fragment** with a given A, Z, N, etc. :

$$Y(Z,A) = 200 \cdot \frac{N(Z,A)}{\sum_{Z,A} N(Z,A)}$$

^{232}Th mass yields exhibit more asymmetric fission than ^{236}U at low excitation energy (6.64 MeV)

The **yields get closer to** the "**common** behaviour" when the **excitation energy is increased**

THORIUM ANOMALY (2)

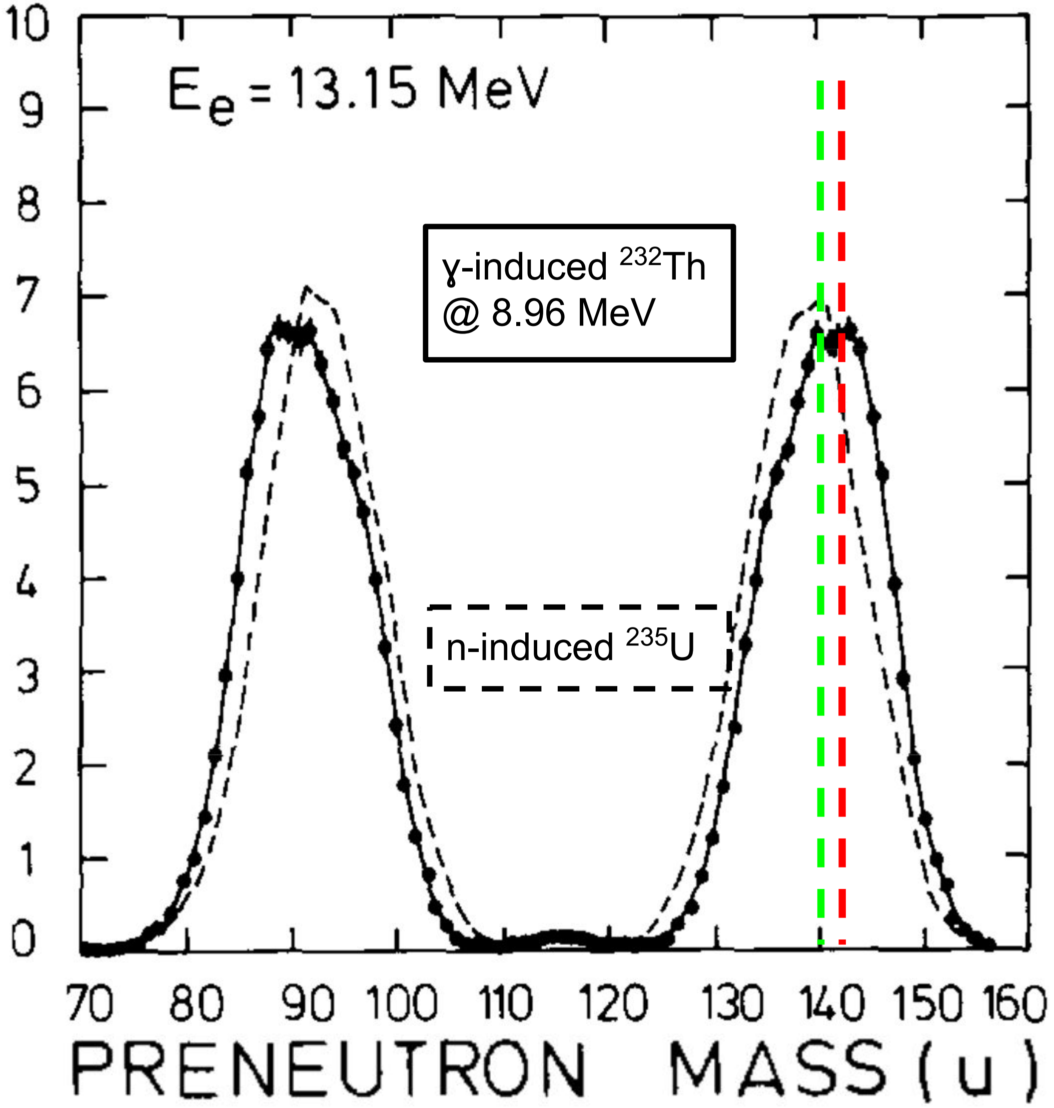

Piessens, M., Jacobs, E., Pommé, S., & De Frenne, D. (1993). Mass and kinetic energy distributions for the photofission of 232Th with 6.44 to 13.15 MeV bremsstrahlung. Nuclear Physics A, 556(1), 88-106.

Anomaly explanation: third barrier

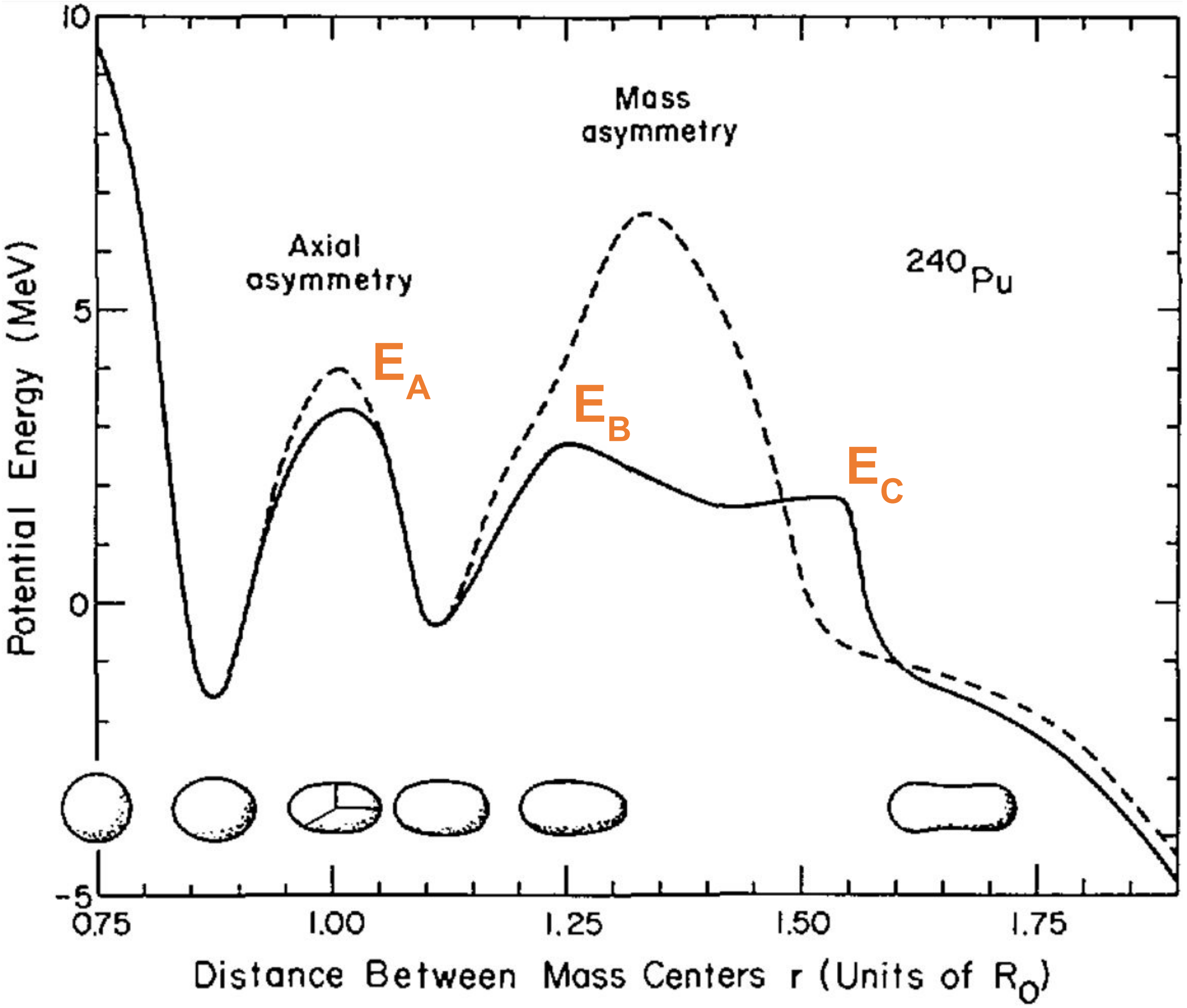

A **third fission barrier** was proposed to **explain** these **anomalous** observations

Möller, P., & Nix, J. R. (1974). Calculation of fission barriers. In Physics and chemistry of fission, 1973.

Anomaly explanation: third barrier

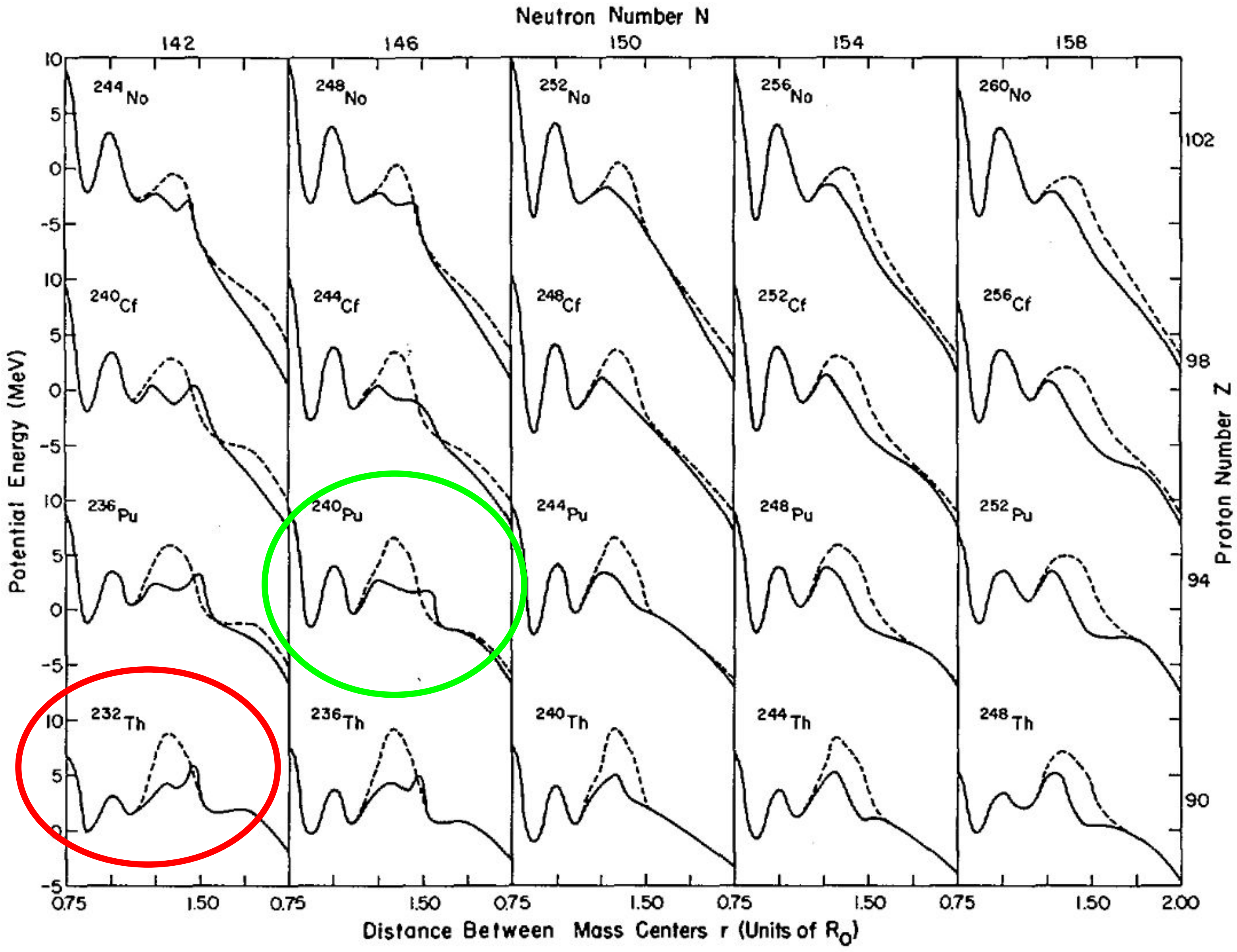

A third fission barrier was proposed to explain these anomalous observations

The **ratio** between the **height of the second and third barrier depends** on **(N,Z)** of the fissioning systems

Möller, P., & Nix, J. R. (1974). Calculation of fission barriers. In Physics and chemistry of fission, 1973.

Anomaly explanation: third barrier

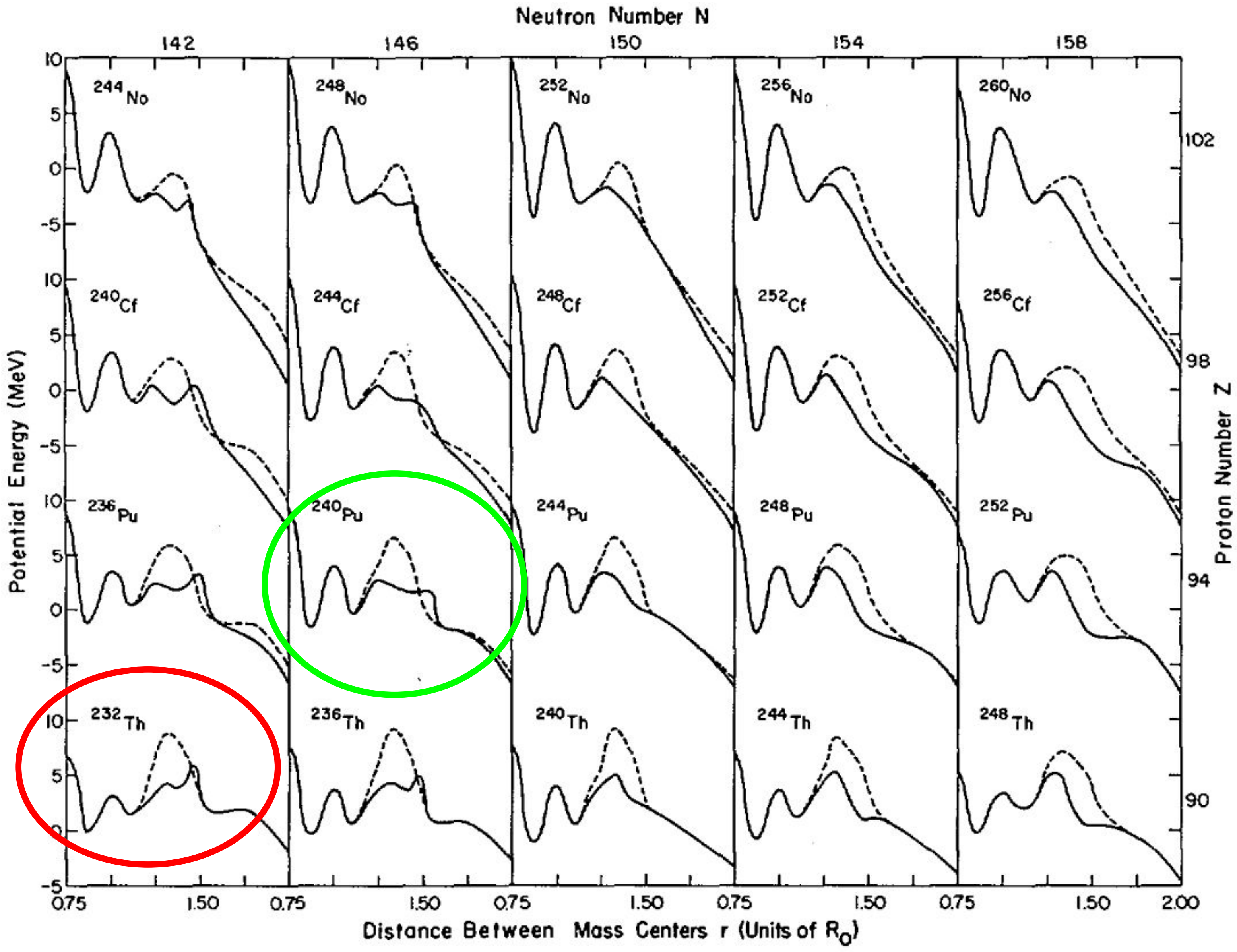

A third fission barrier was proposed to explain these anomalous observations

The ratio between the height of the second and third barrier depends on (N,Z) of the fissioning systems

↓

Only for **N ≤ 146** (in these calculations)

Möller, P., & Nix, J. R. (1974). Calculation of fission barriers. In Physics and chemistry of fission, 1973.

Anomaly explanation: third barrier

Nucleus	Ref	E_A MeV	$\hbar\omega_A$ MeV	E_{IS} MeV	E_{Min} MeV	$\hbar\omega_{Min}$ MeV	E_B MeV	$\hbar\omega_B$ MeV	E_B-E_A MeV
Theory:									
^{232}Th	a	4.8	-	2.8	-	-	7.3	-	2.5
	b	4.3	-	1.9	1.4	-	8.6	-	4.3
	c	3.4	-	2.3	1.8	-	6.6	-	3.2
Experiment:									
^{232}Th	Present	5.50	0.90	4.43	4.25	0.36	6.18	0.47	0.68

A third fission barrier was proposed to explain these anomalous observations

The ratio between the height of the second and third barrier depends on (N,Z) of the fissioning systems

Only for N ≤ 146 (in these calculations)

(1) The observed **height difference** would be E_C-E_B instead of E_B-E_A

Back, B. B., Britt, H. C., Garrett, J. D., & Hansen, O. (1972). Subbarrier fission resonances in Th isotopes. Physical Review Letters, 28(26), 1707.

Anomaly explanation: third barrier

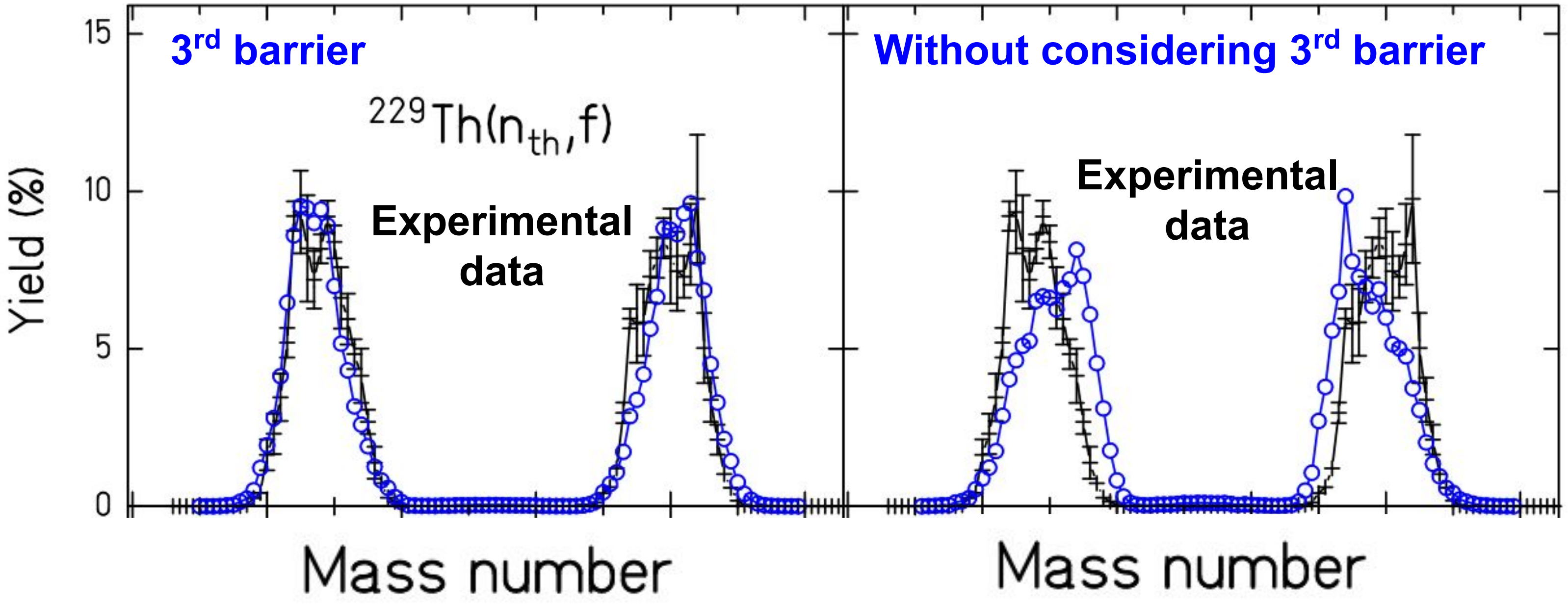

A third fission barrier was proposed to explain these anomalous observations

The ratio between the height of the second and third barrier depends on (N,Z) of the fissioning systems

Only for N ≤ 146 (in these calculations)

(1) The observed height difference would be E_C-E_B instead of E_B-E_A

(2) The **mass yields** are **better reproduced** by the **semi-empirical model (GEF) when** the **third barrier** is included

Schmidt, K. H., Schmitt, C., Heinz, A., & Jurado, B. (2024). Identifying and overcoming deficiencies of nuclear data on the fission of light actinides by use of the GEF code. Annals of Nuclear Energy, 208, 110784.

Anomaly explanation: third barrier

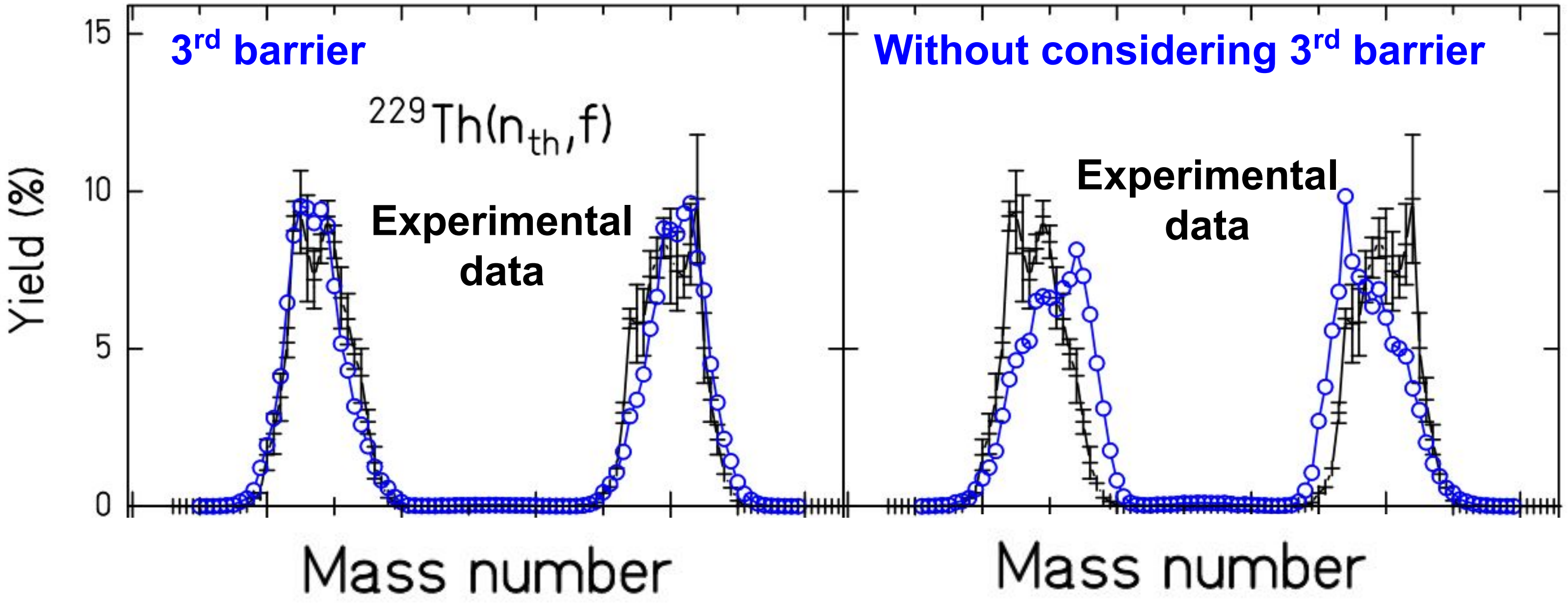

A third fission barrier was proposed to explain these anomalous observations

The ratio between the height of the second and third barrier depends on (N,Z) of the fissioning systems

Only for N ≤ 146 (in these calculations)

(1) The observed height difference would be E_C-E_B instead of E_B-E_A

(2) The mass yields are better reproduced by the semi-empirical model (GEF) when the third barrier is included

- What **structural effects** (proton/neutron) **drives** this anomaly ?
- **How** do they **vary** with **excitation energy**?
- Is it just an **anomaly?**

Schmidt, K. H., Schmitt, C., Heinz, A., & Jurado, B. (2024). Identifying and overcoming deficiencies of nuclear data on the fission of light actinides by use of the GEF code. Annals of Nuclear Energy, 208, 110784.

Experimental technique: inverse-kinematics

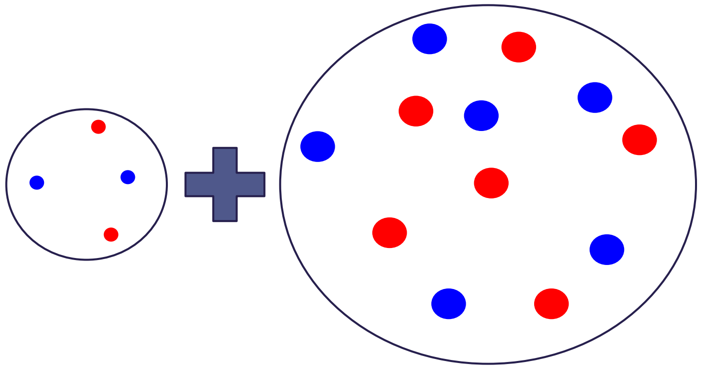

Reaction kinematics:
direct

Experimental technique: inverse-kinematics

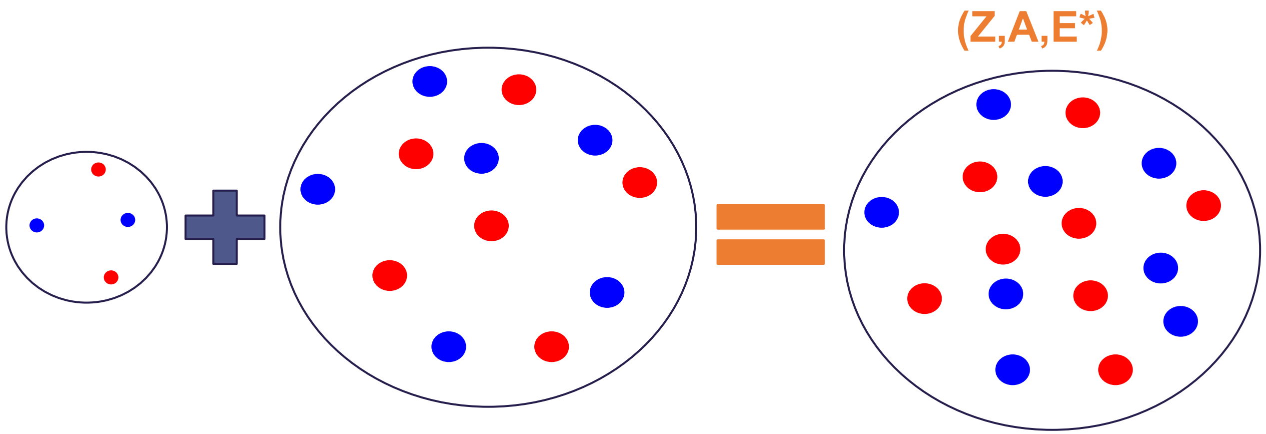

Reaction kinematics:
direct

Experimental technique: inverse-kinematics

(Z,A,E*)

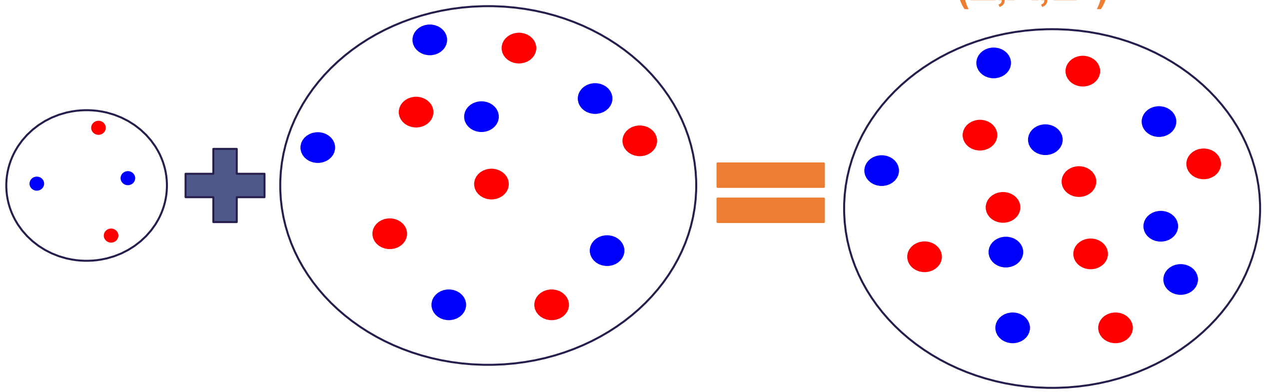

In fission, Total Kinetic Energy (TKE) ~ 200 MeV

Reaction kinematics:
direct

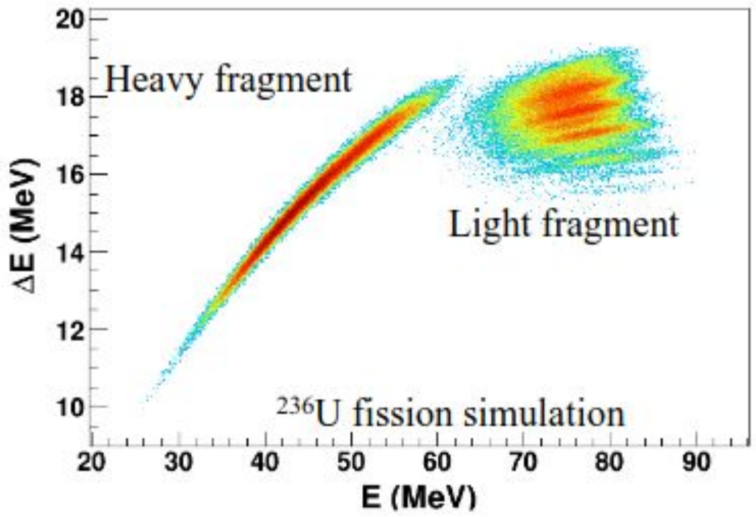

Bethe-Bloch : $-dE/dx \propto Z^2/\beta^2$

Experimental technique: inverse-kinematics

(Z,A,E*)

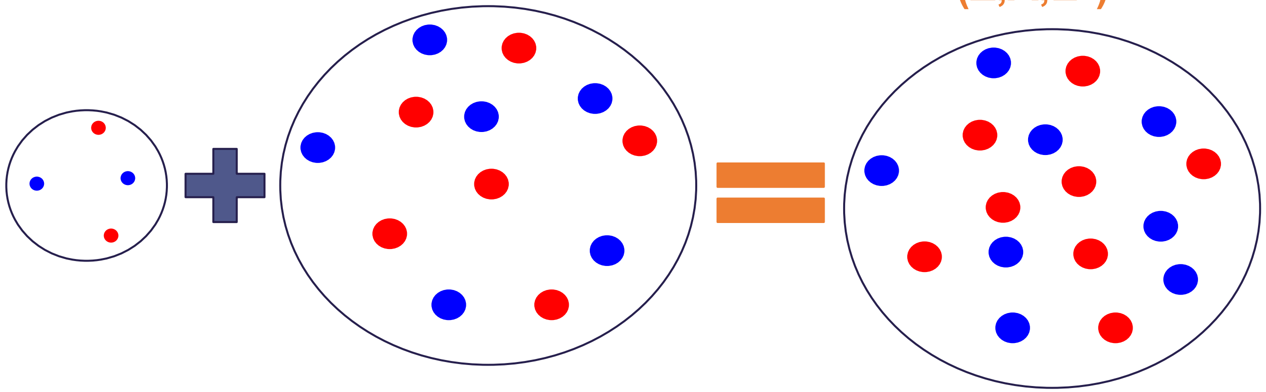

In fission, Total Kinetic Energy (TKE) ~ 200 MeV

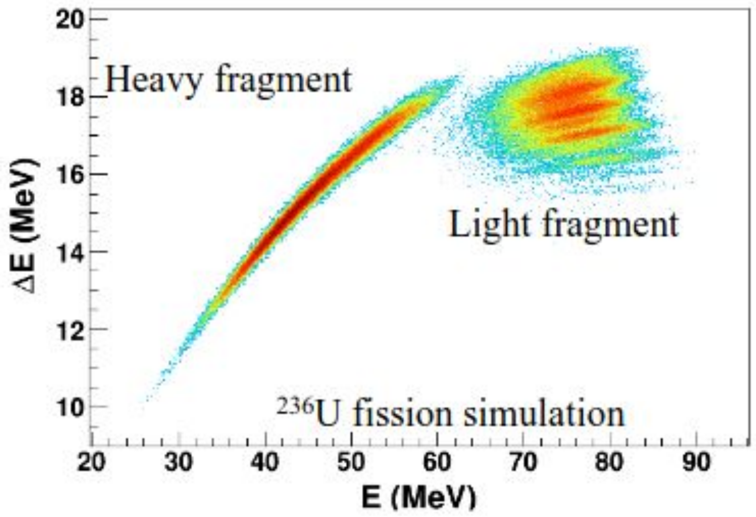

Reaction kinematics:
direct

Reaction kinematics:
inverse

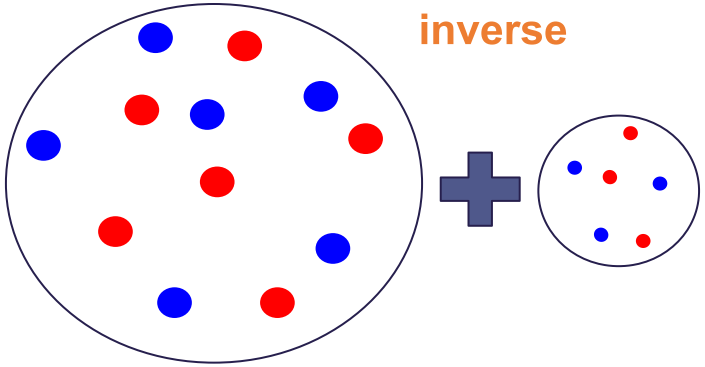

Experimental technique: inverse-kinematics

(Z,A,E*)

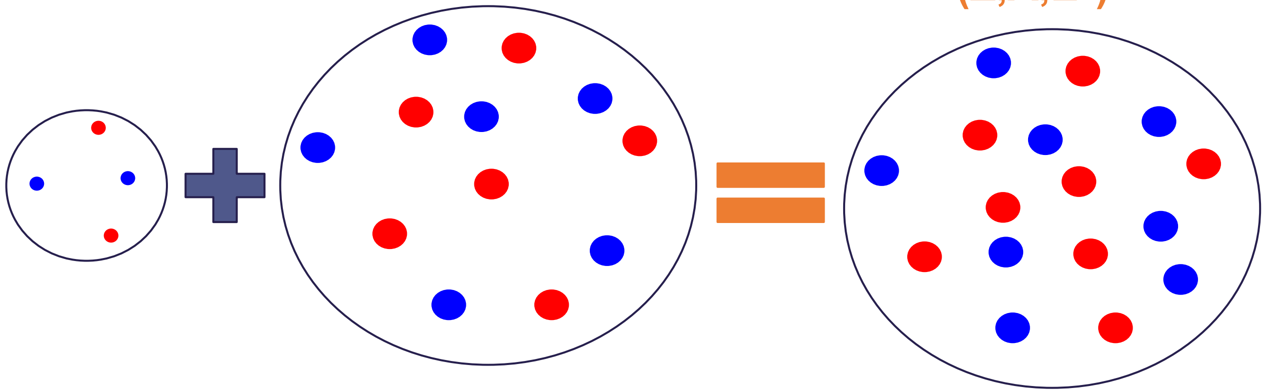

In fission, Total Kinetic Energy (TKE) ~ 200 MeV

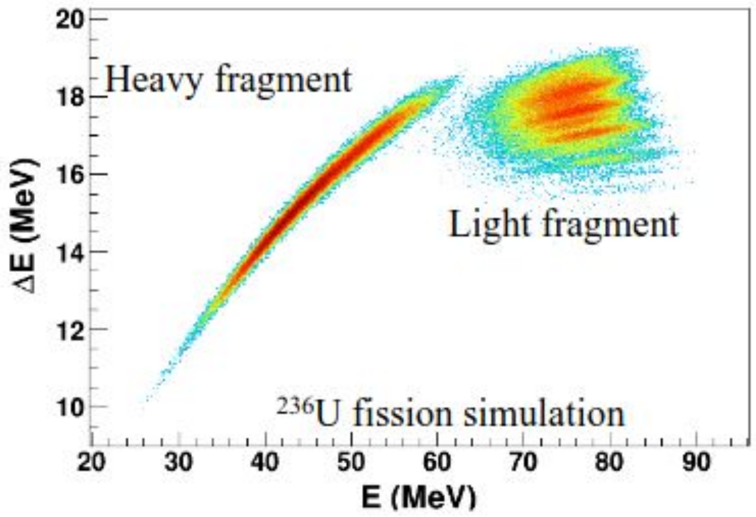

<u>Reaction kinematics:</u>
direct

<u>Reaction kinematics:</u>
inverse

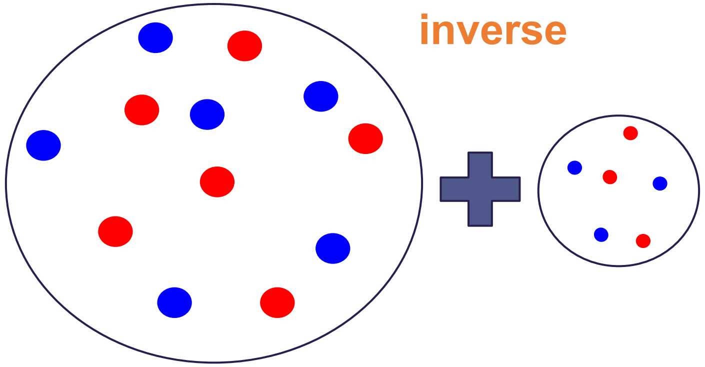

Kinematic boost:

TKE up to ~1000 MeV

Experimental technique: inverse-kinematics

(Z,A,E*)

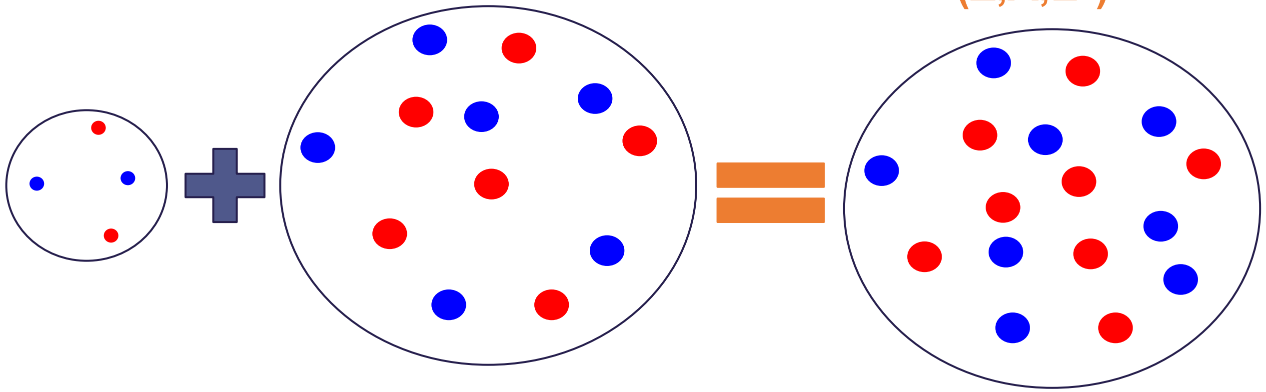

In fission, Total Kinetic Energy (TKE) ~ 200 MeV

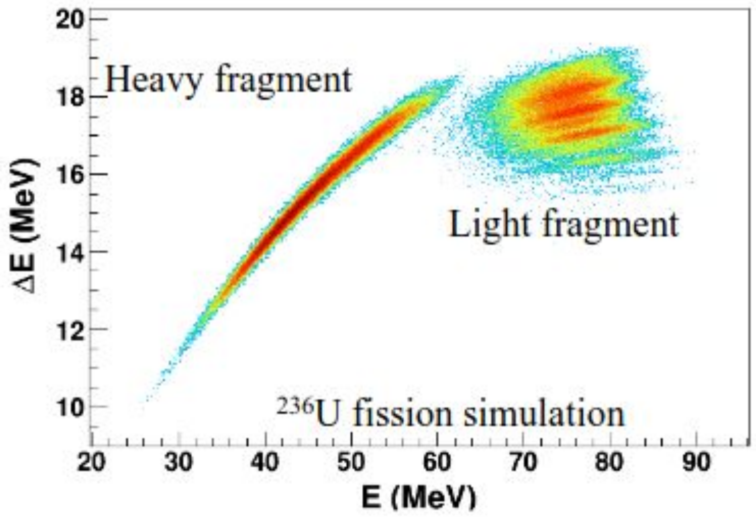

Reaction kinematics: direct

Reaction kinematics: inverse

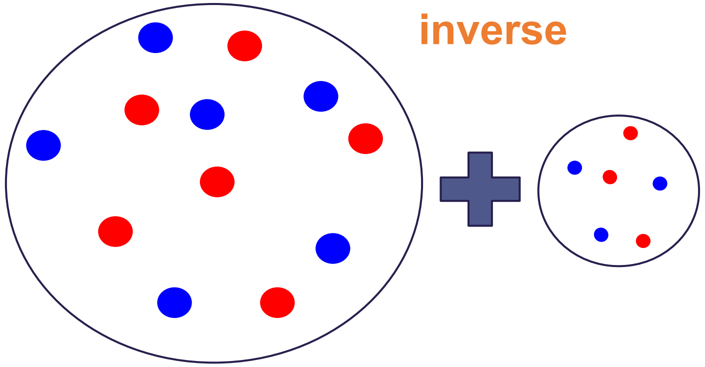

Kinematic boost:

TKE up to ~1000 MeV

-dE/dx ∝ Z^2/β^2

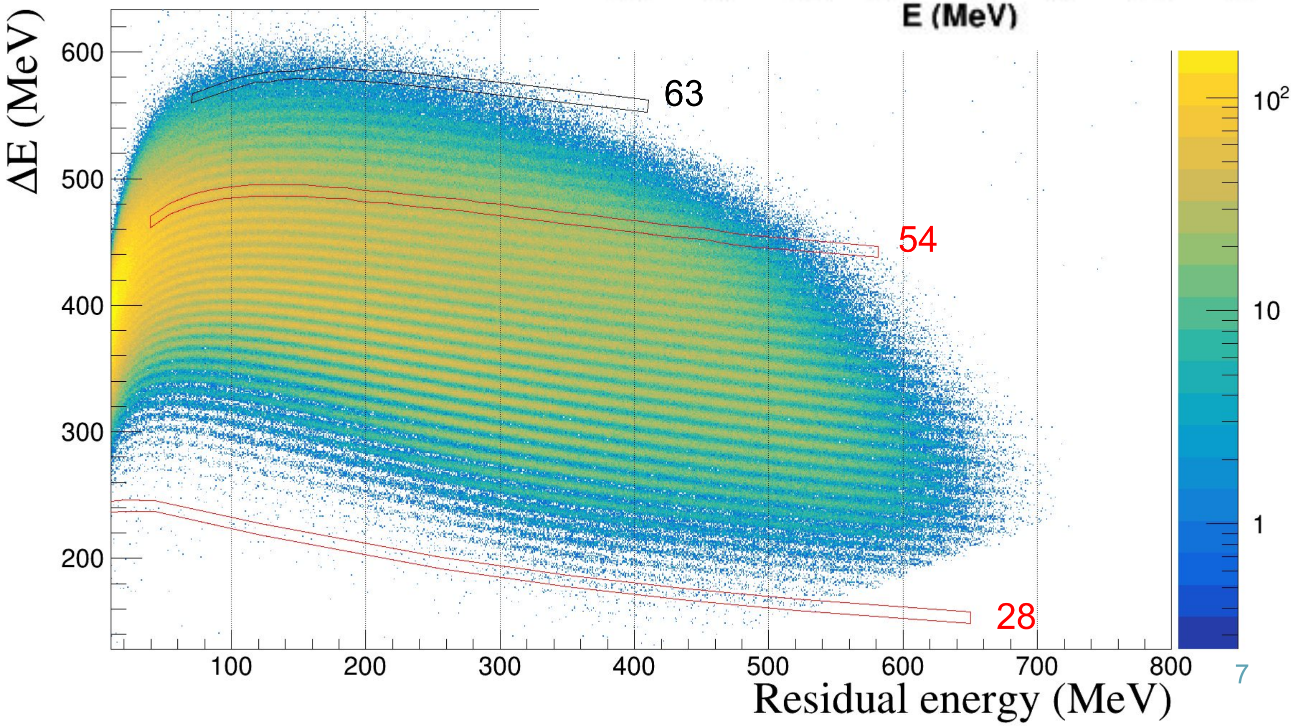

Experimental setup

^{232}Th beam of 6 MeV/u impinging on a ^{12}C target.

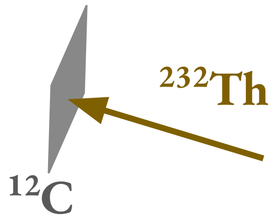

Experimental setup

^{232}Th beam of 6 MeV/u impinging on a ^{12}C target.
Produce fissioning systems through fusion (^{244}Cm) , transfer reactions (10+ systems like ^{234}U, ^{230}Th, ^{238}Pu, …) and inelastic scattering (^{232}Th)

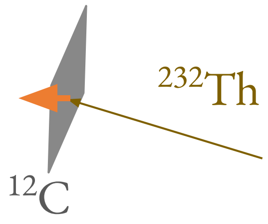

Experimental setup

^{232}Th beam of 6 MeV/u impinging on a ^{12}C target.
Produce fissioning systems through fusion (^{244}Cm) , transfer reactions (10+ systems like ^{234}U, ^{230}Th, ^{238}Pu, …) and inelastic scattering (^{232}Th)

- **Beam-like** at high E* => **fission fragments**
- **Target-like** recoil => **Correlated to the fissioning nucleus**

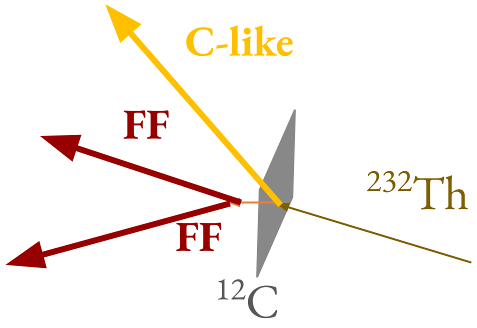

Experimental setup

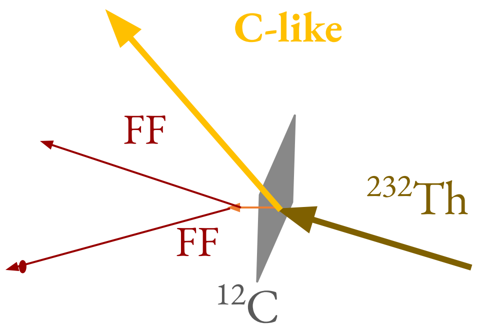

Experimental setup

Carbon-like particle identified by **PISTA**: **8 ΔE - E segmented silicon telescopes** => (**E, θ**)

Bégué–Guillou, et al. (2026). Performance of the Particle-Identification Silicon-Telescope Array coupled with the VAMOS++ magnetic spectrometer. Nuclear Instruments and Methods in Physics Research Section A: Accelerators, Spectrometers, Detectors and Associated Equipment, 1090, 171671.

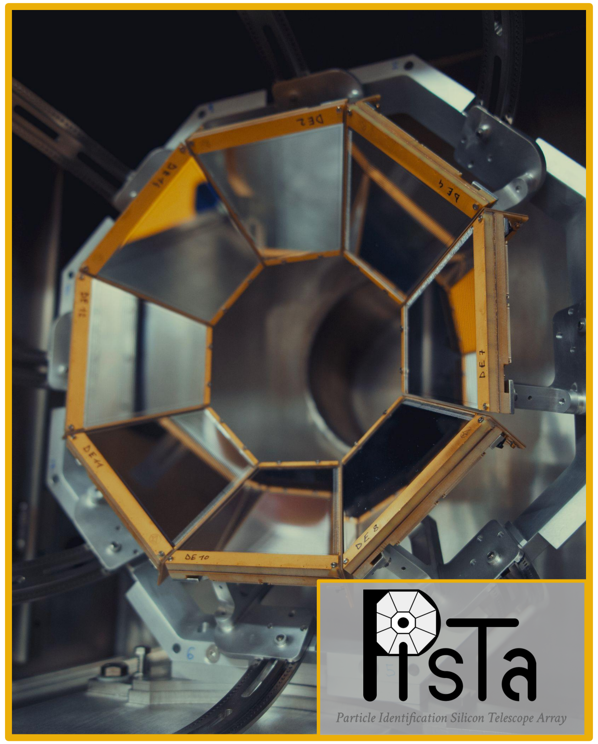

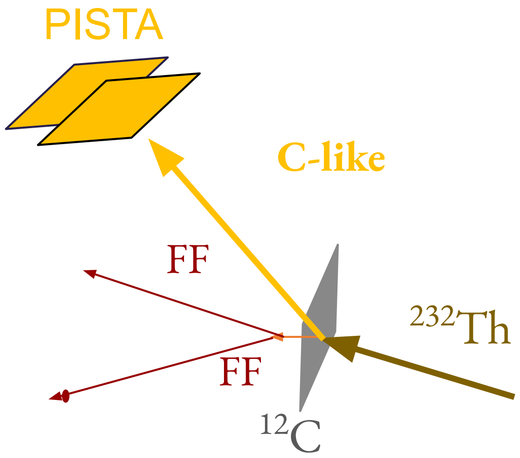

PISTA: Entrance channel information

Bégué–Guillou, et al. (2026). Performance of the Particle-Identification Silicon-Telescope Array coupled with the VAMOS++ magnetic spectrometer. Nuclear Instruments and Methods in Physics Research Section A: Accelerators, Spectrometers, Detectors and Associated Equipment, 1090, 171671.

1) What is the fissioning system that was formed (Z,A)

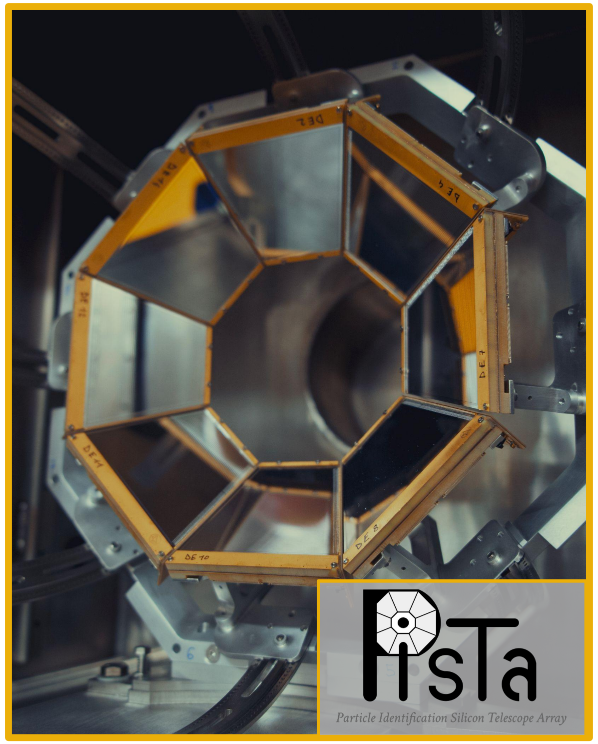

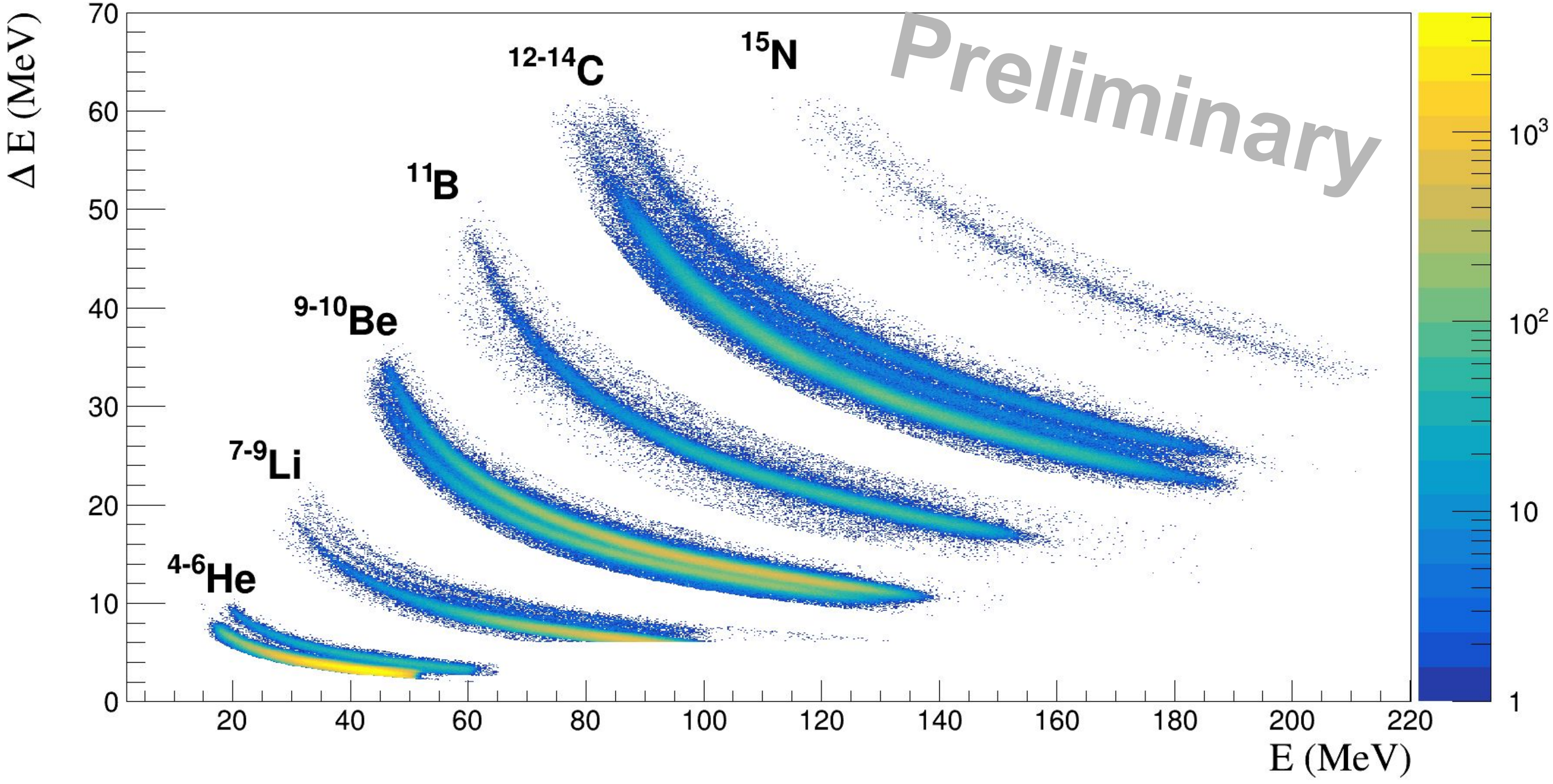

PISTA: Entrance channel information

Bégué–Guillou, et al. (2026). Performance of the Particle-Identification Silicon-Telescope Array coupled with the VAMOS++ magnetic spectrometer. Nuclear Instruments and Methods in Physics Research Section A: Accelerators, Spectrometers, Detectors and Associated Equipment, 1090, 171671.

1) What is the fissioning system that was formed (Z,A)

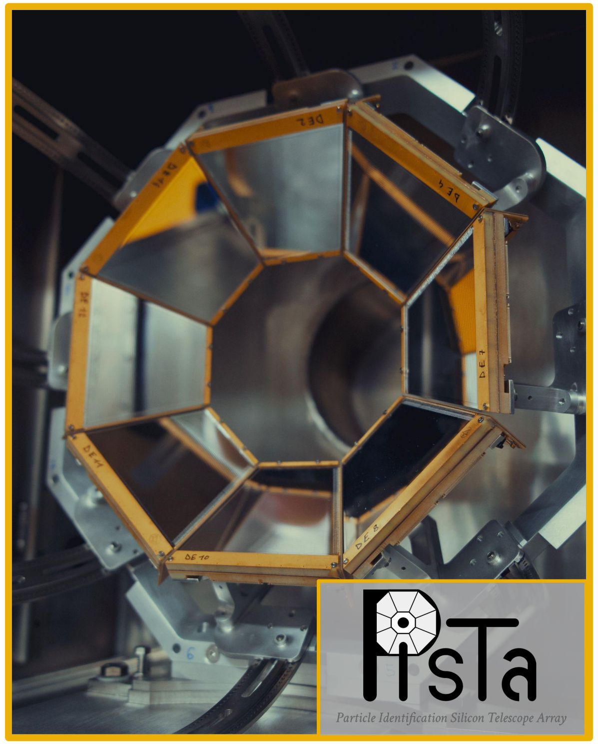

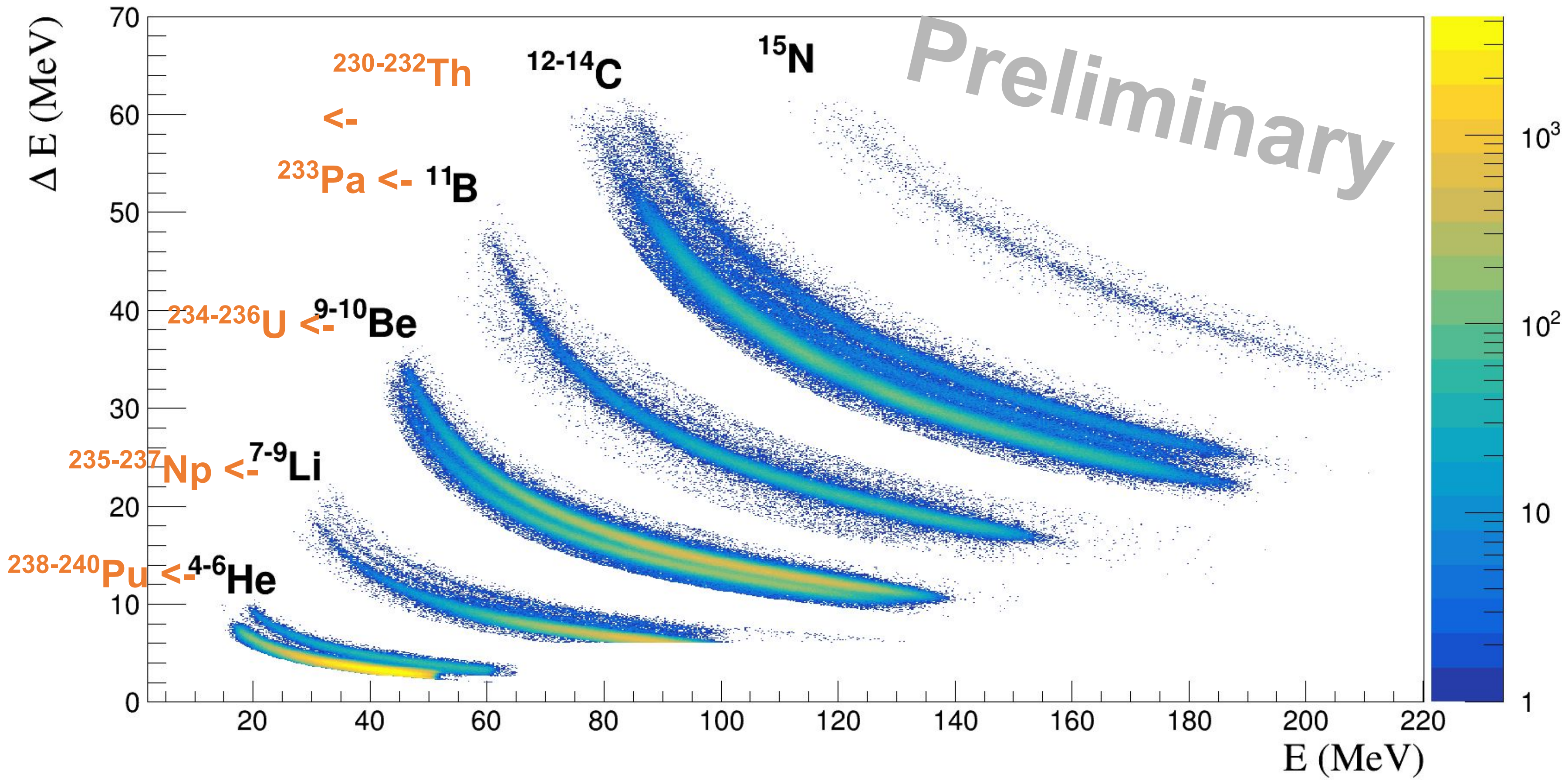

PISTA: Entrance channel information

GANIL

Bégué–Guillou, et al. (2026). Performance of the Particle-Identification Silicon-Telescope Array coupled with the VAMOS++ magnetic spectrometer. Nuclear Instruments and Methods in Physics Research Section A: Accelerators, Spectrometers, Detectors and Associated Equipment, 1090, 171671.

1) What is the fissioning system that was formed (Z,A)
2) **What is the excitation energy (E*)**

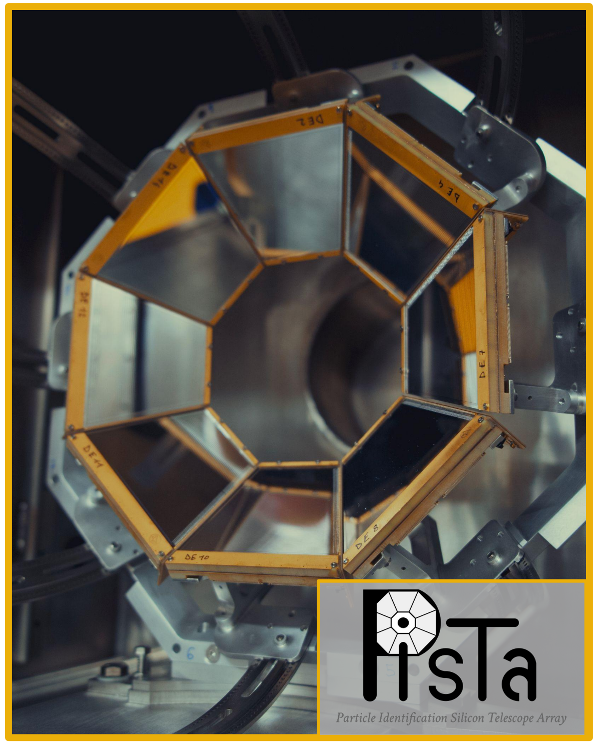

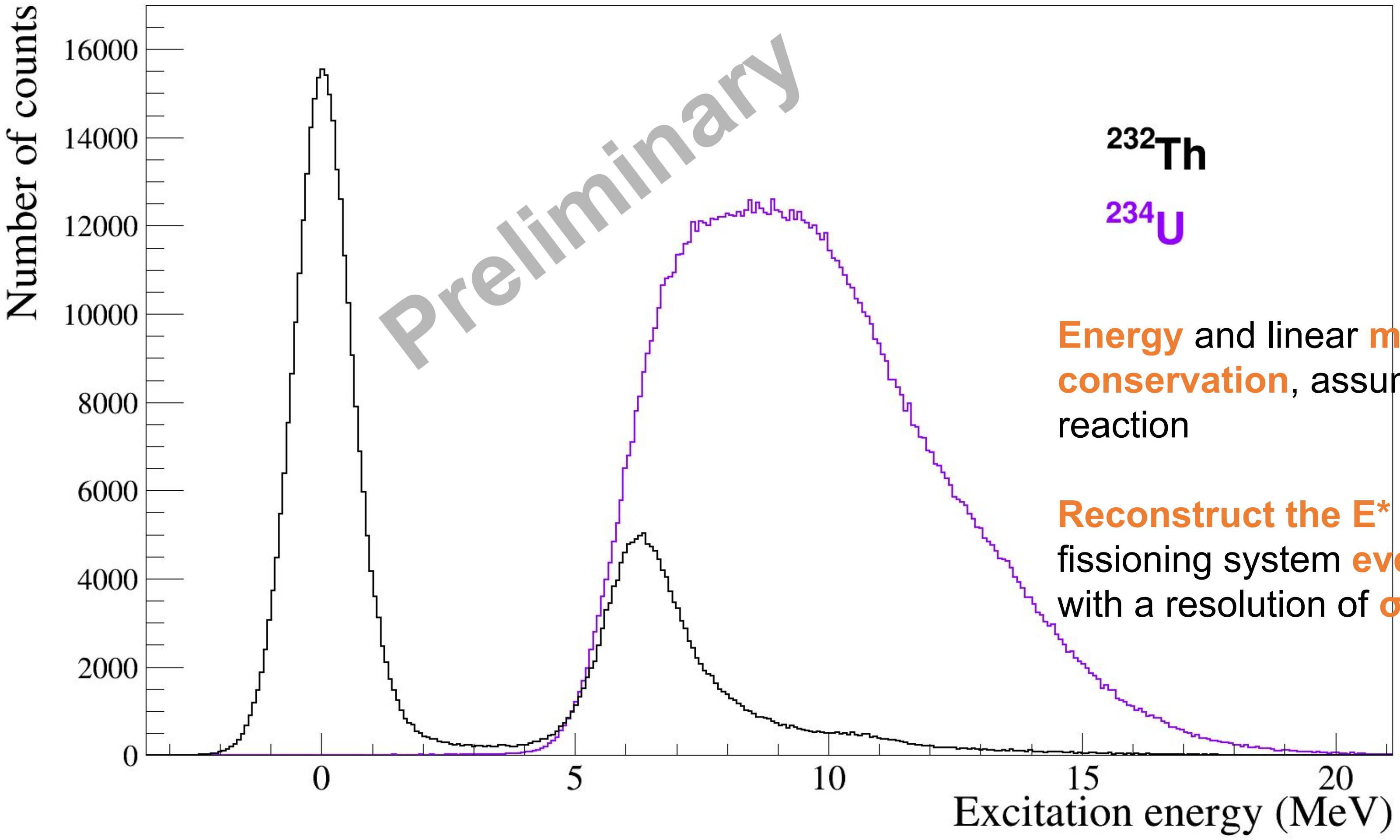

Energy and linear **momentum conservation**, assuming binary reaction

Reconstruct the E* of the fissioning system **event-by-event** with a resolution of **σ ~ 500 keV**

Experimental setup

Need to **identify** a **fission fragment mass** event by event
The **mass of the fragments is high** for good resolution through a Energy vs Time-of-Flight (ToF) identification

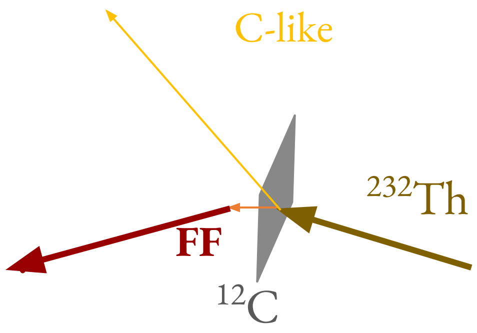

VAMOS ++ : Exit channel information

Need to identify a fission fragment mass event by event
The mass of the fragments is high for good resolution through a Energy vs Time-of-Flight (ToF) identification
Use a **magnetic spectrometer** => mass **resolution** depends on magnetic rigidity ($B\rho$) an ToF resolution

VAMOS: A Dipole, a Wien Filter (not used) and a pair of Quadrupoles

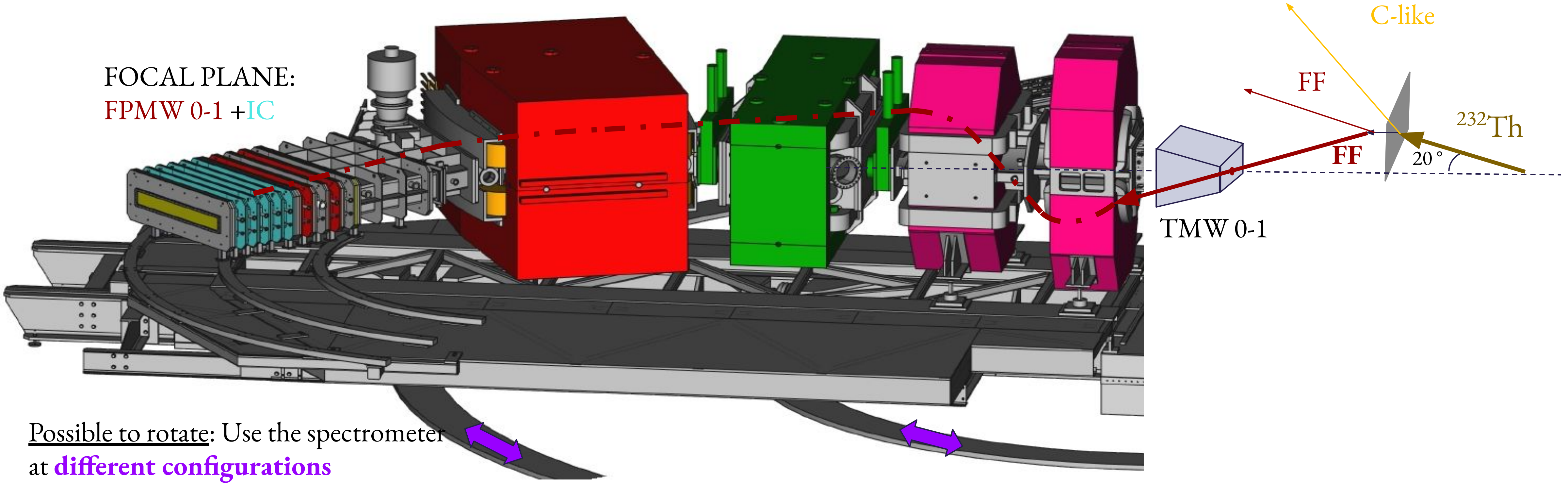

Possible to rotate: Use the spectrometer at **different configurations**

$B\rho$ = p/q →Unique for one nucleus of a given velocity and charge state (q)

VAMOS ++ : Ionization Chamber

GANIL

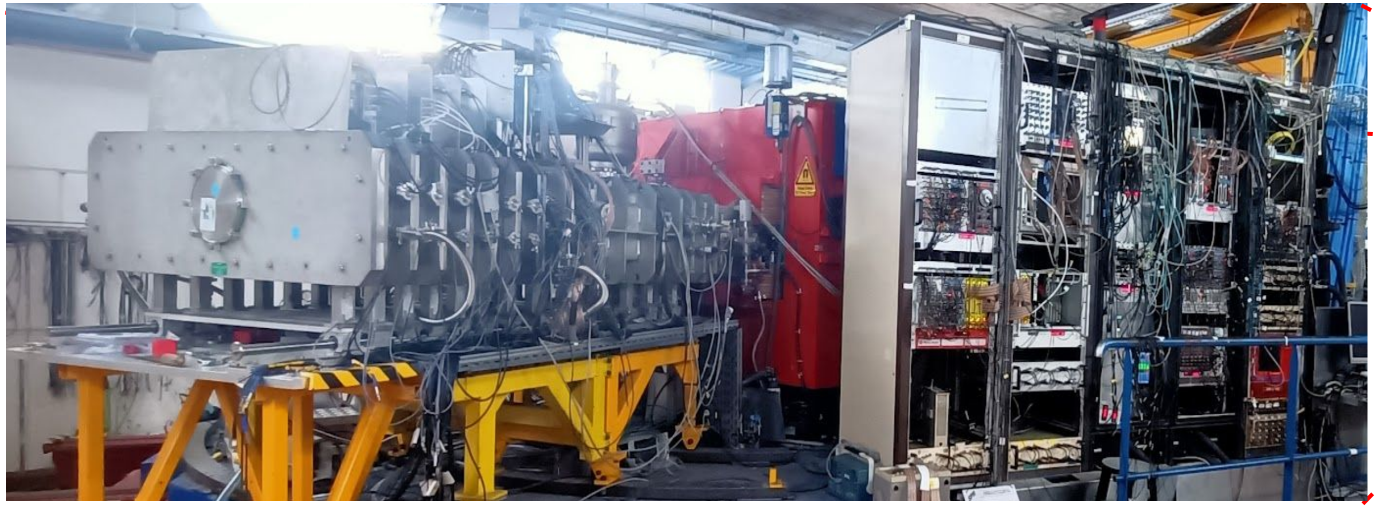

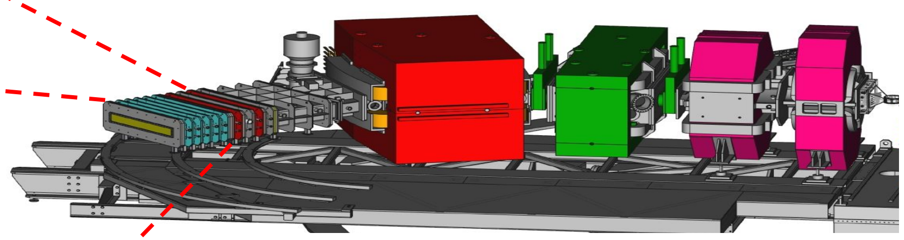

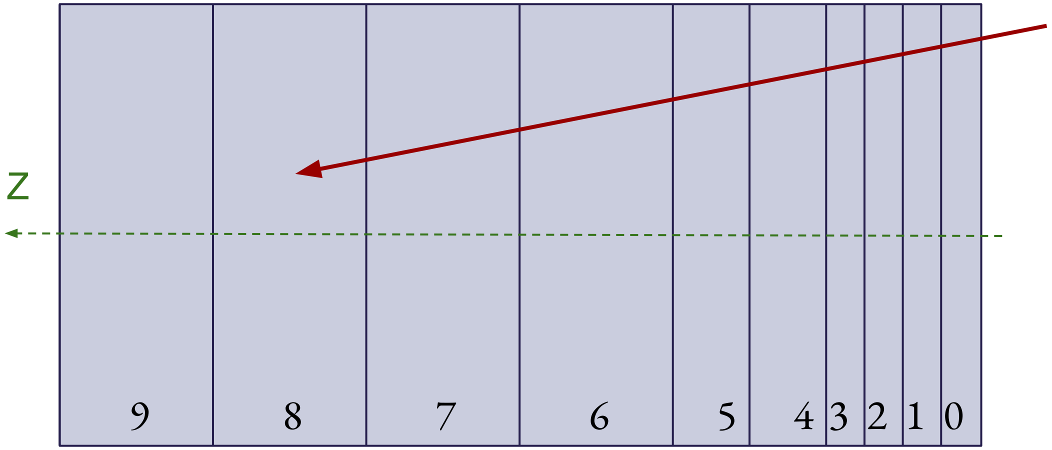

The **kinetic energy (E_{Kin})** of the fragment is proportional to the **mass** and the **velocity (γ)**

Through a **minimization method**, **scale** the contribution of **each IC** section for every time section

$E_{Kin} = \Sigma a_i * IC_i + b_0$
$A_{IC} = E_{Kin} / (\gamma_{VAMOS} - 1)$

The **A_{IC} is not enough** (~1%) for our goal :
$Q = A_{IC}/(A/Q)$

Fission fragment identification: Q vs A/Q

GANIL

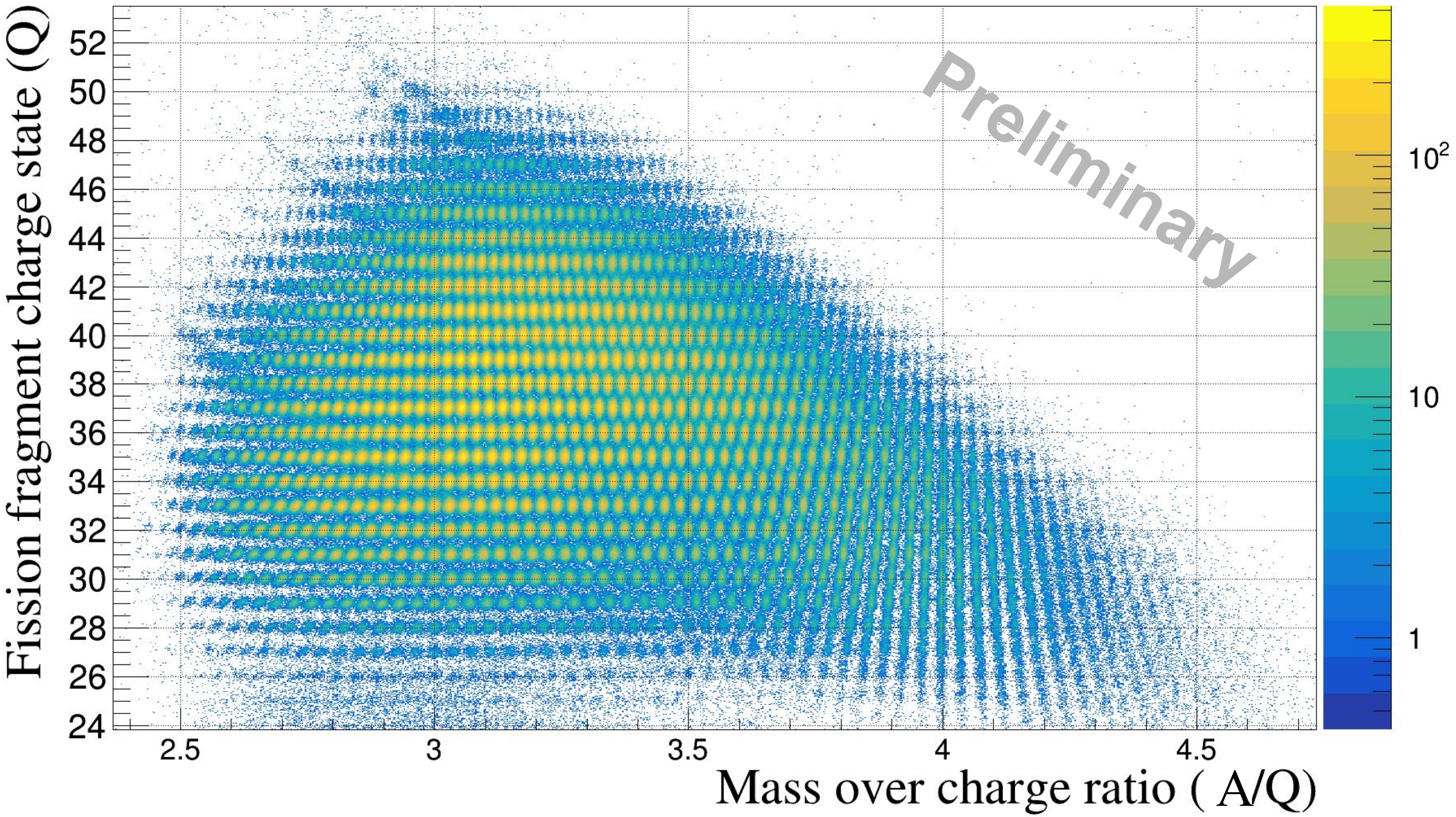

Fission fragment identification: A

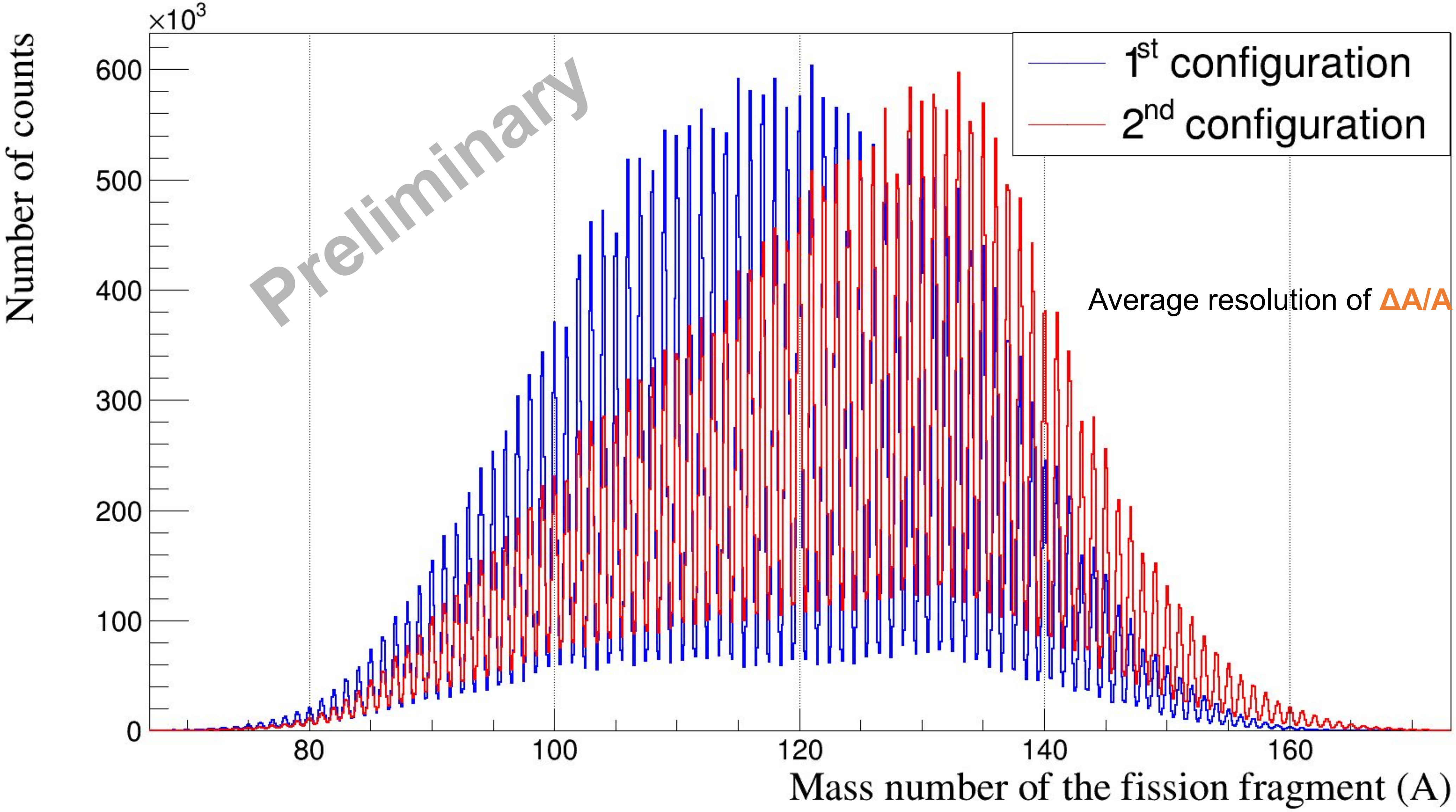

Average resolution of **ΔA/A ~** 1/234 = **4.27 ‰**

Fission fragment identification: Z

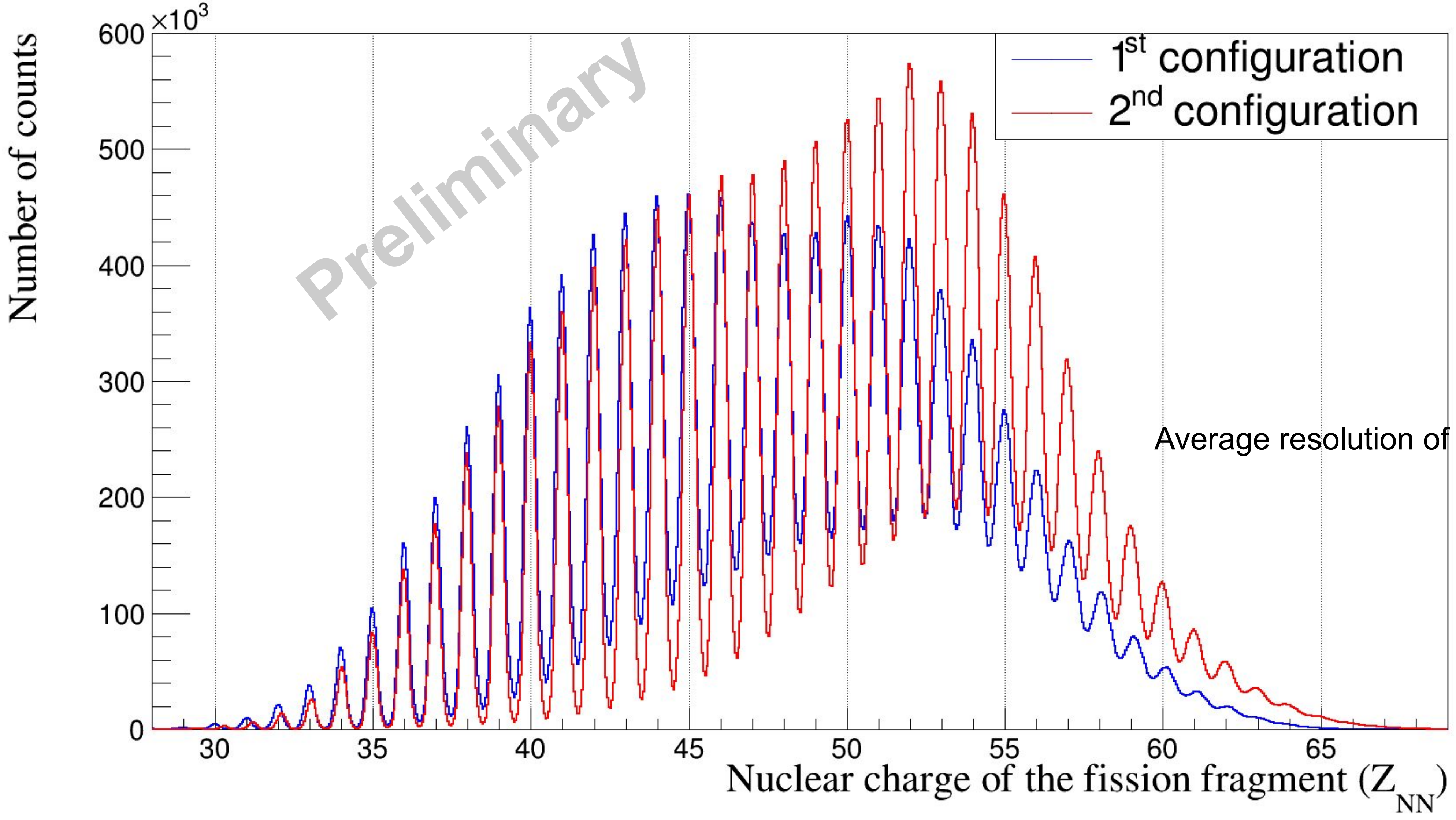

Average resolution of **ΔZ/Z ~** 1/86 = **1.16 %**

Fission fragment isotopic identification

GANIL

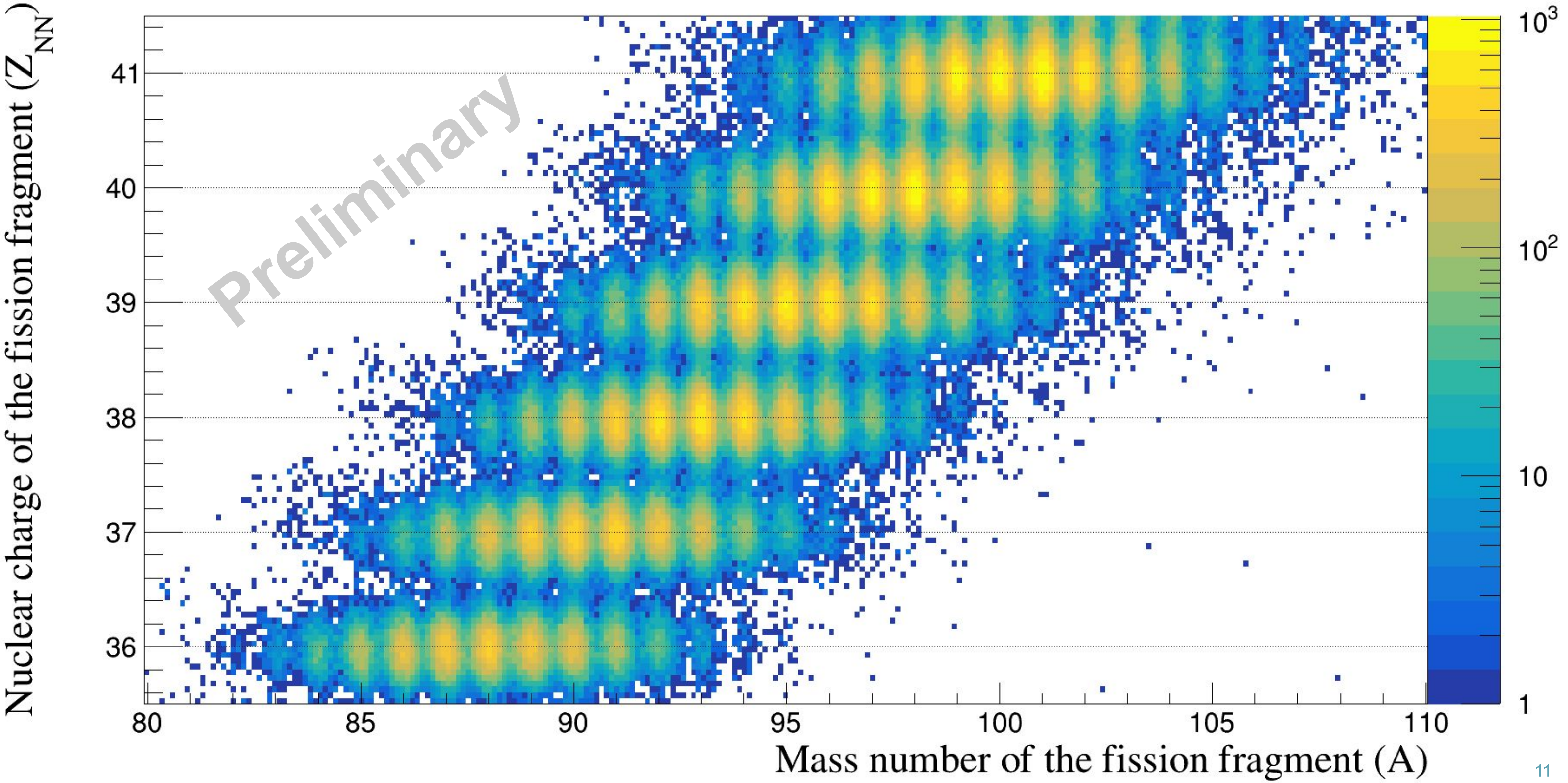

Mass yields of ^{232}Th

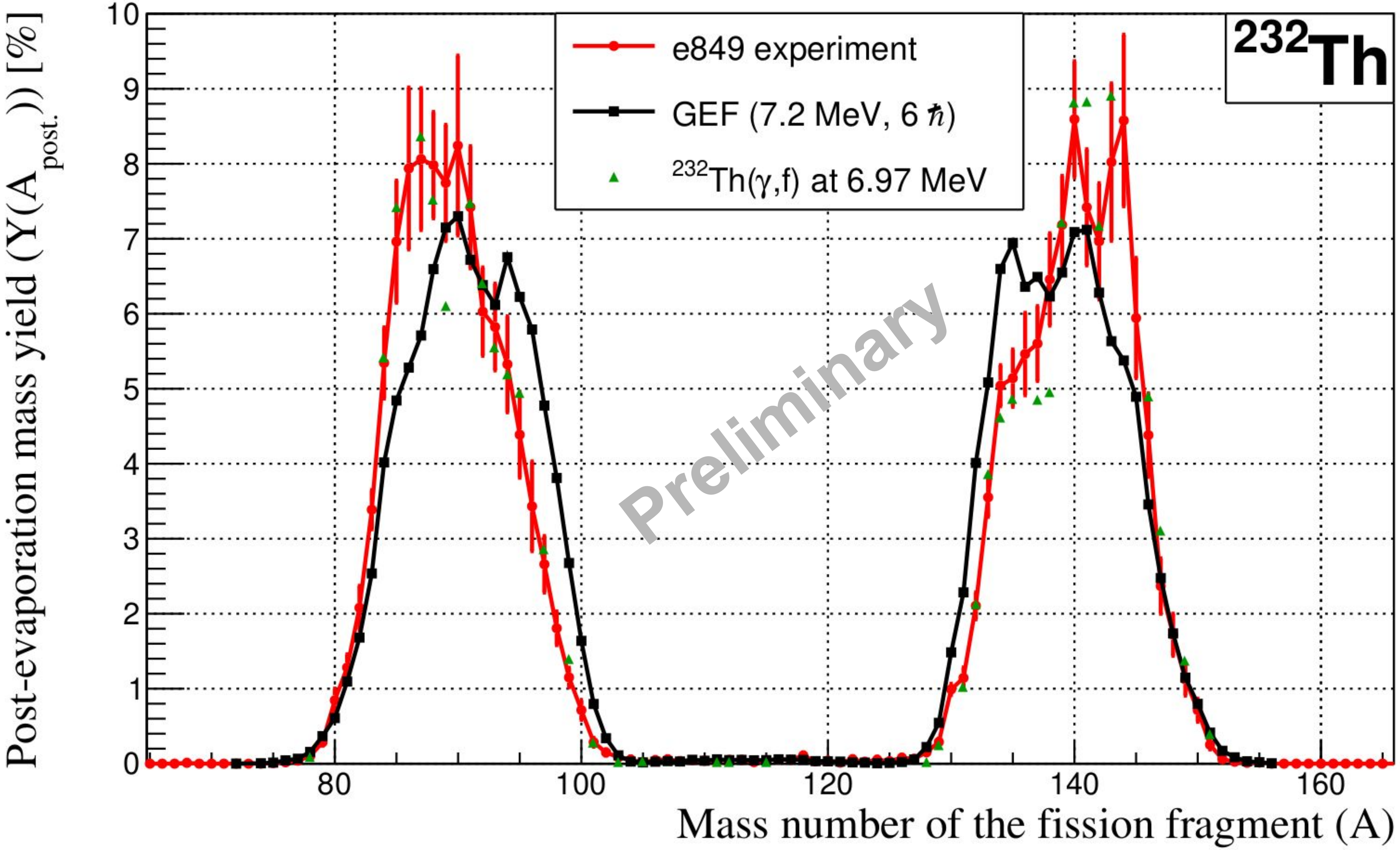

Elemental yields of ^{232}Th

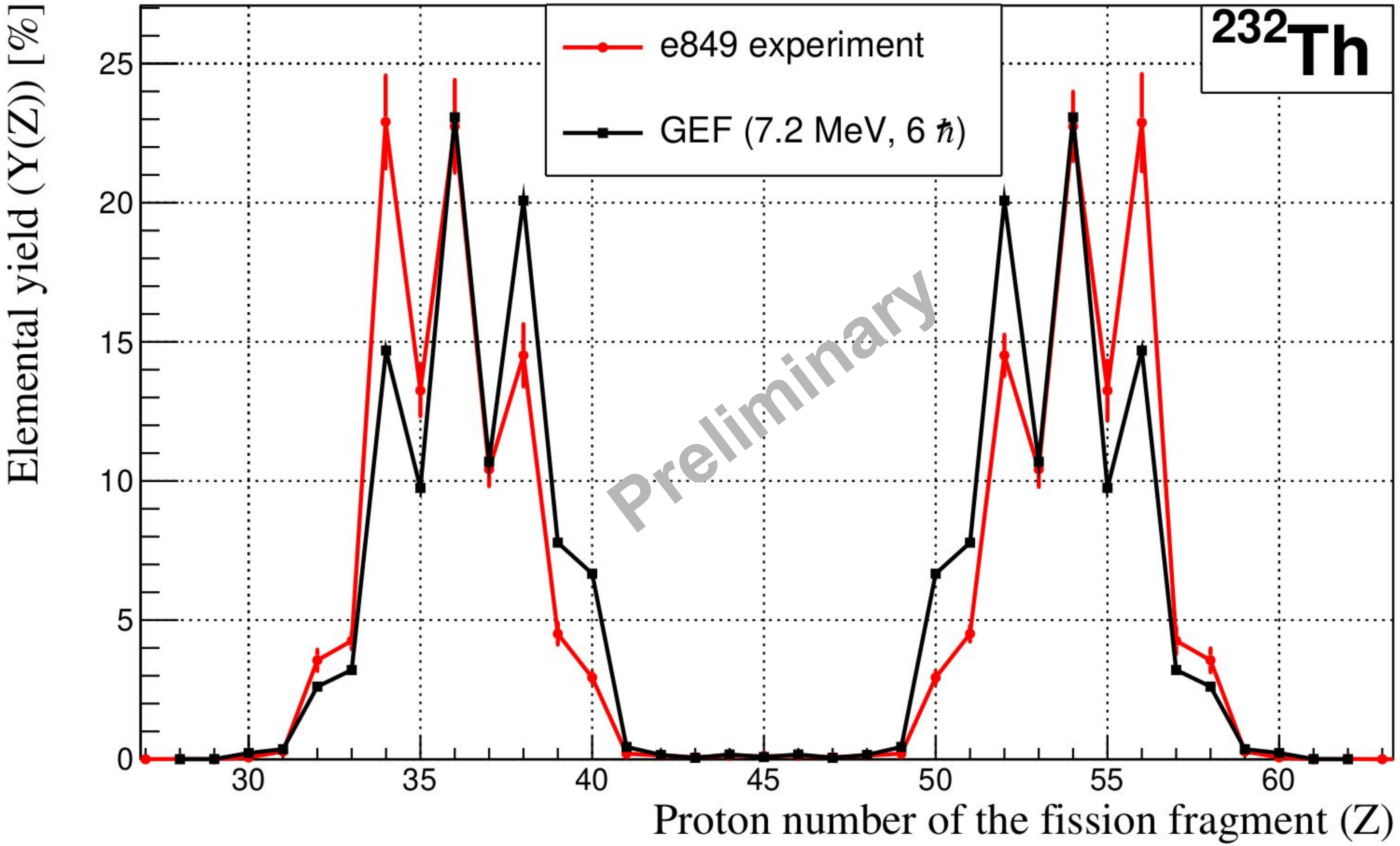

Elemental yields of ^{232}Th

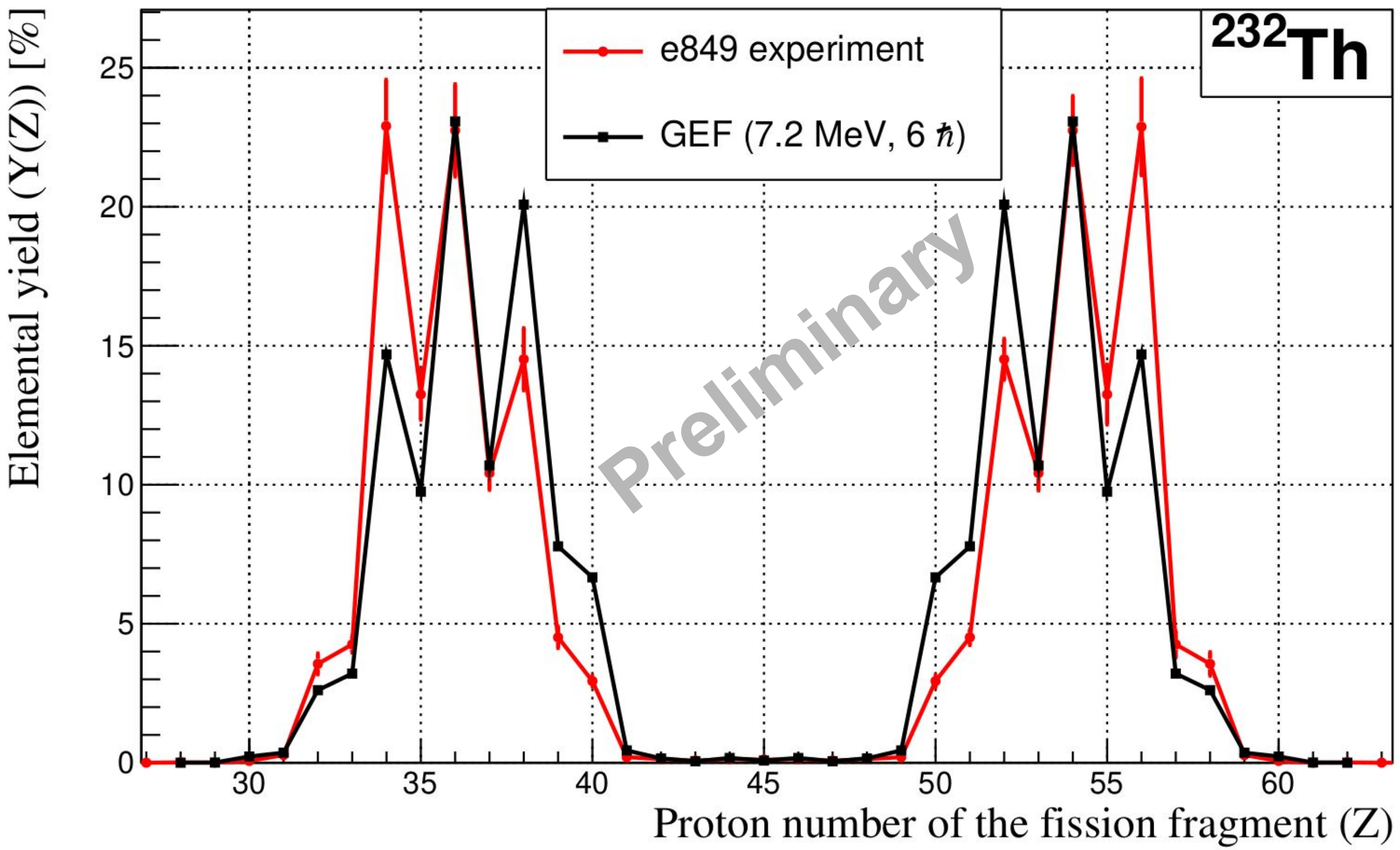

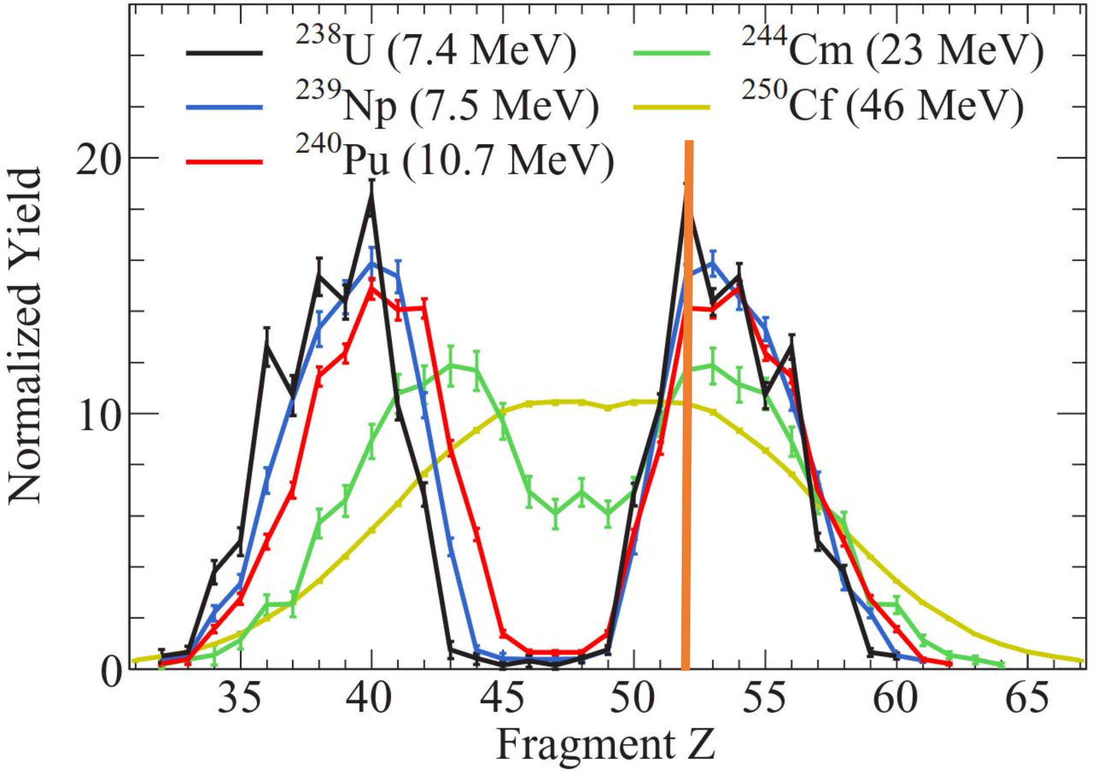

Ramos, D., Caamaño, M., Farget, F., Rodríguez-Tajes, C., Audouin, L., Benlliure, J., ... & Schmitt, C. (2018). Isotopic fission-fragment distributions of U 238, Np 239, Pu 240, Cm 244, and Cf 250 produced through inelastic scattering, transfer, and fusion reactions in inverse kinematics. Physical review C, 97(5), 054612.

Elemental yields of ^{233}Pa

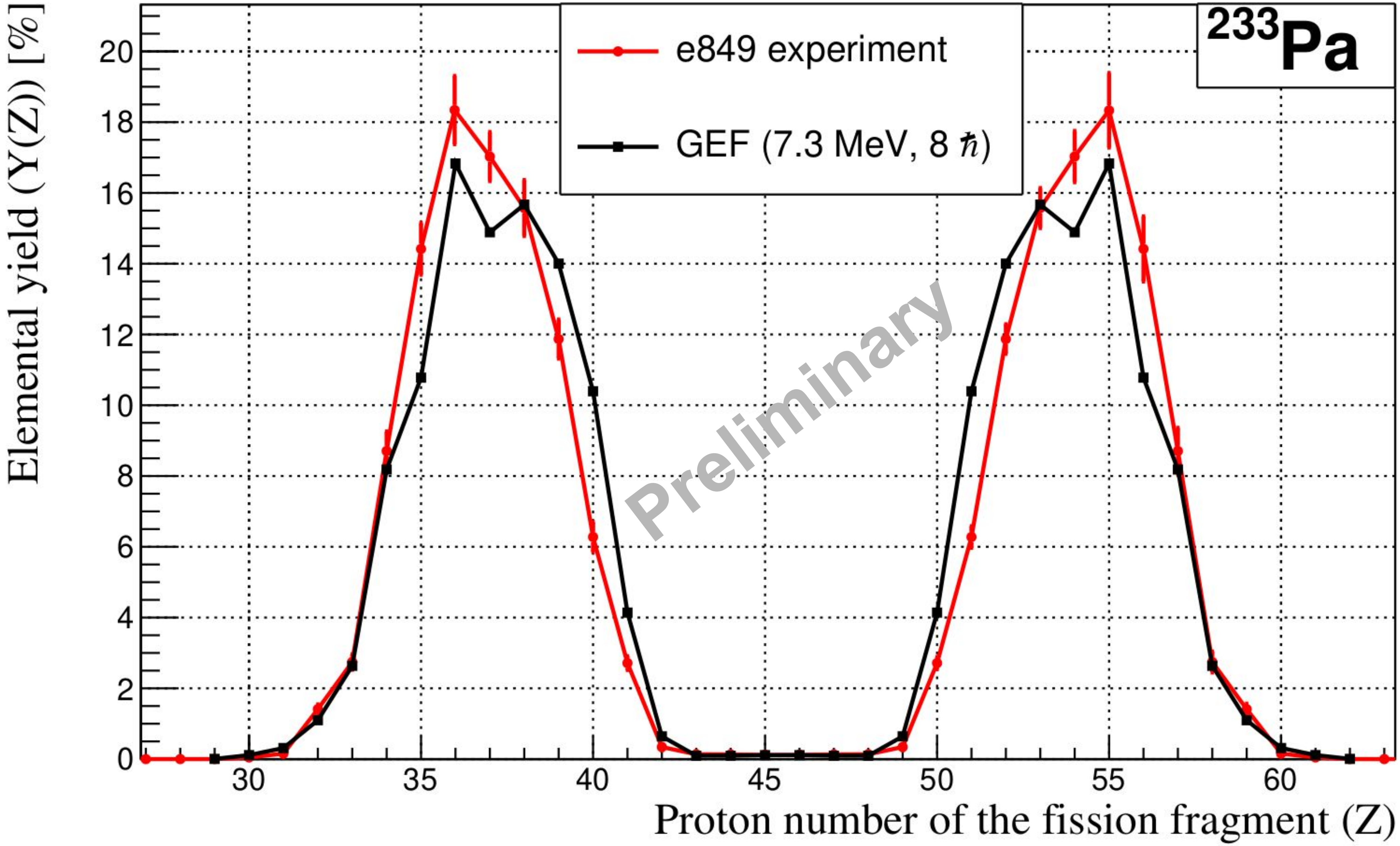

Elemental yields of ^{234}U

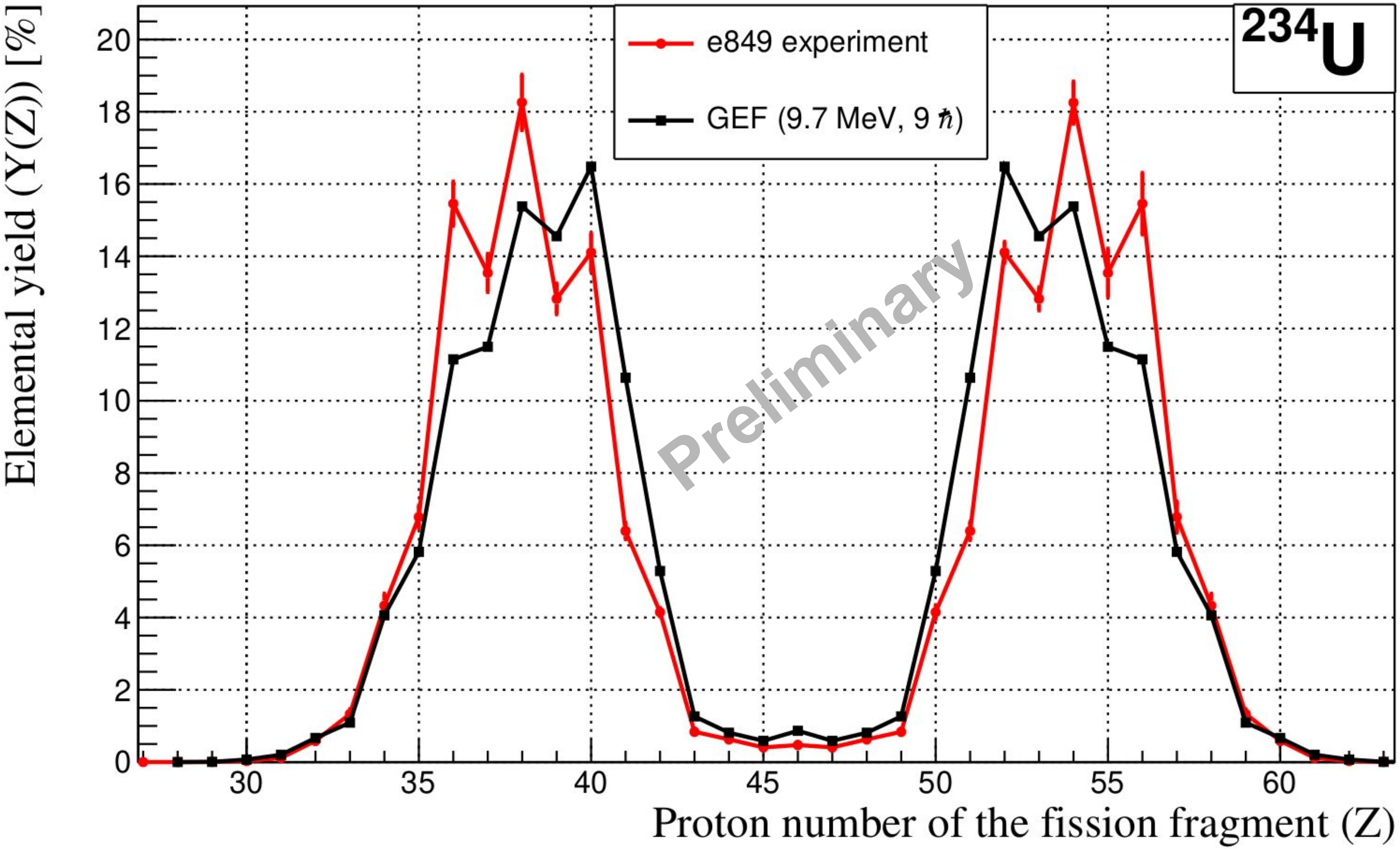

Elemental yields of $^{234-236}U$

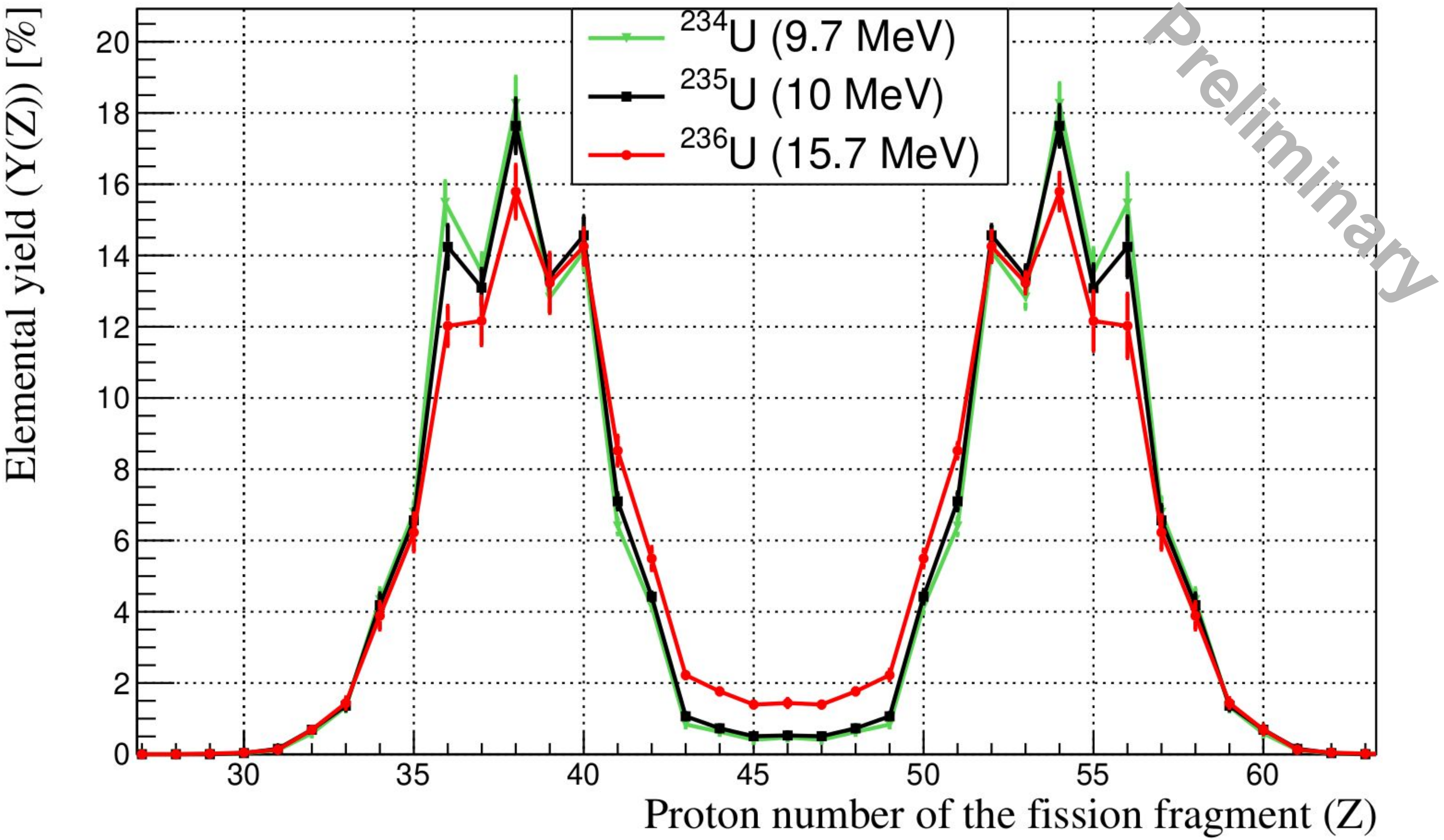

Elemental yields as a function of E*

GANIL

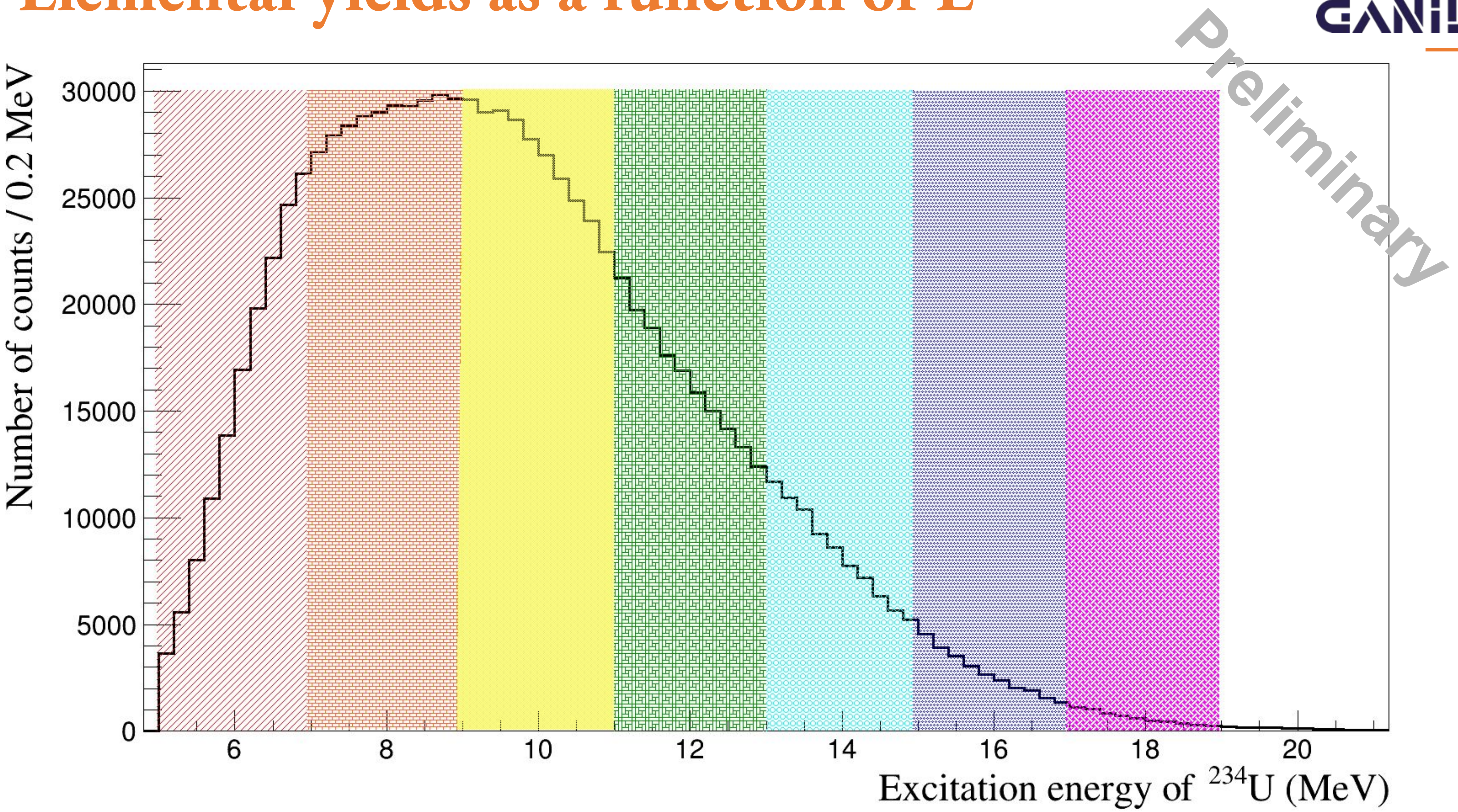

Elemental yields of ^{232}Th as a function of E*

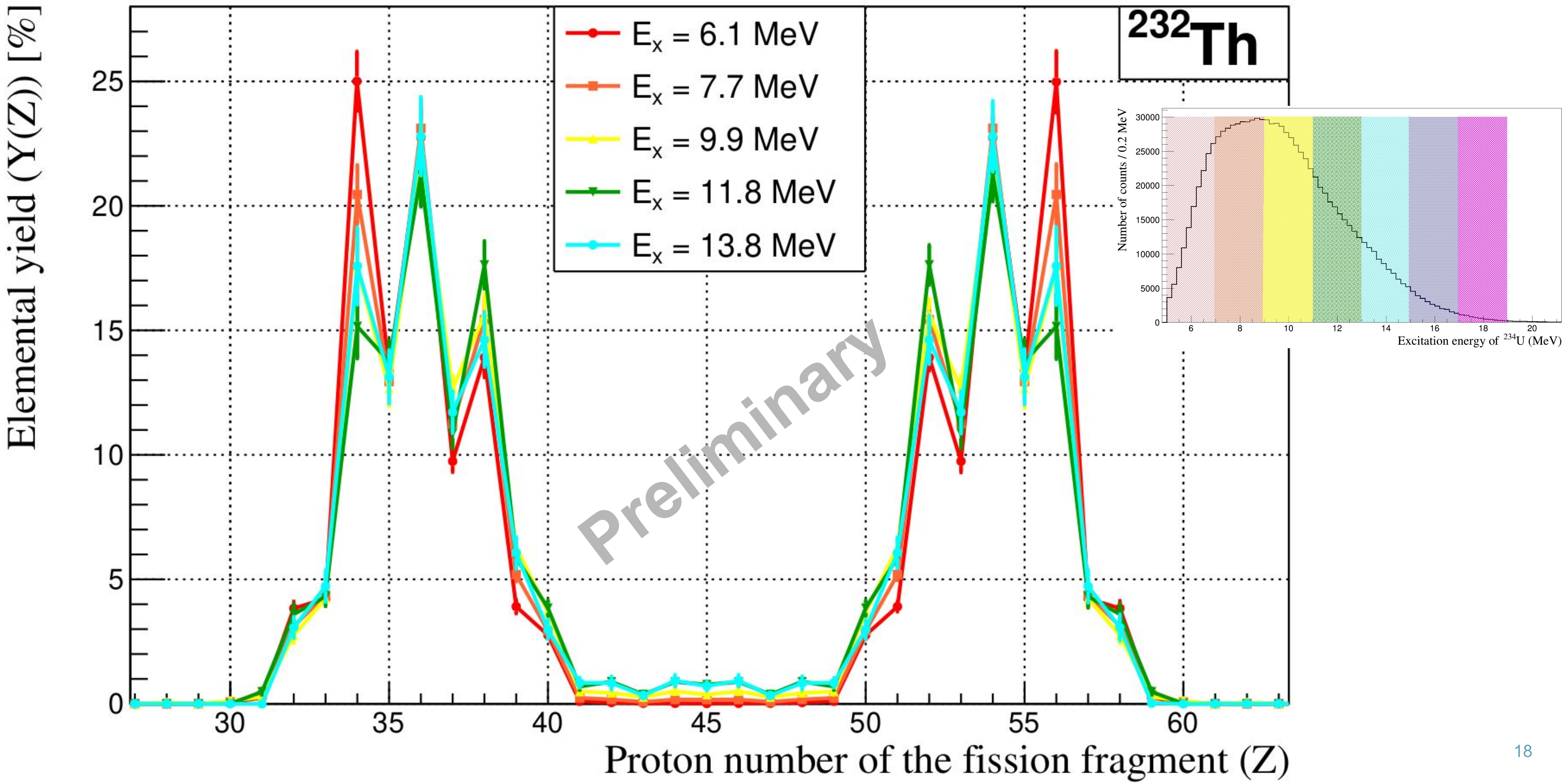

Elemental yields of ^{233}Pa as a function of E*

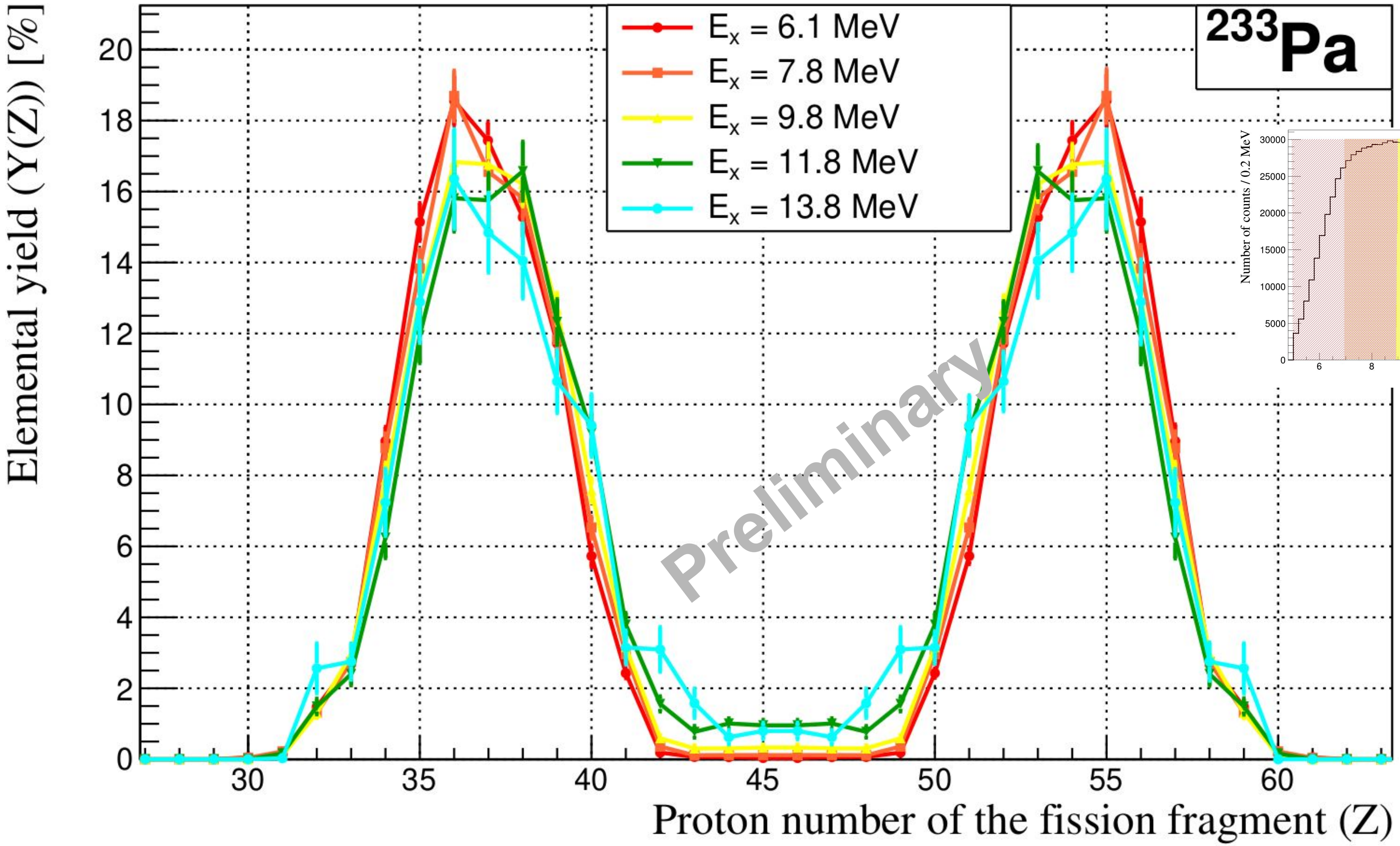

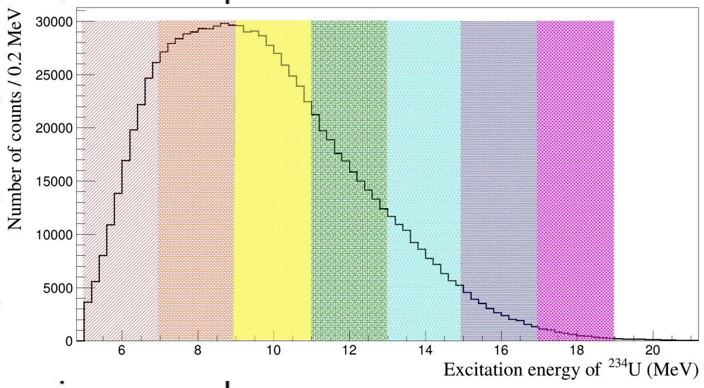

Elemental yields of ^{234}U as a function of E*

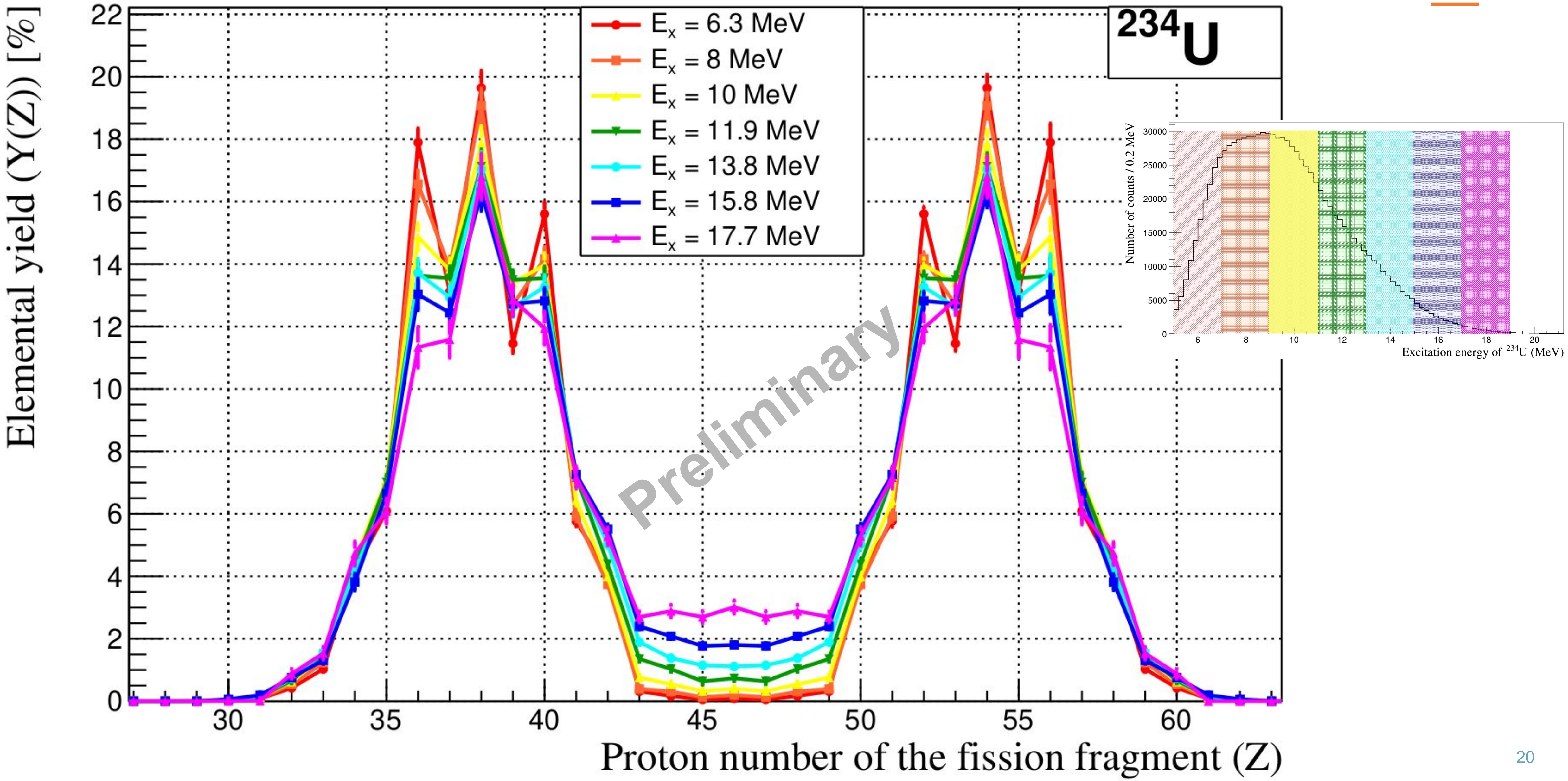

Elemental yields ratio as a function of E*

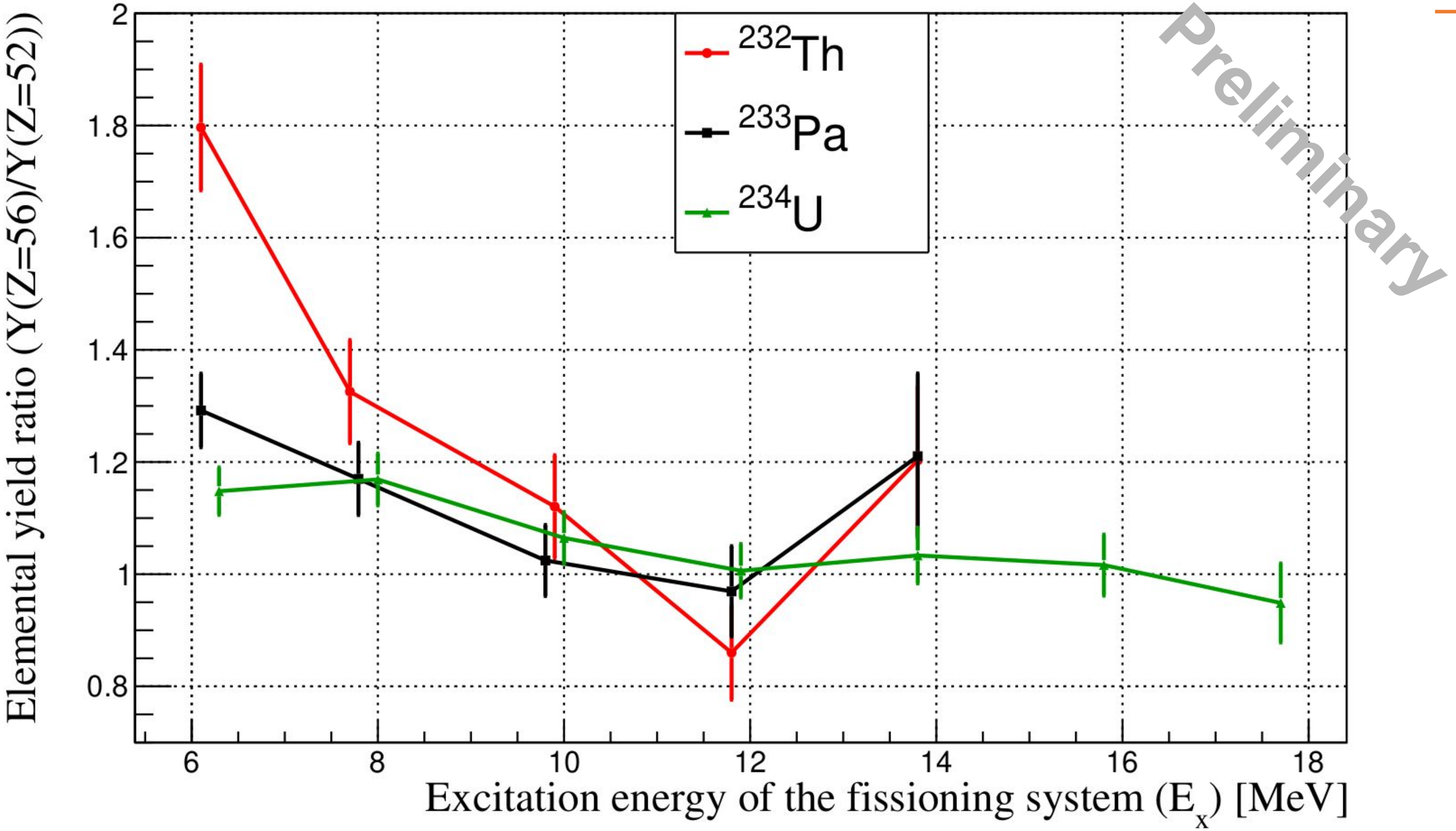

Elemental yields ratio as a function of E*

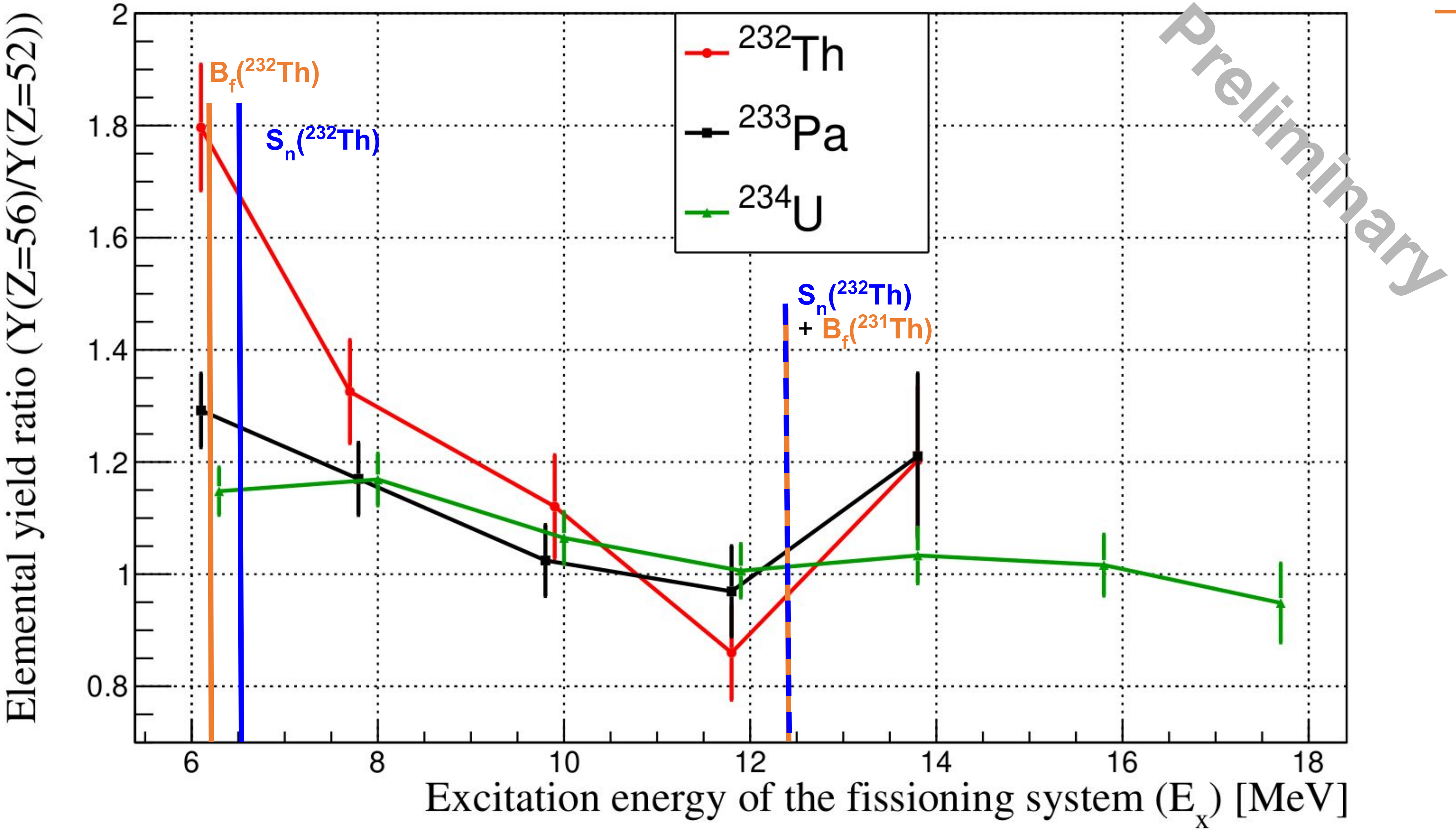

Elemental yields ratio as a function of E*

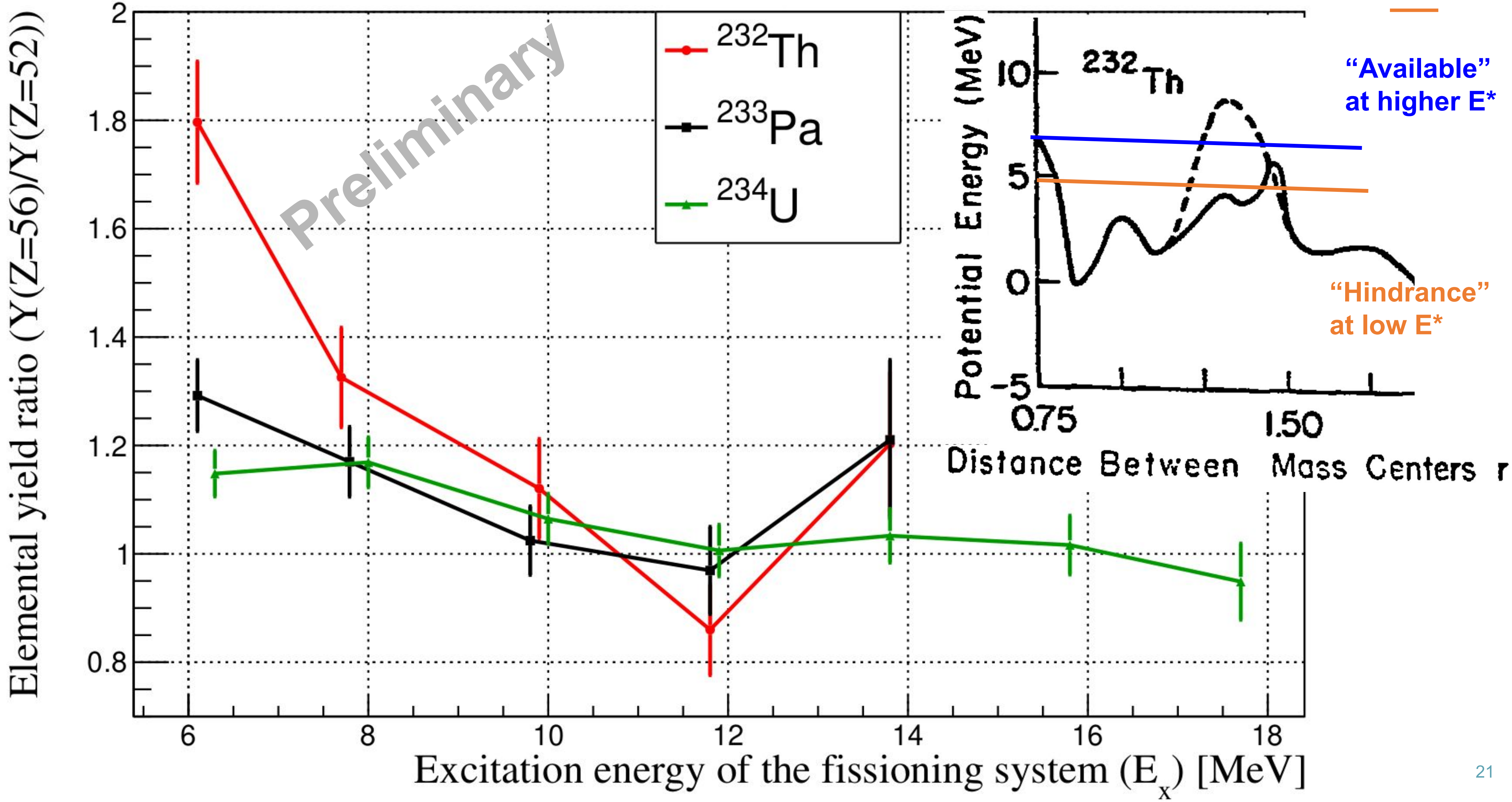

THANK YOU

Thanks to VAMOS group and collaborators from e849 experiment

Back up slides

Neutron excess of ^{234}U as a function of E*

GANIL

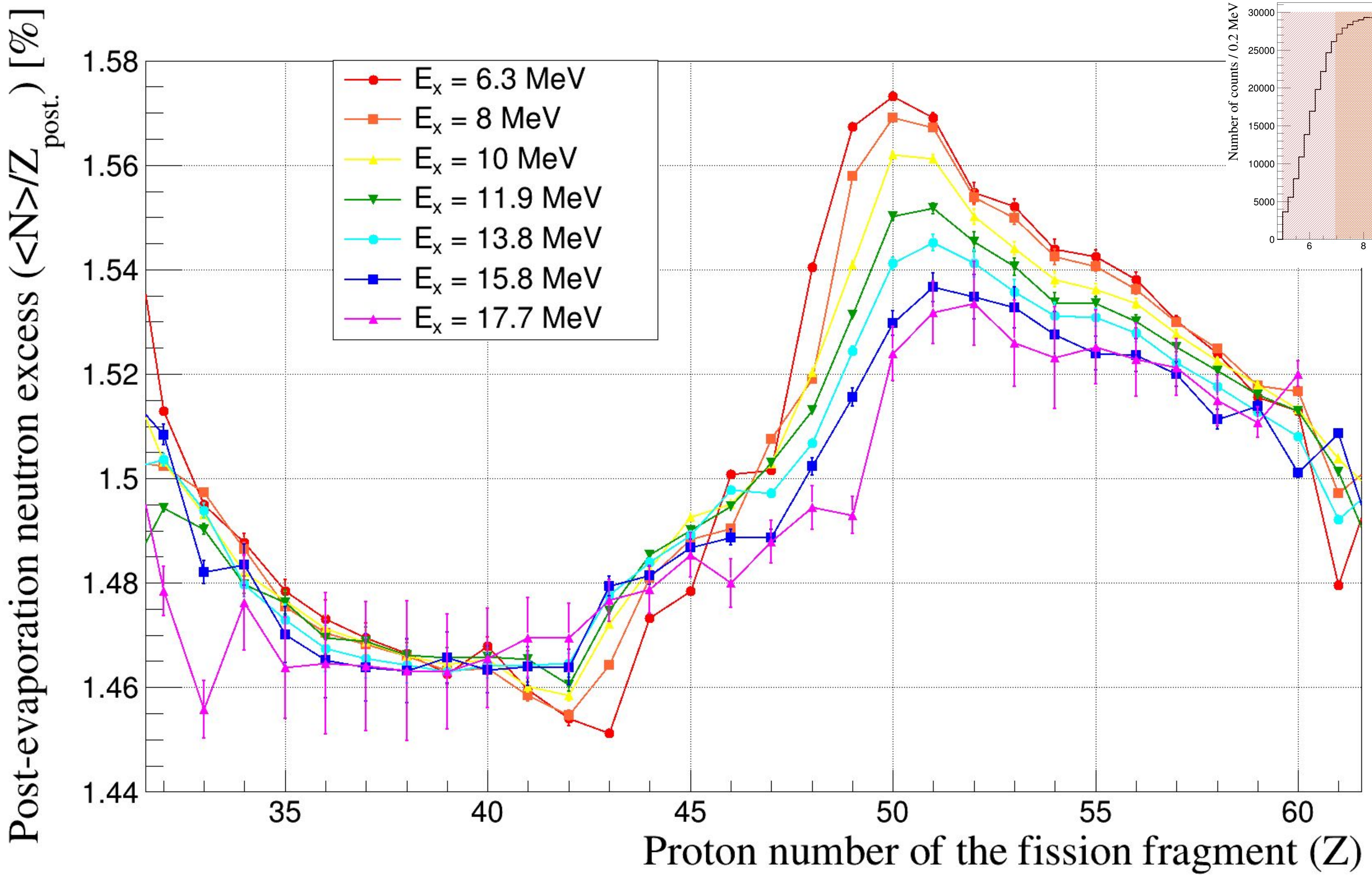

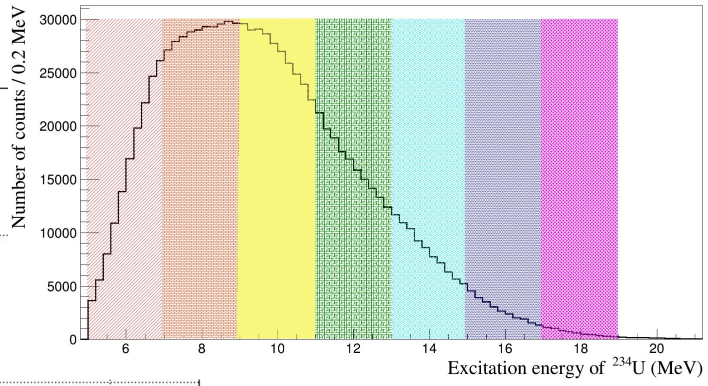

Elemental yields of ^{230}Th

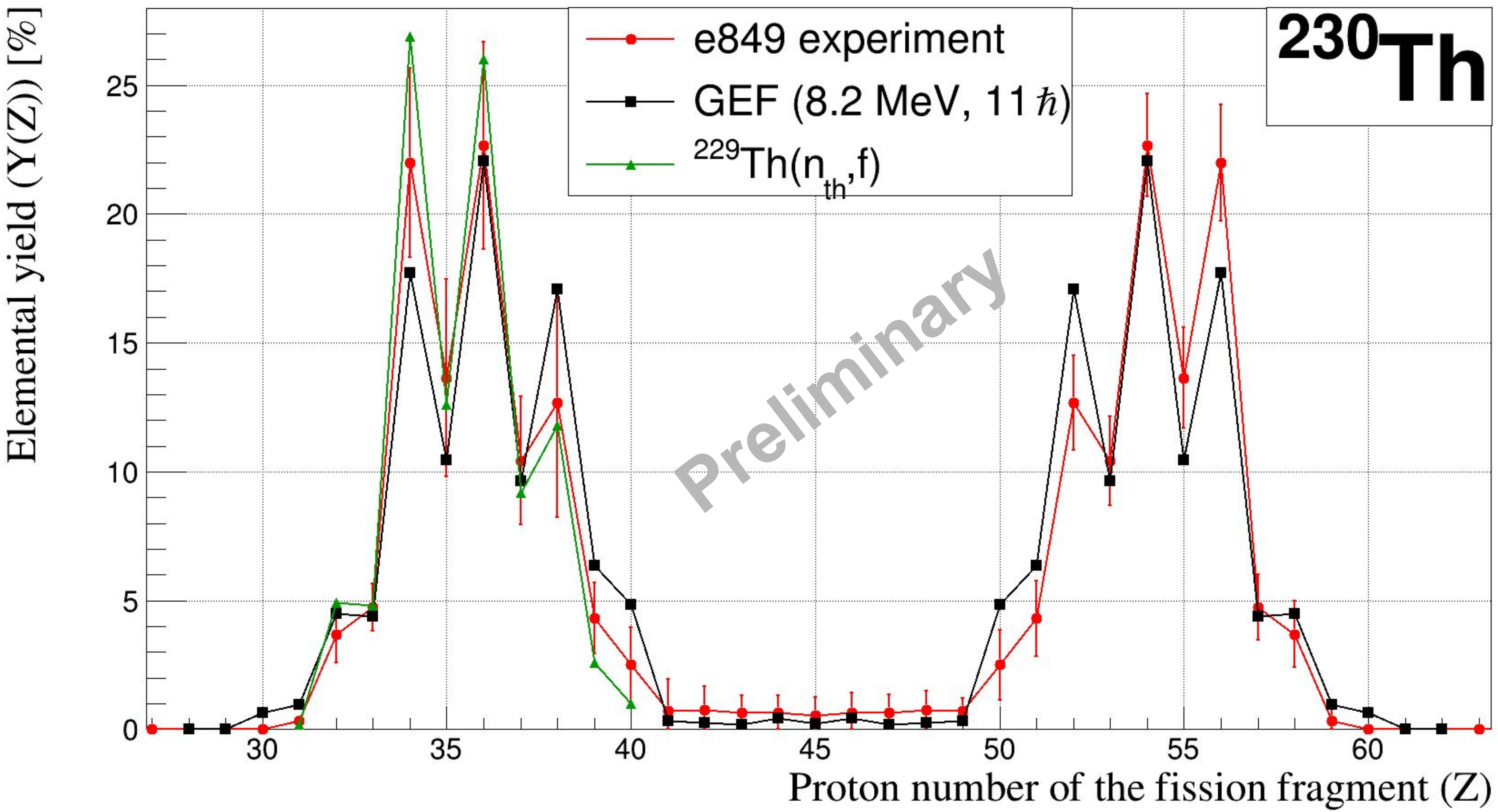

Neutron yields of ^{230}Th

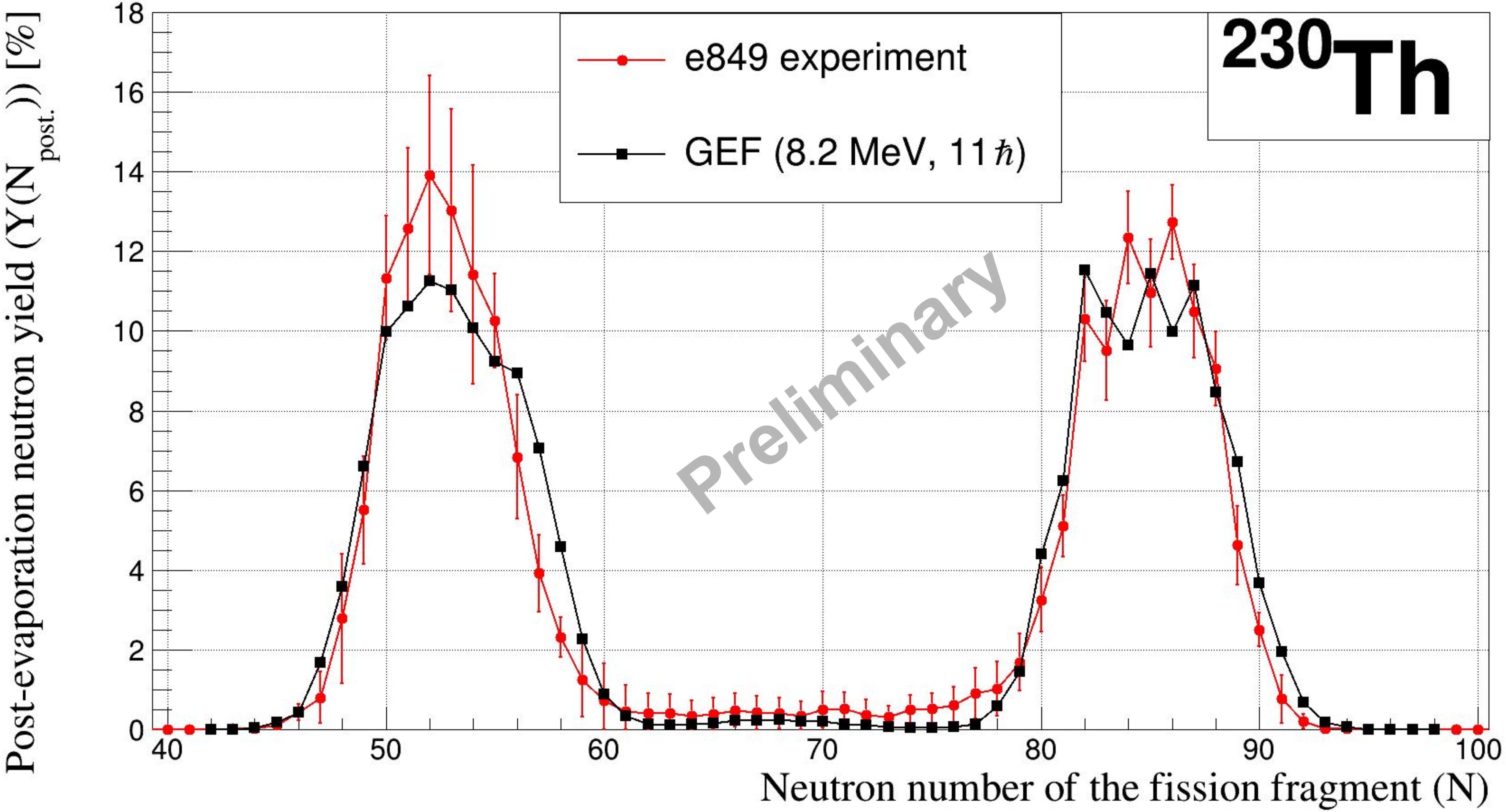

Neutron yields of ^{232}Th

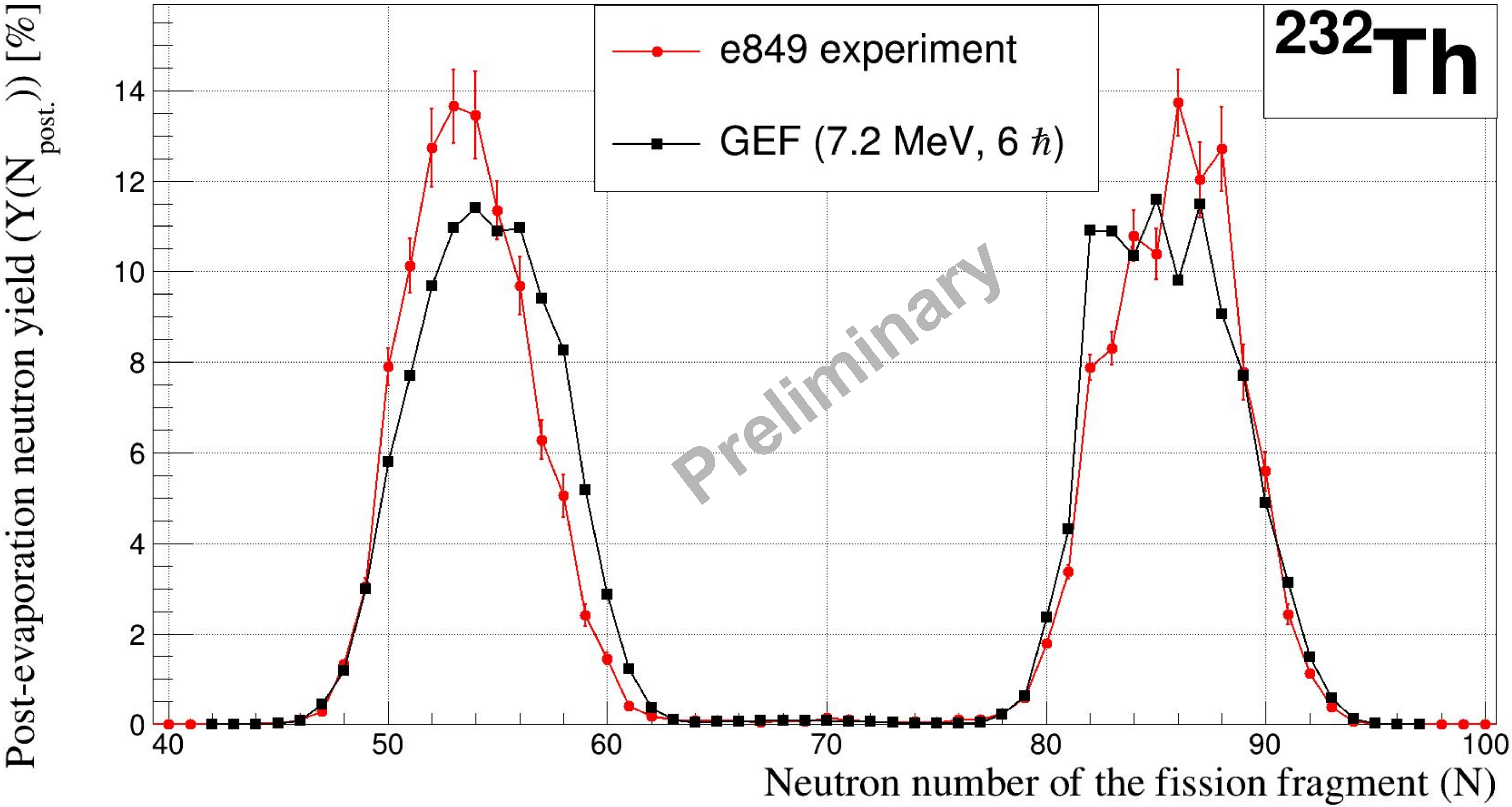

Neutron yields of ^{233}Pa

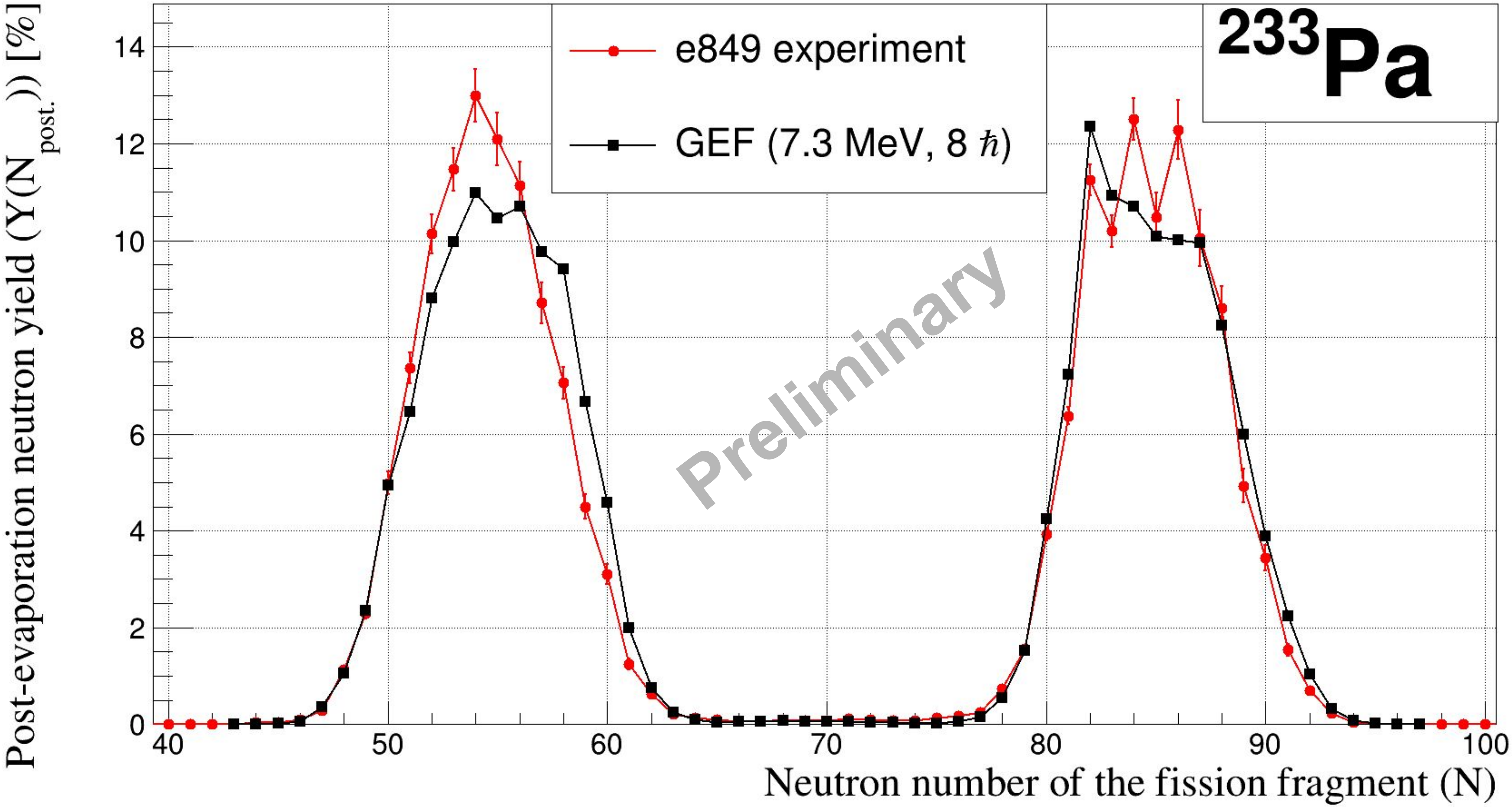

Neutron yields of ^{234}U

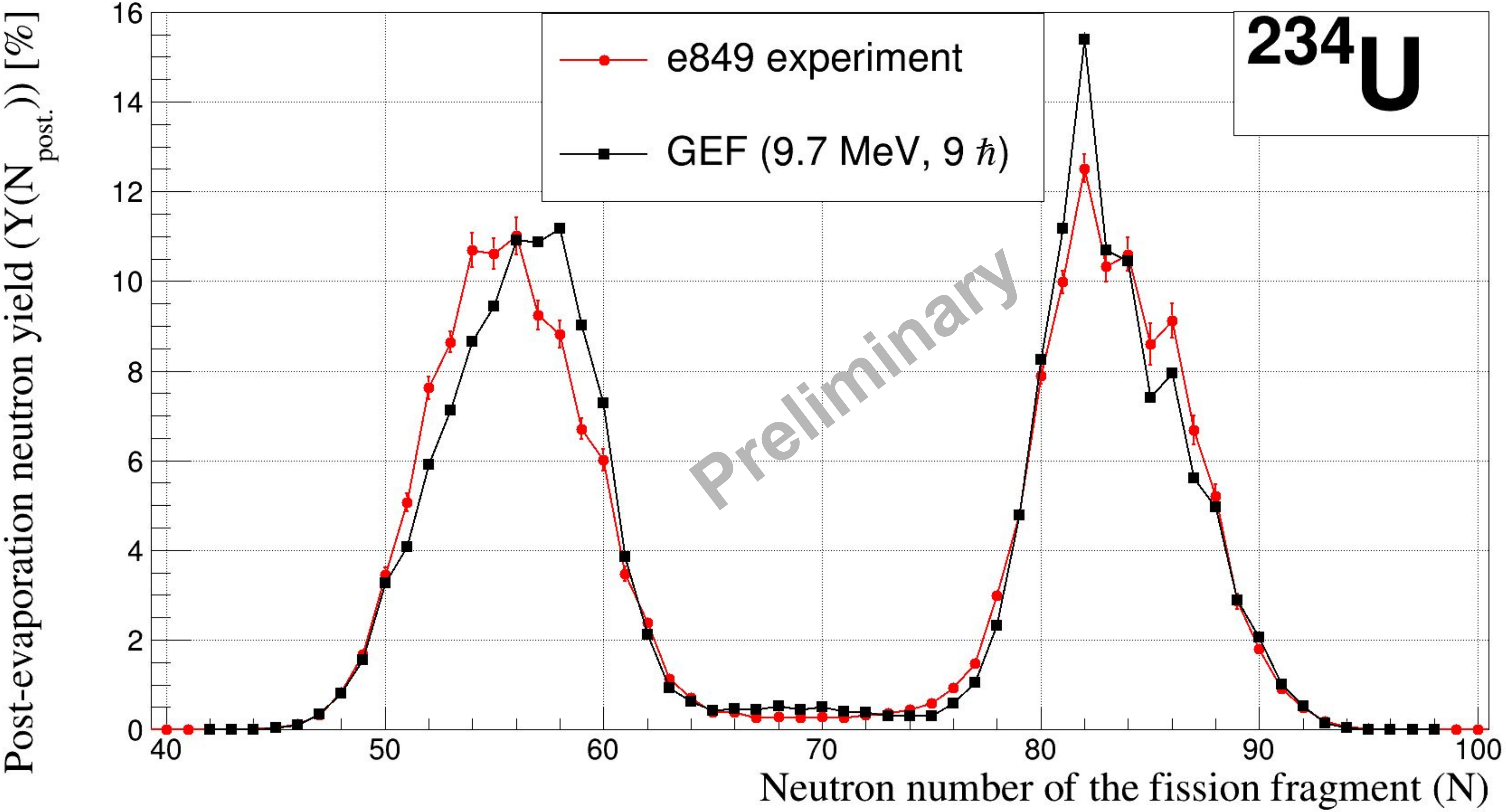

Mass yields of ^{236}U

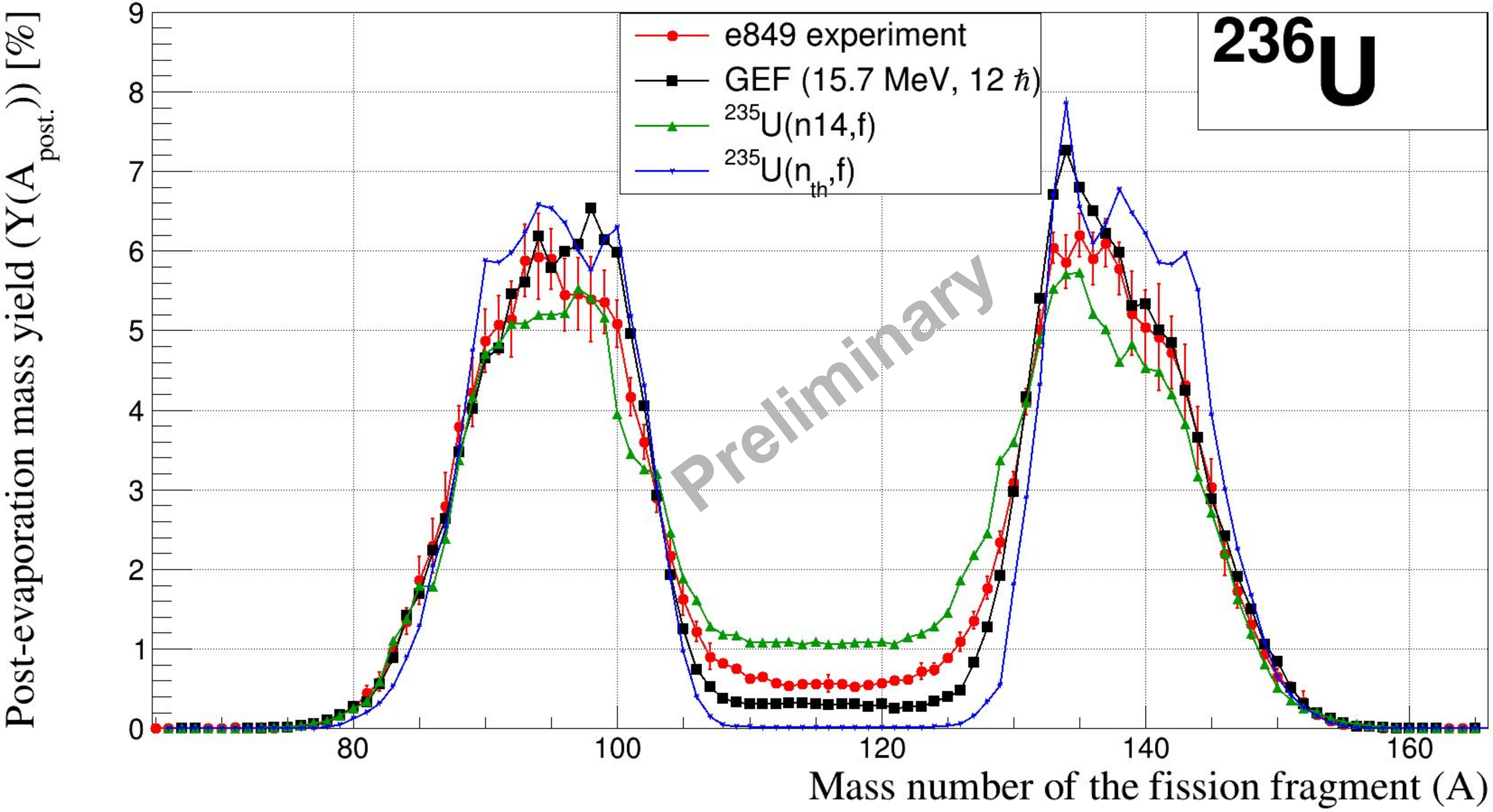

Entrance channel information

GANIL

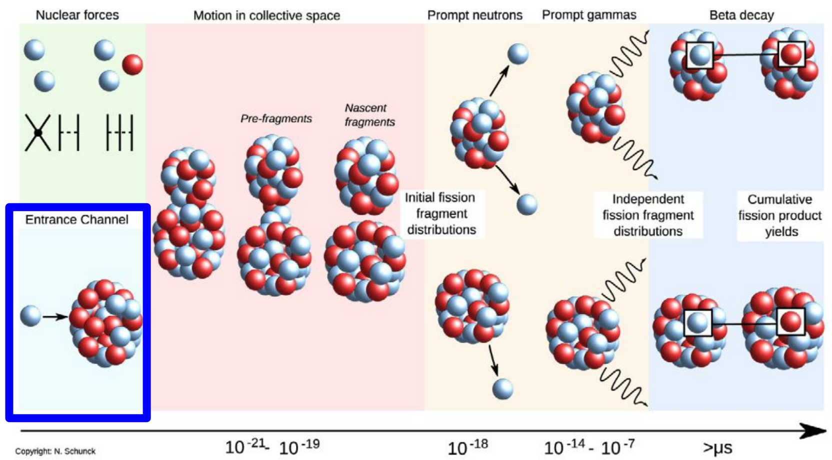

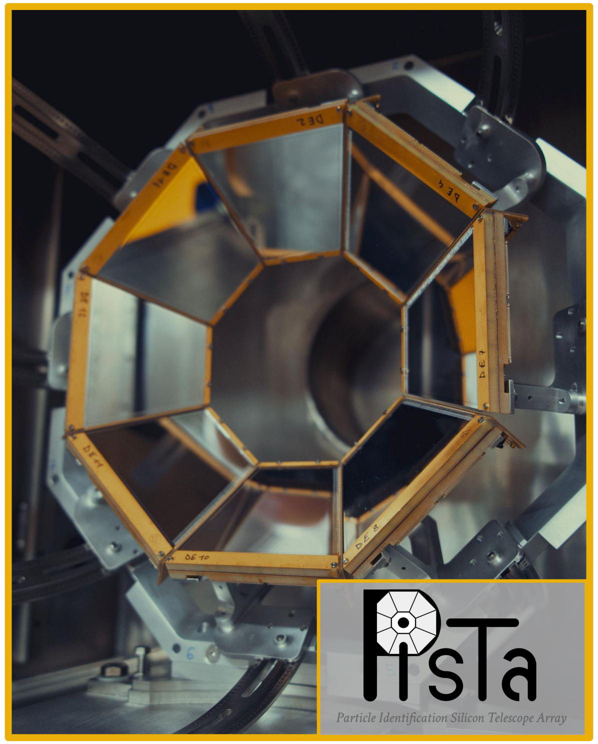

1) What is the fissioning system that was formed (Z,A)?
2) **What is the probability of fissioning for a given excitation energy?**

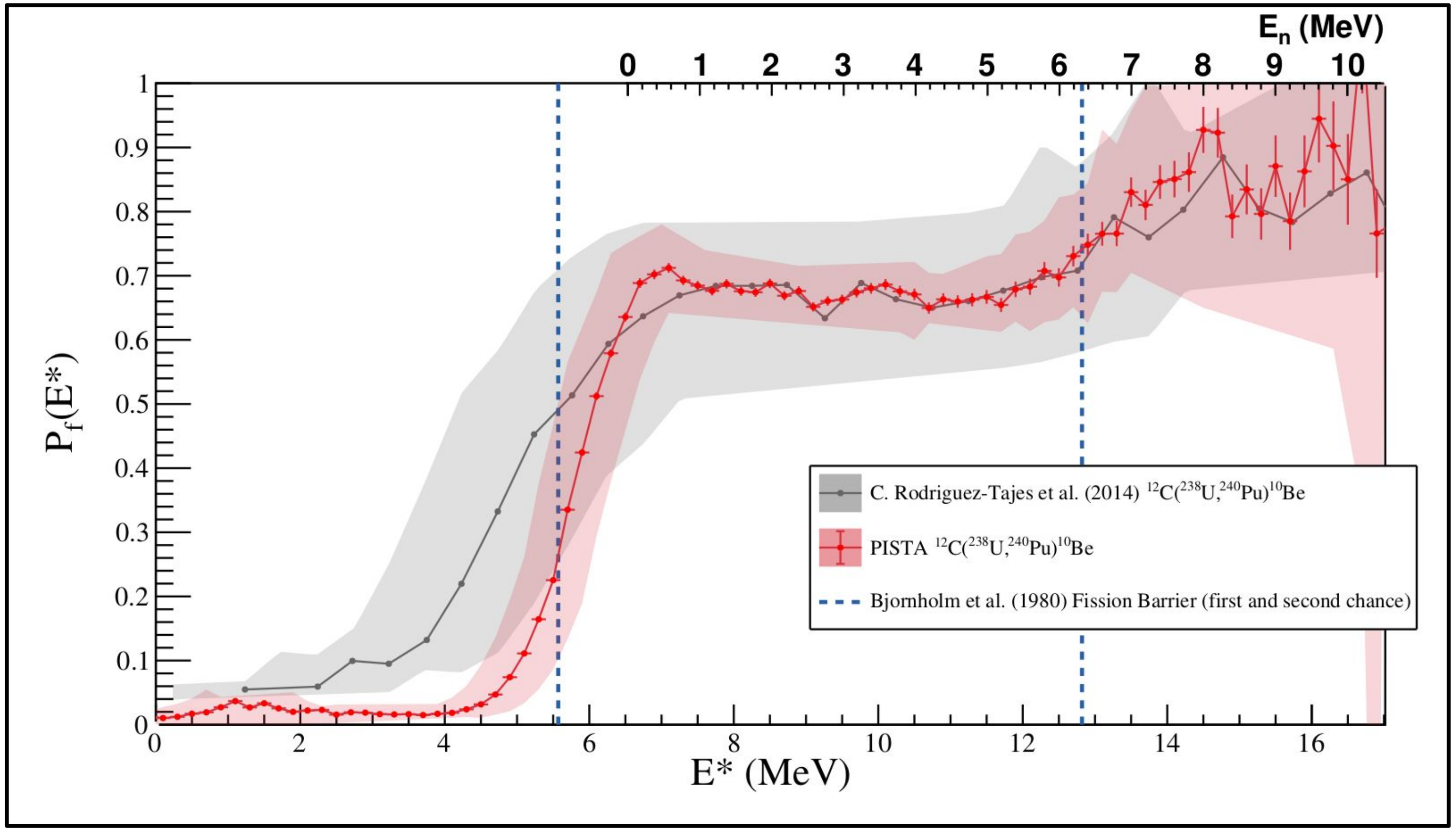

PhD thesis of Lucas Bégué-Guillou

Entrance channel information

1) What is the fissioning system that was formed (Z,A)
2) What is the excitation energy (E*)
3) **What is the probability of fissioning for a given excitation energy?**

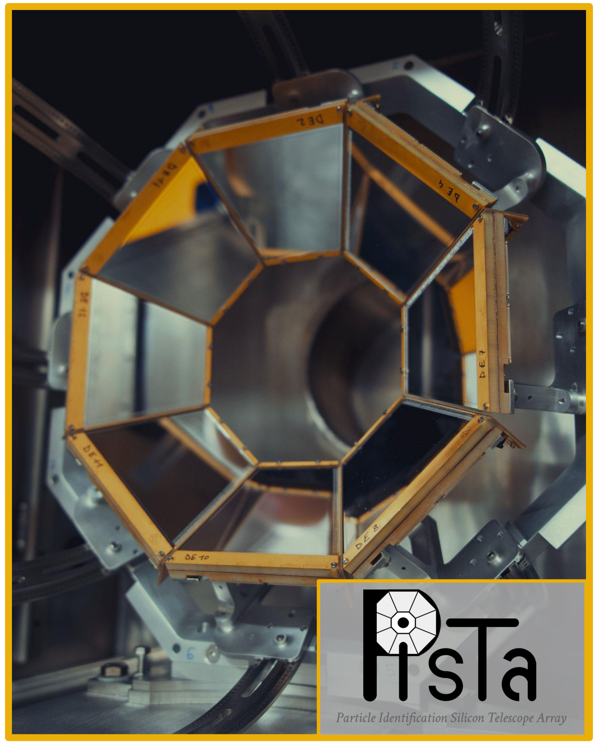

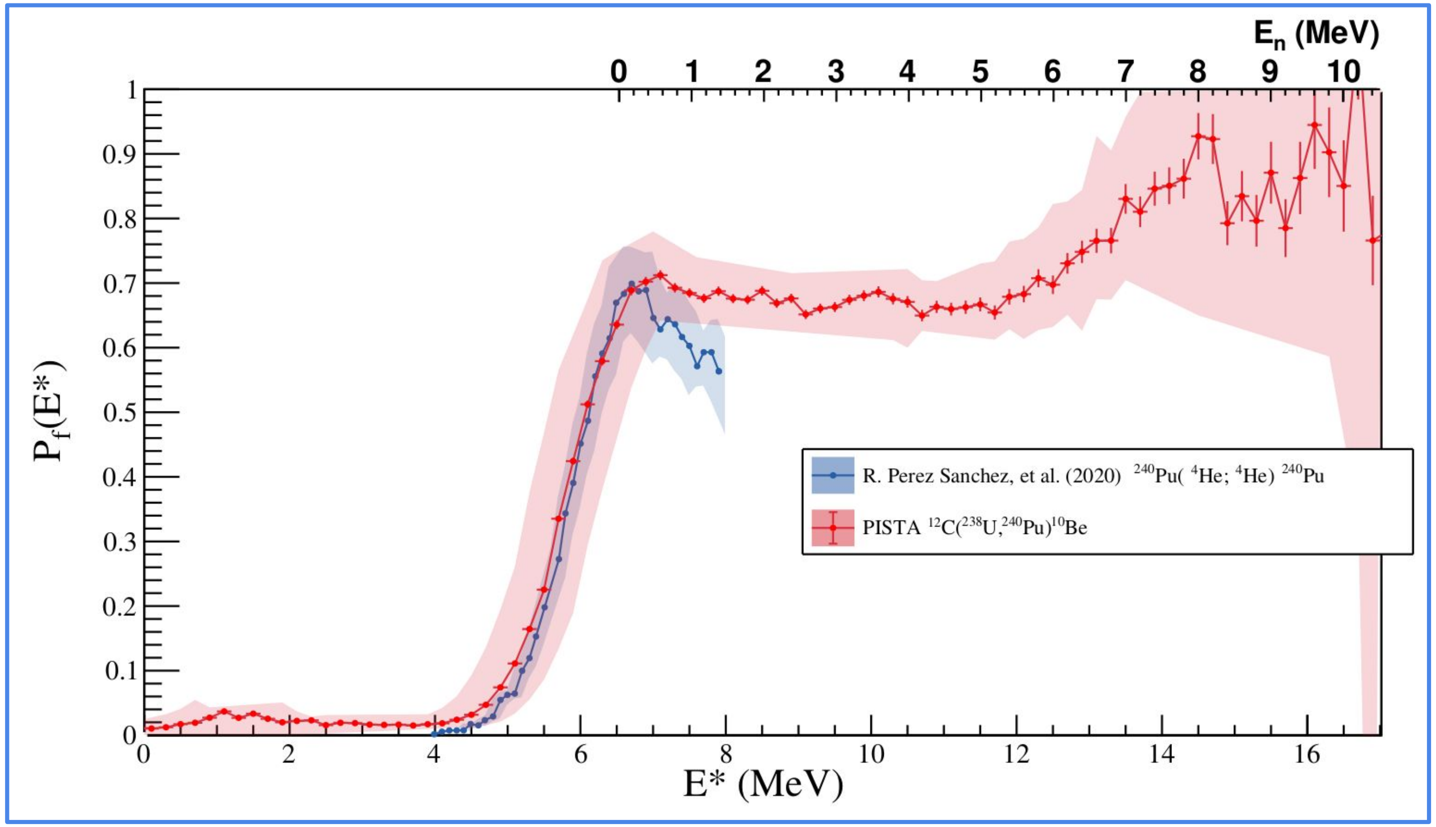

PhD thesis of Lucas Bégué-Guillou ($^{238}U + ^{12}C$)

Excitation energy distributions

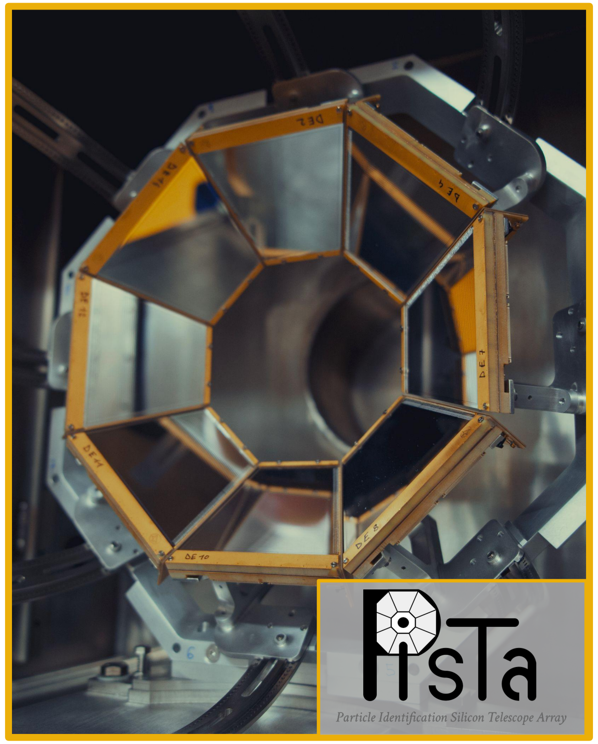

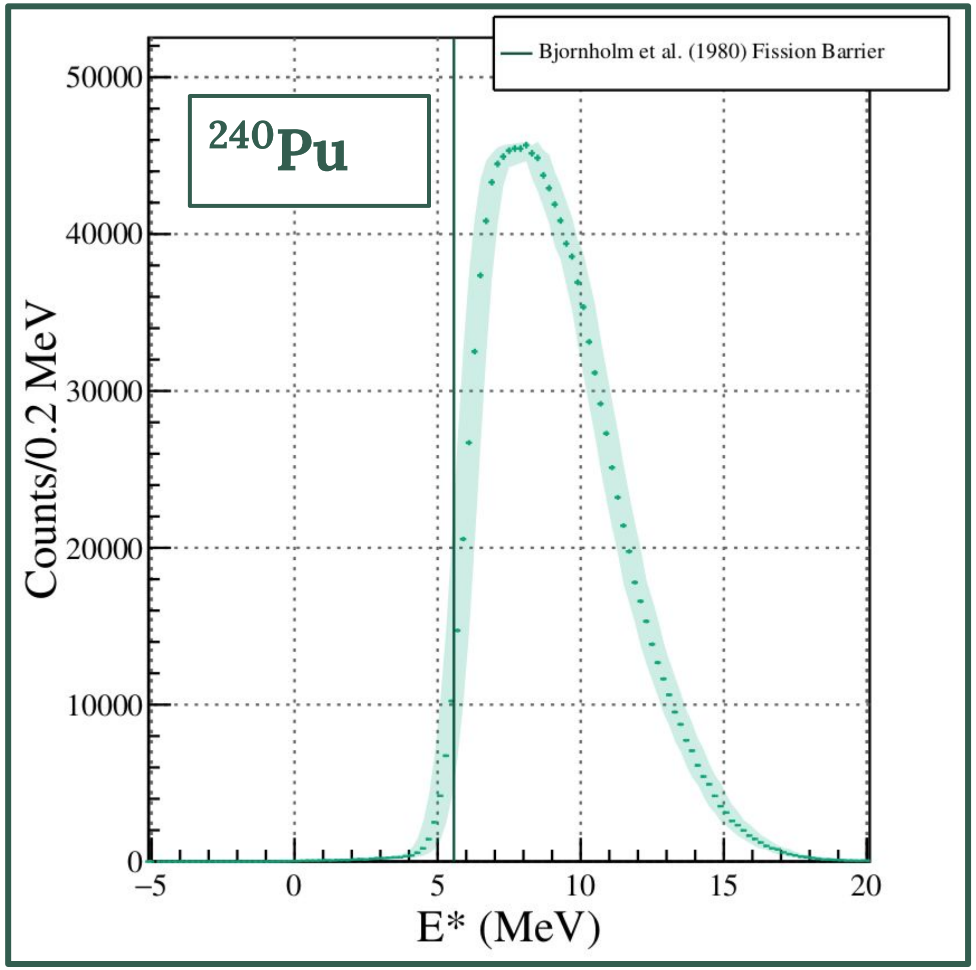

PhD thesis of Lucas Bégué-Guillou (^{238}U + ^{12}C)

Experimental setup: VAMOS++

Concept basis

Simulations of trajectories propagating particles through the spectrometer from the target until the focal plane.

Particles with **different Bρ and entrance coordinates** ($\vec{r}_t$,θ_t ,φ_t) will travel a **different path (l)** and arrive at **different position** (x_f ,θ_f) at the Focal Plane (FP)

[7] Rejmund, M., & Lemasson, A. (2025). Seven-dimensional trajectory reconstruction for VAMOS++. Nuclear Instruments and Methods in Physics Research Section A: Accelerators, Spectrometers, Detectors and Associated Equipment, 1076, 170445.

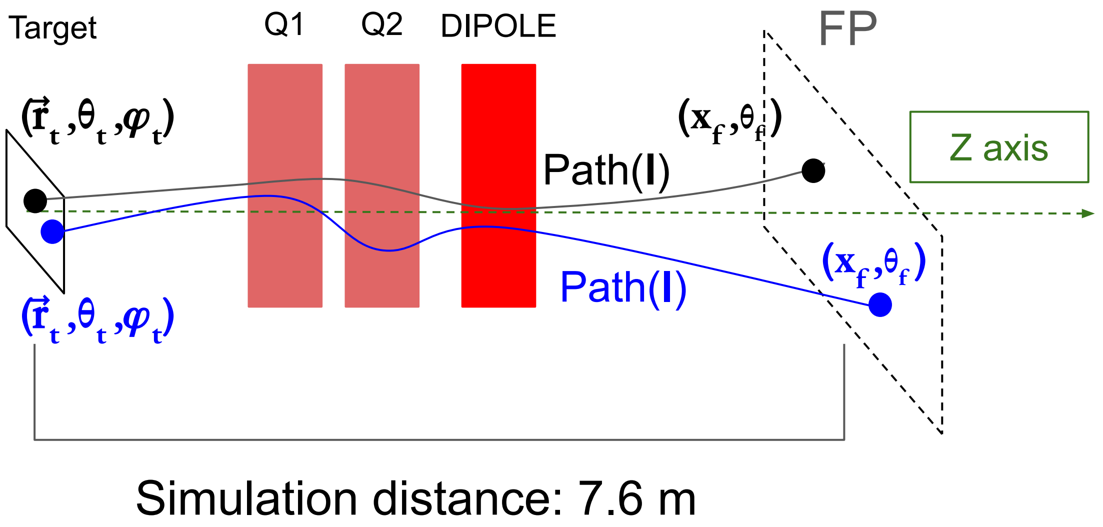

Experimental setup: VAMOS++

Concept basis

Simulations of trajectories propagating particles through the spectrometer from the target until the focal plane.

Particles with **different Bϱ and entrance coordinates** ($\vec{r}_t$,θ_t ,φ_t) will travel a **different path (l)** and arrive at **different position** (x_f ,θ_f) at the Focal Plane (FP)

[7] Rejmund, M., & Lemasson, A. (2025). Seven-dimensional trajectory reconstruction for VAMOS++. Nuclear Instruments and Methods in Physics Research Section A: Accelerators, Spectrometers, Detectors and Associated Equipment, 1076, 170445.

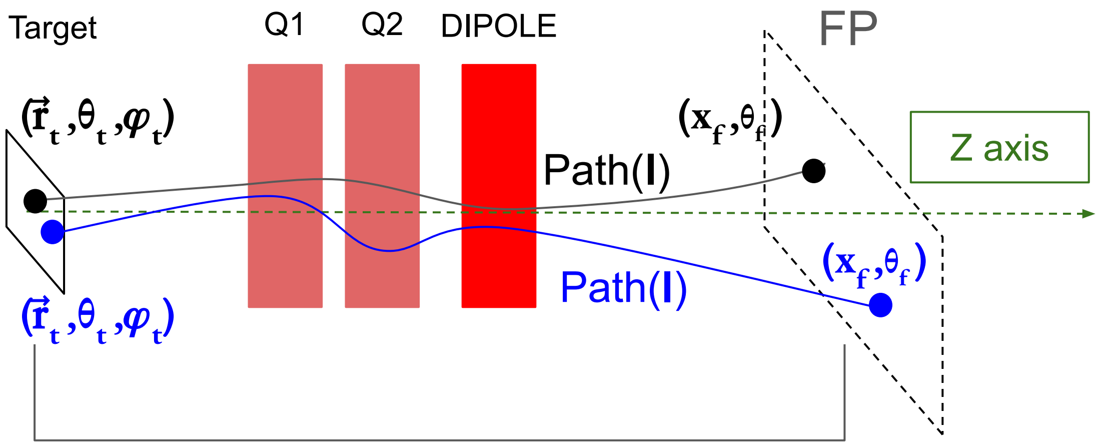

Simulation distance: 7.6 m

Experimentally

A pair of Multi-Wire Proportional counters (MWPC) at the target determine the **entrance coordinates** and **start time** (t_i)
A pair of MWPCs at the exit determine the **focal plane coordinates** and **20 stop times** (t_f)

From measured positions, we extract the **Bϱ and l** of a fragment
Combining it with the **ToF (t_f - t_i)**, we get the **velocity and M/Q**:

V = D/T => β,γ
M/Q = **Bϱ**/(3.107*β*γ)

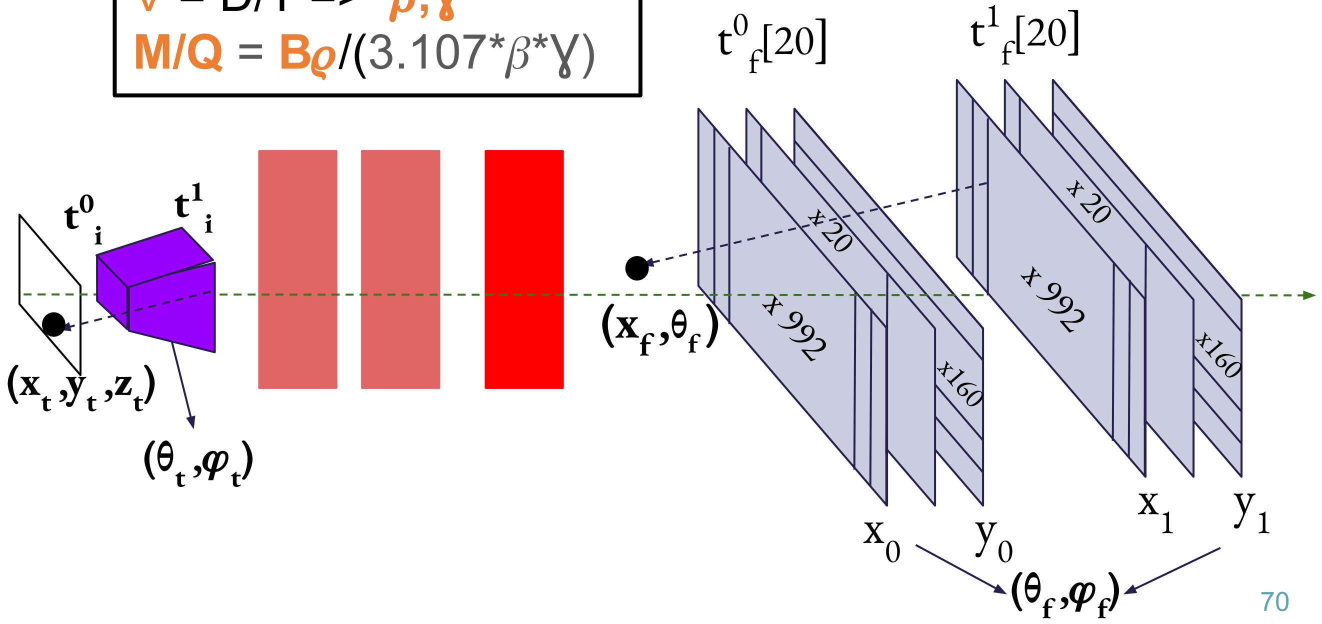

Experimental result: M/Q

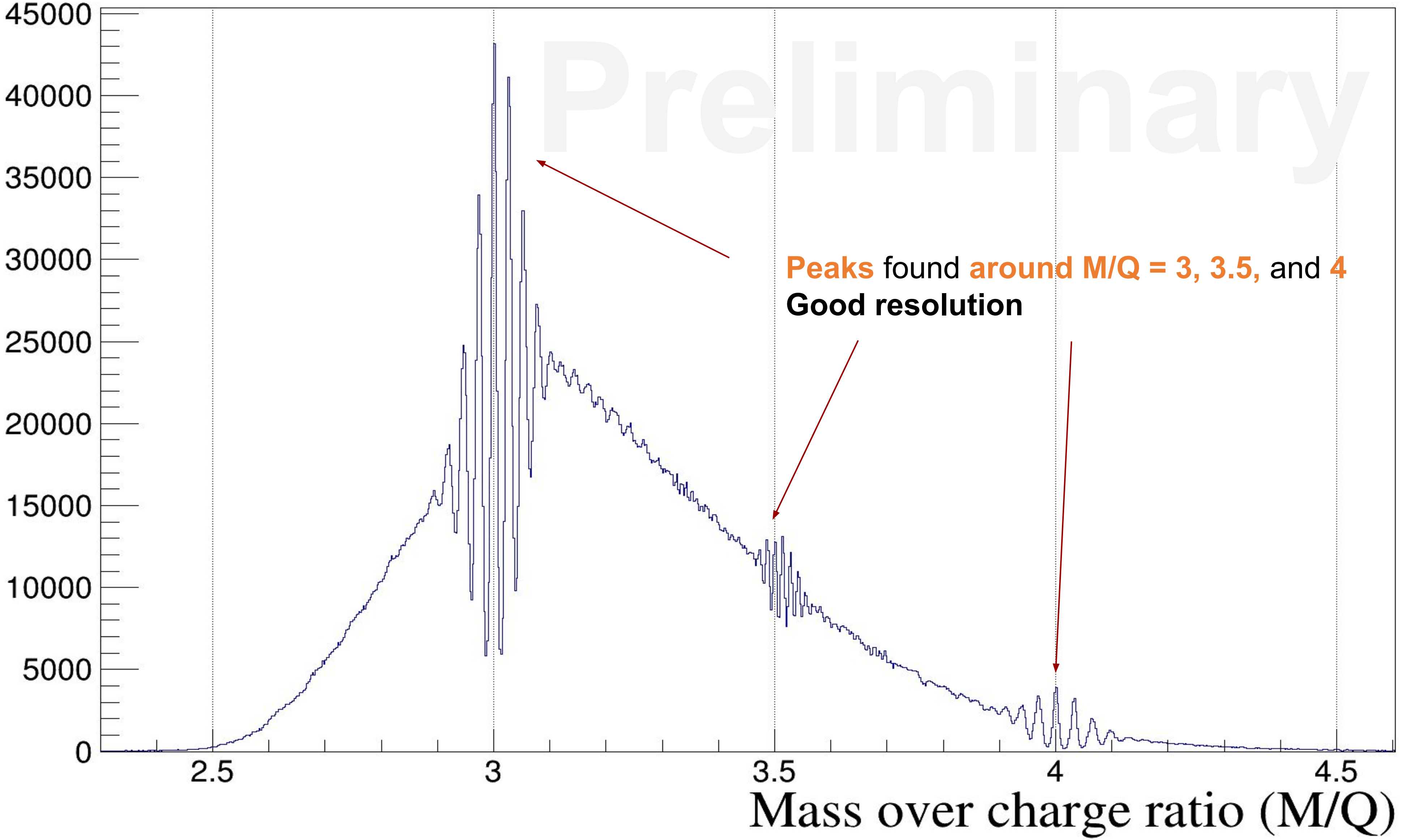

Peaks found **around M/Q = 3, 3.5,** and **4**

Good resolution

Experimental setup: Ionization Chamber (Q)

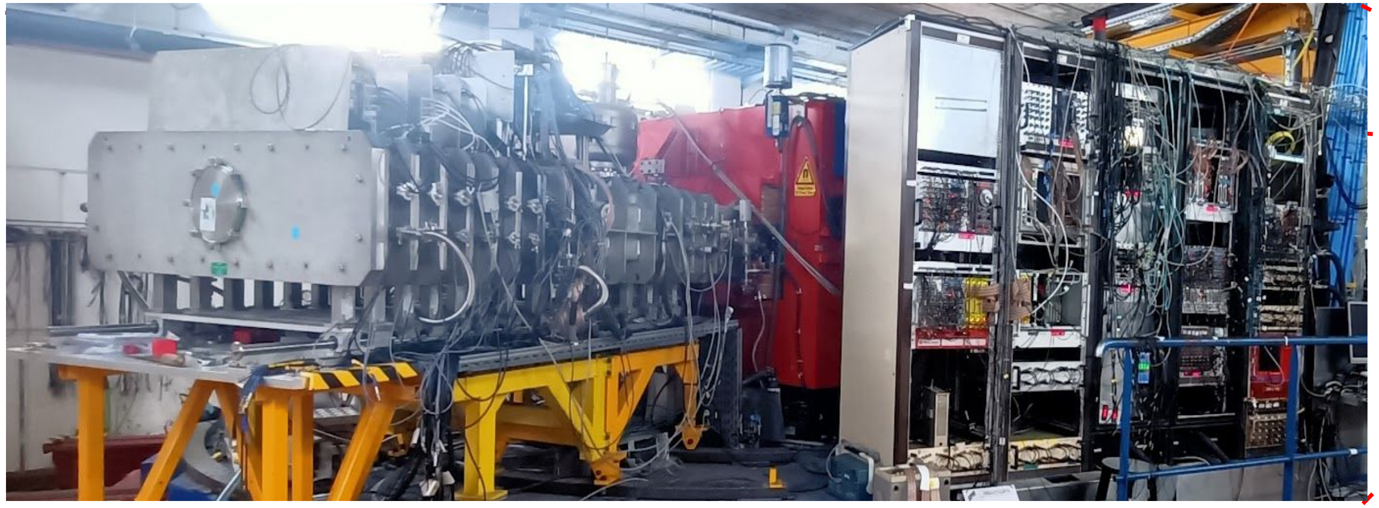

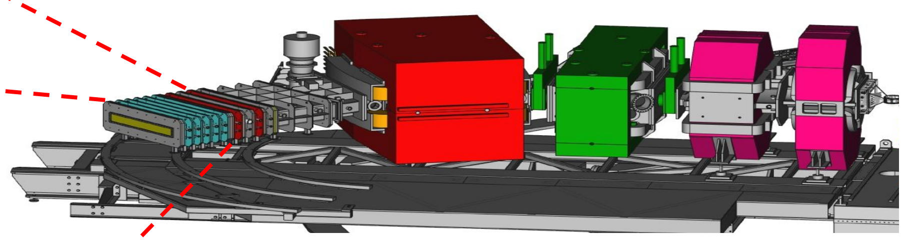

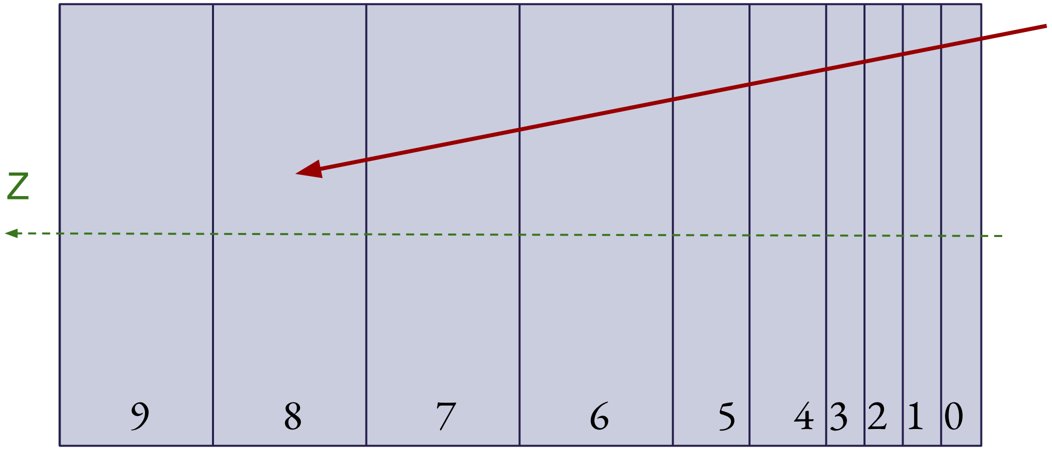

The **kinetic energy (E_{Kin})** of the fragment is proportional to the **mass** and the **velocity (γ)**

Through a **minimization method**, **scale** the contribution of **each IC** section for every time section

$E_{Kin} = \Sigma a_i * IC_i + b_0$

$M_{IC} = E_{Kin} / (\gamma_{VAMOS} - 1)$

The **M_{IC} is not enough** (~1%) for our goal :

$Q = M_{IC}/(M/Q)$

Experimental result: Q

GANIL

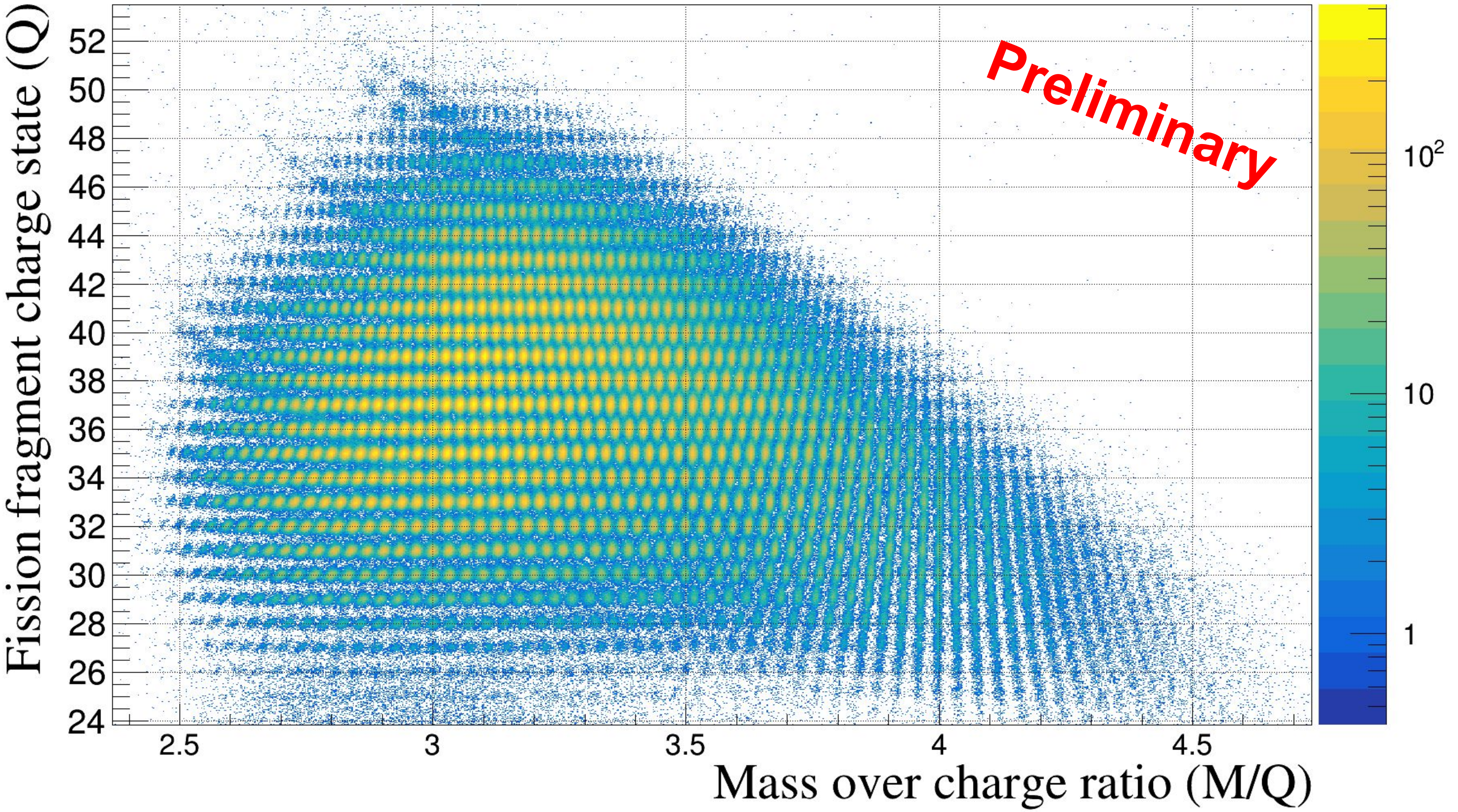

Experimental result: Q and M

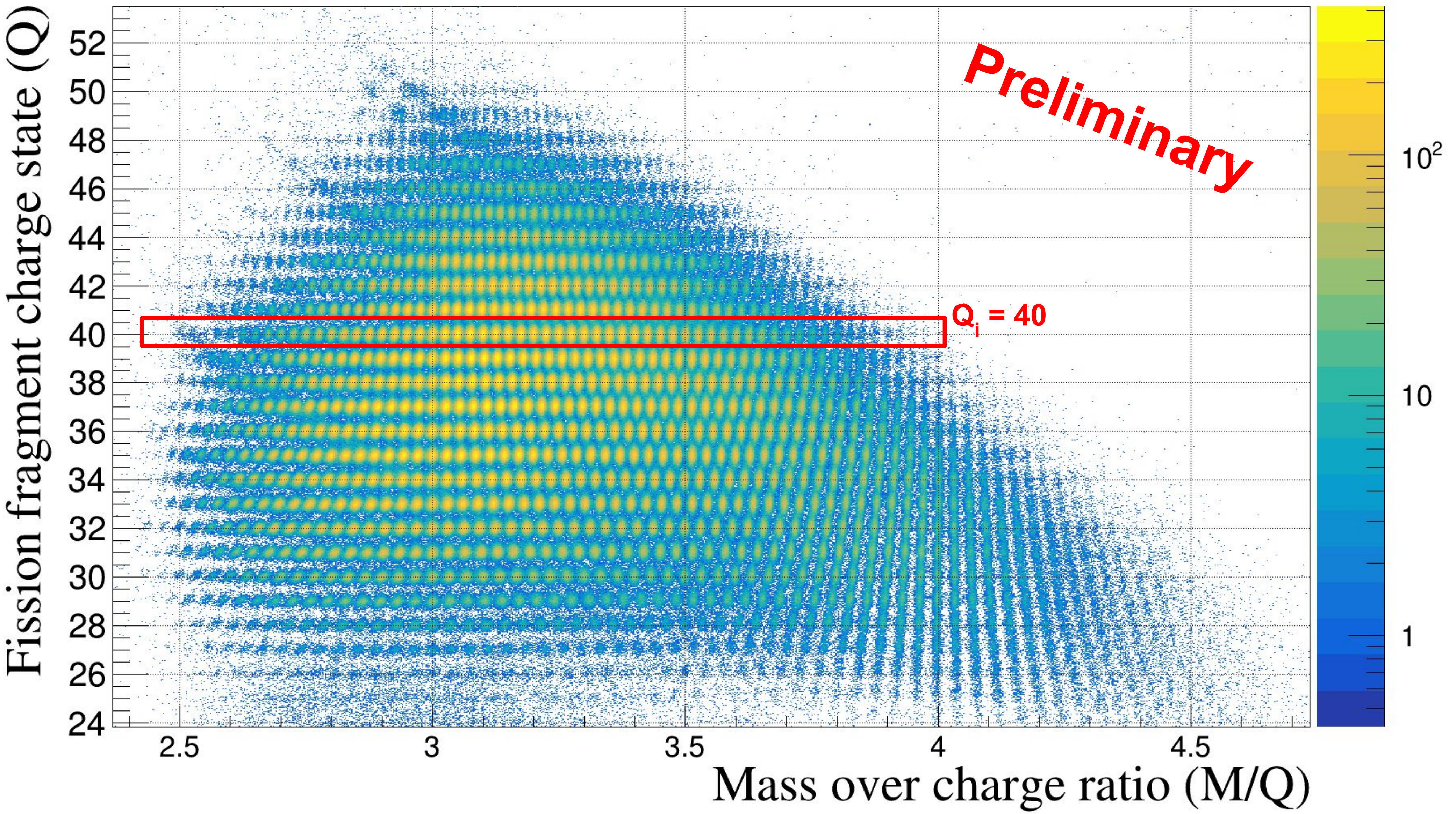

Experimental result: Q and M

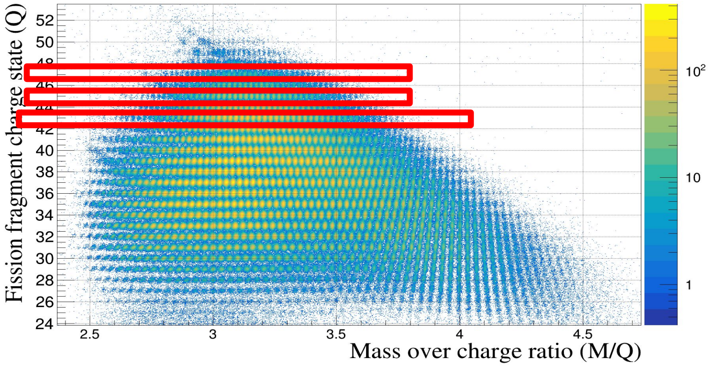

M = Q_i * M/Q

Average resolution of **ΔA/A ~** 1/234 = **4.27 ‰**

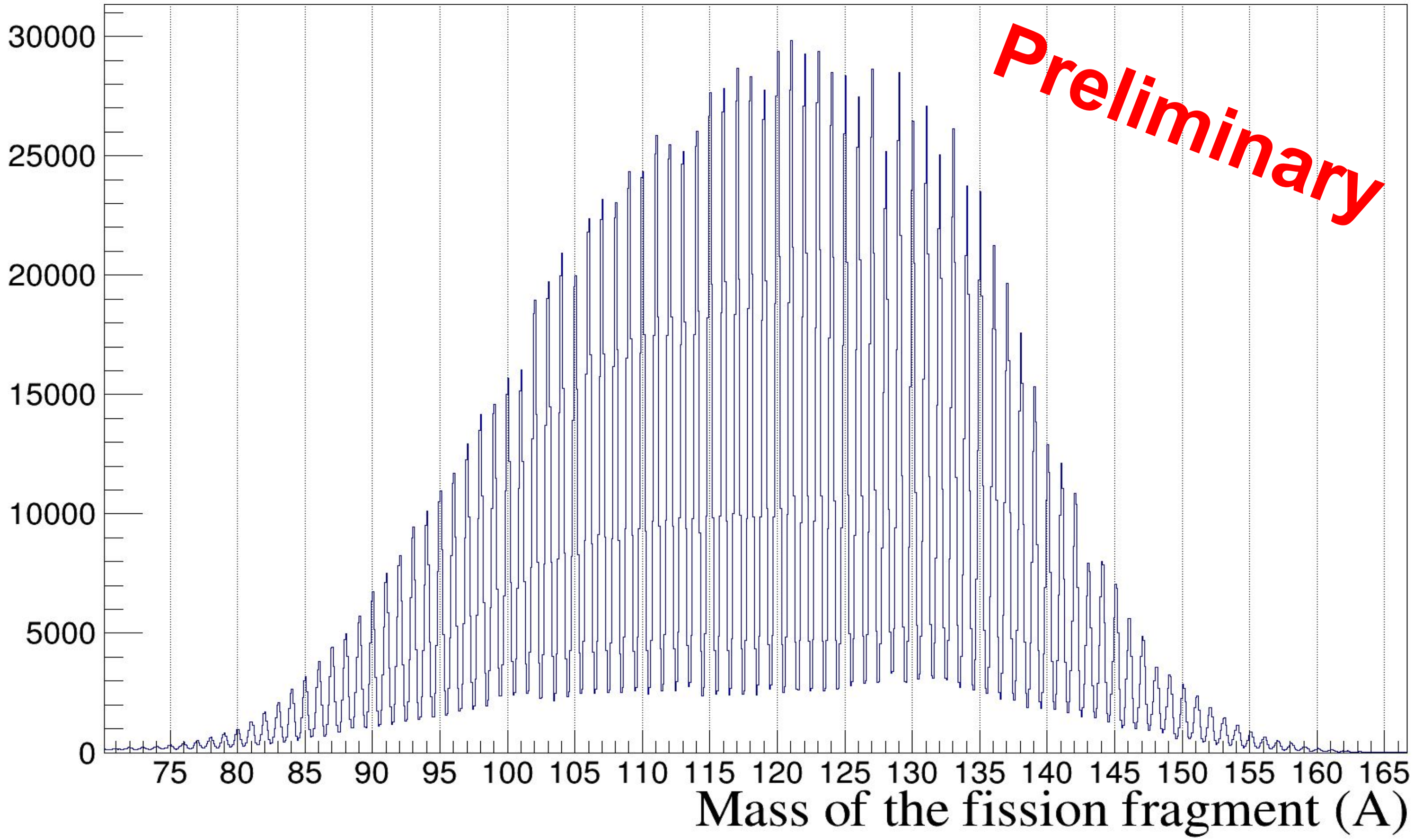

Experimental result: Q and M

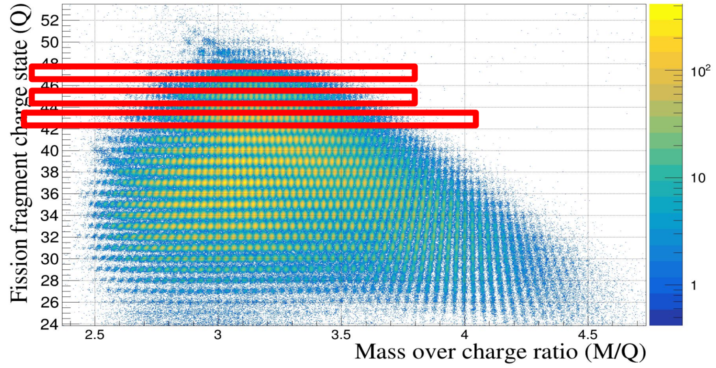

Preliminary

Mass resolution improvement thanks to the **VAMOS++ spectrometer**

M = Q_i * M/Q

Average resolution of **ΔA/A ~** 1/234 = **4.27 ‰**

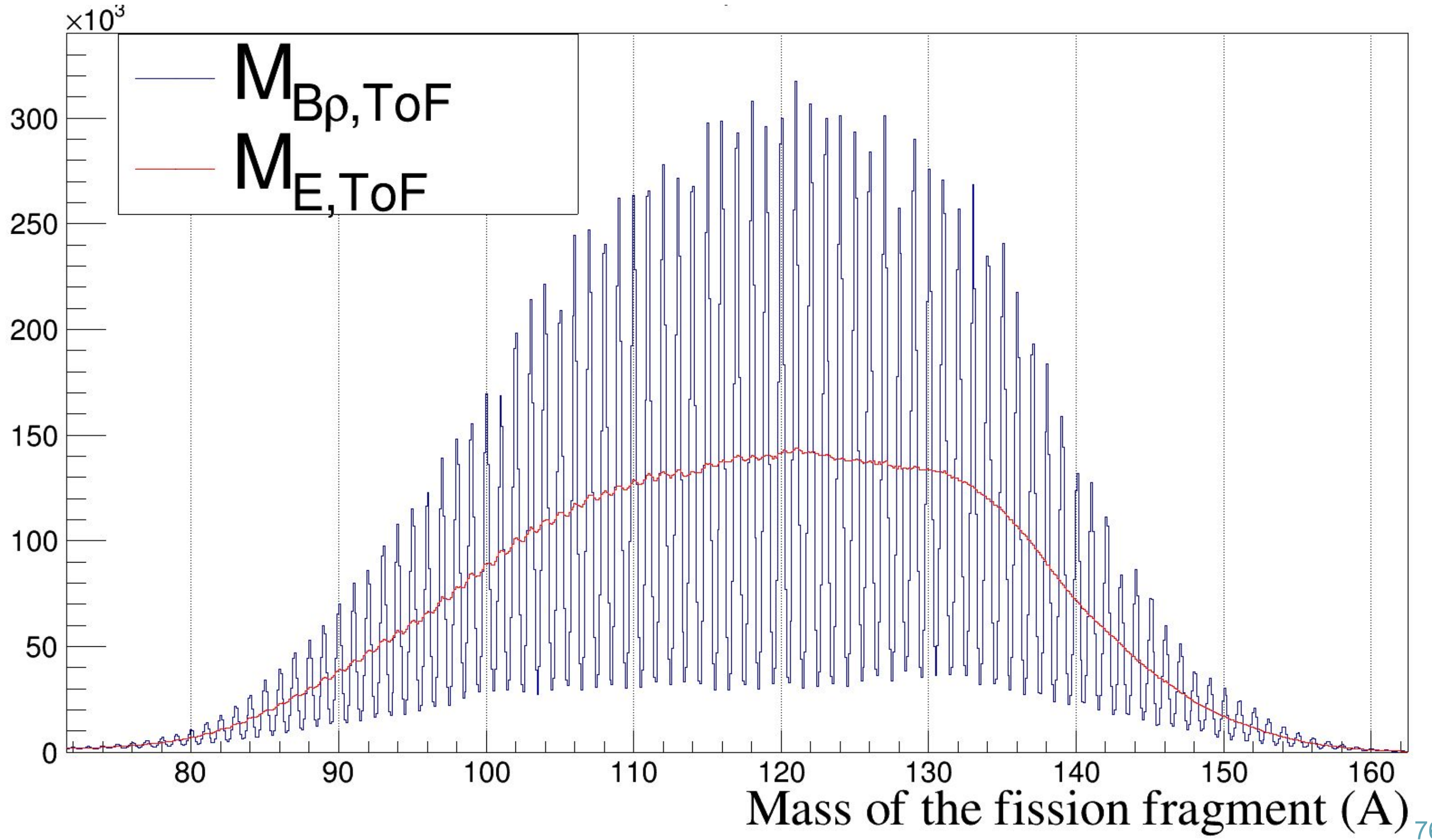

Fission fragment identification: A

GANIL

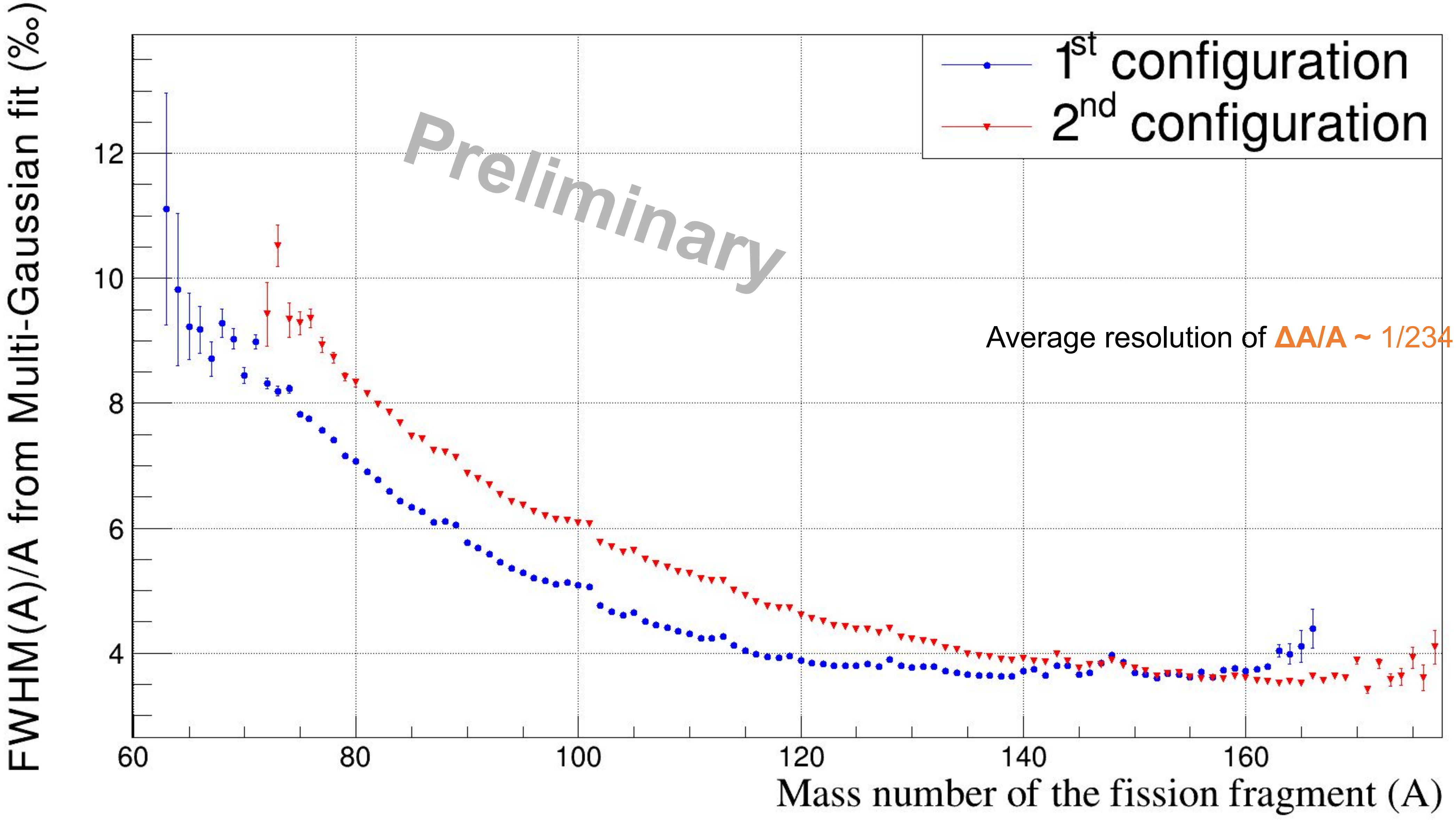

Average resolution of **ΔA/A** ~ 1/234 = **4.27 ‰**

Fission fragment identification: Z

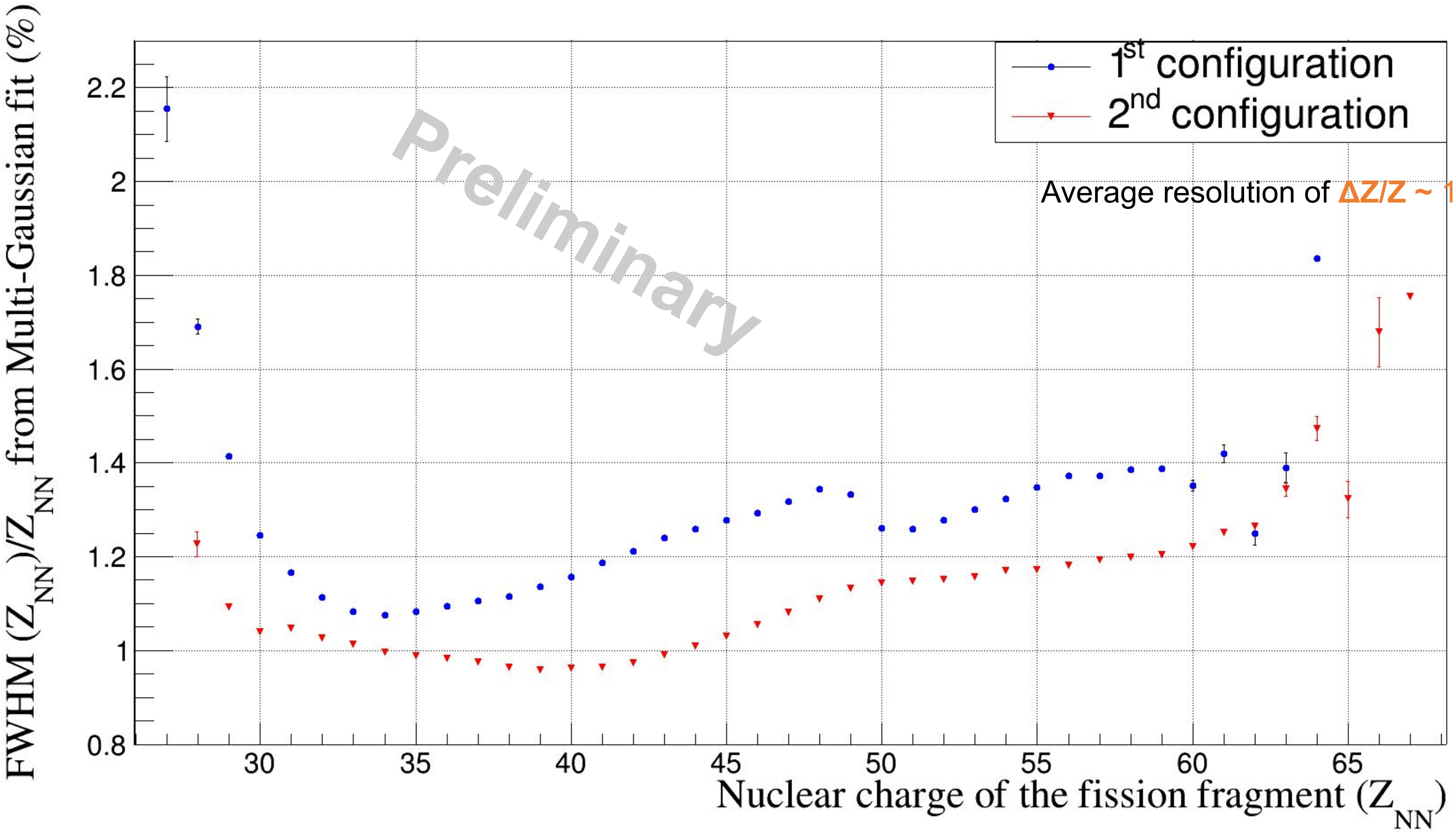

Average resolution of **ΔZ/Z ~** 1/86 = **1.16 %**

Experimental identification confirmation

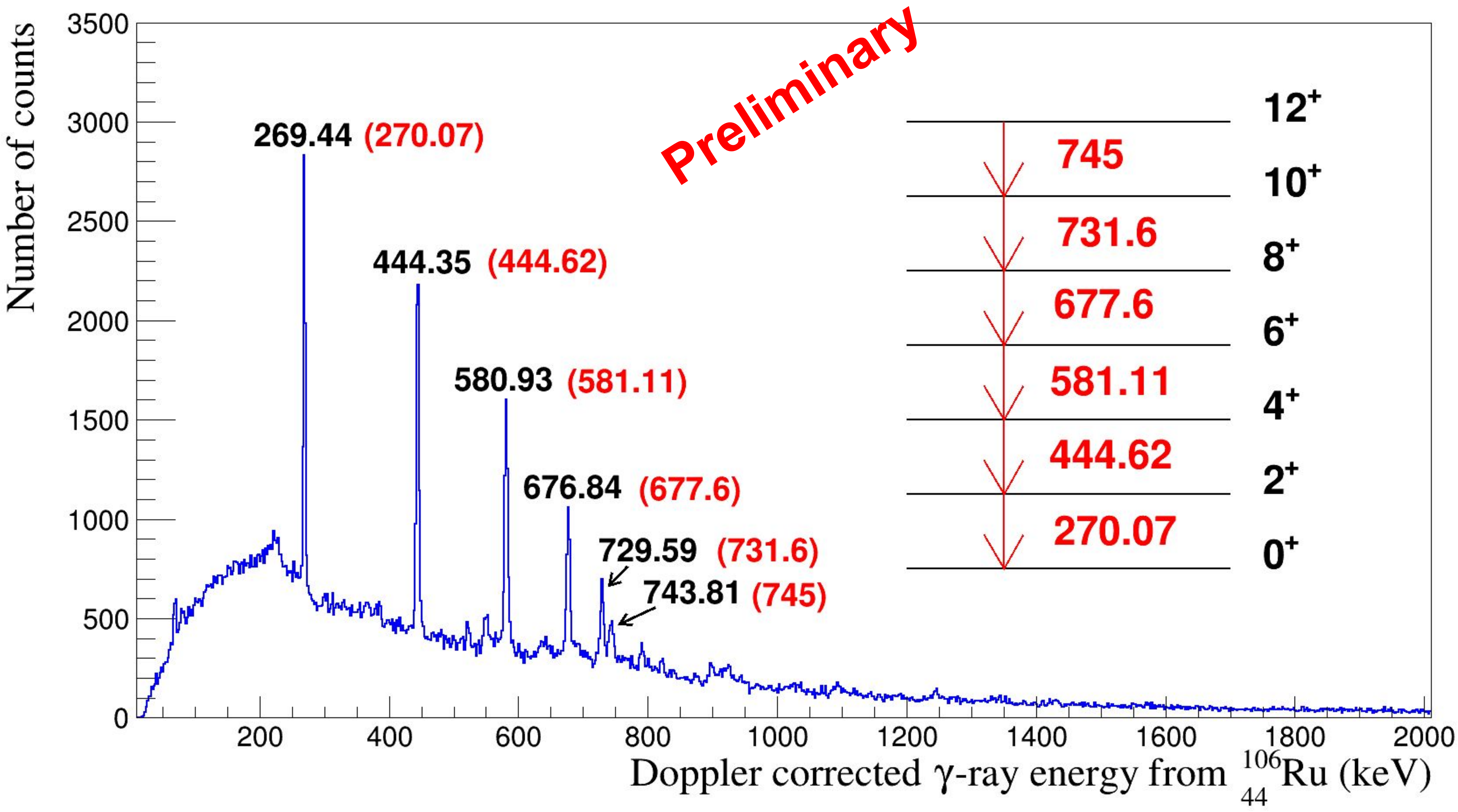

The fission process

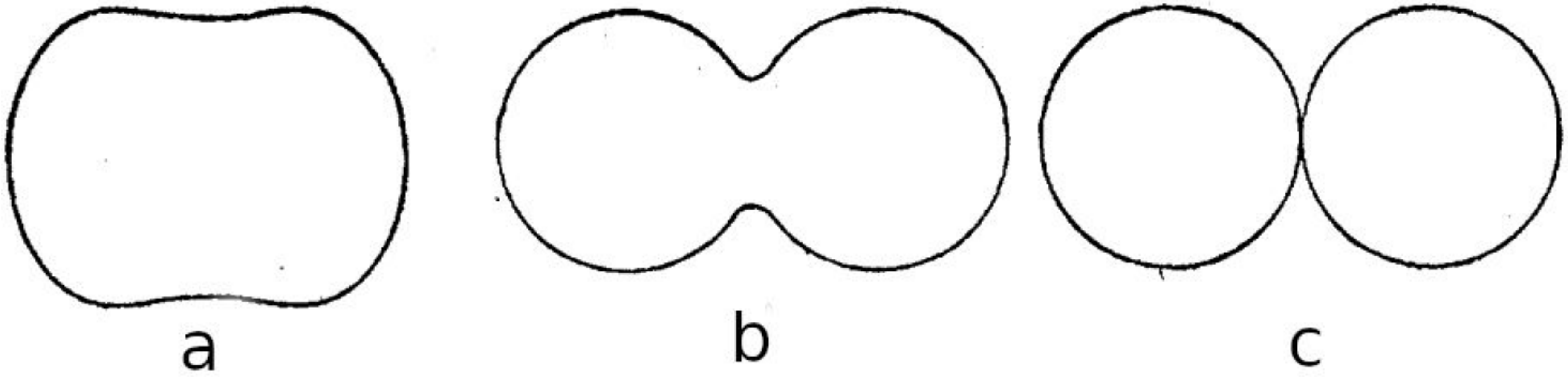

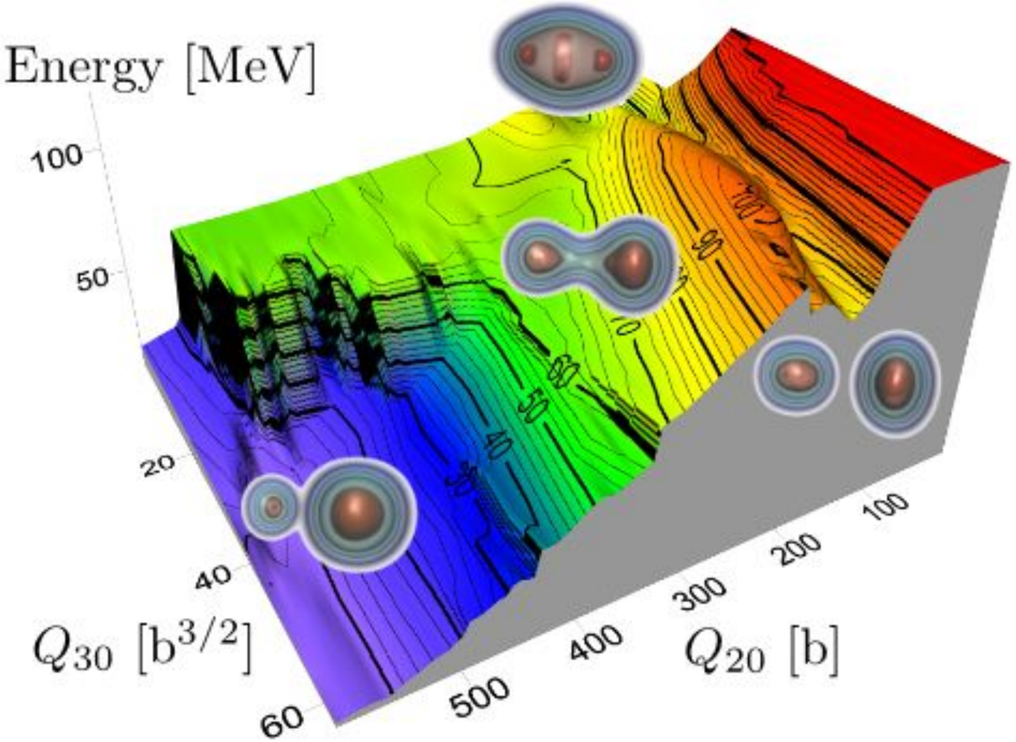

Unestable competition between surface tension (Nuclear force) and repulsion (Coulomb) leads to deformation and split of a heavy nucleus into 2 fragments

The potential energy surface (PES) represents the energy of the system at a given deformation

More **complex PES** can be calculated for **2, 3, etc. deformation parameters**

The fission process

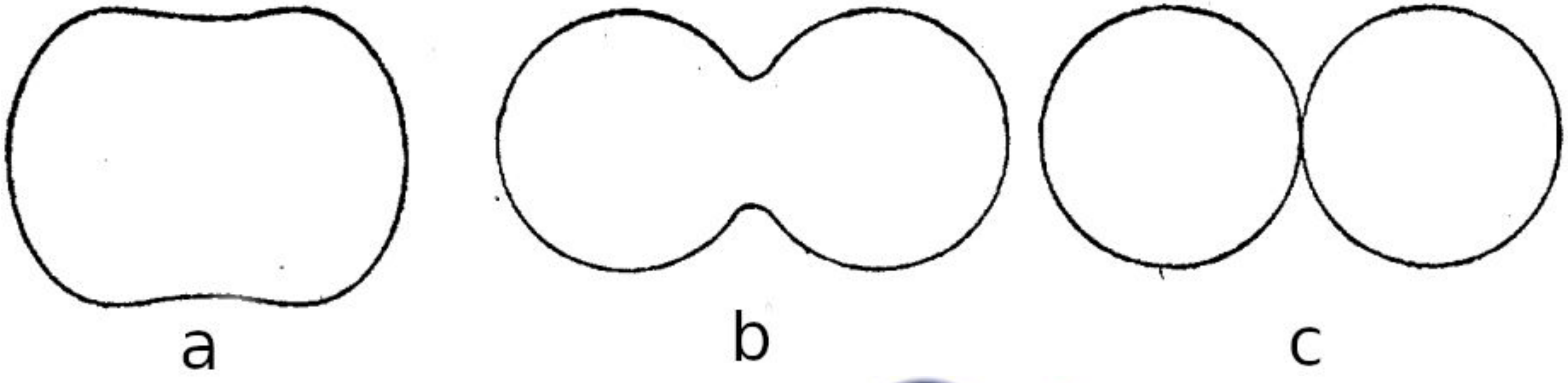

Unestable competition between surface tension (Nuclear force) and repulsion (Coulomb) leads to deformation and split of a heavy nucleus into 2 fragments

The potential energy surface (PES) represents the energy of the system at a given deformation

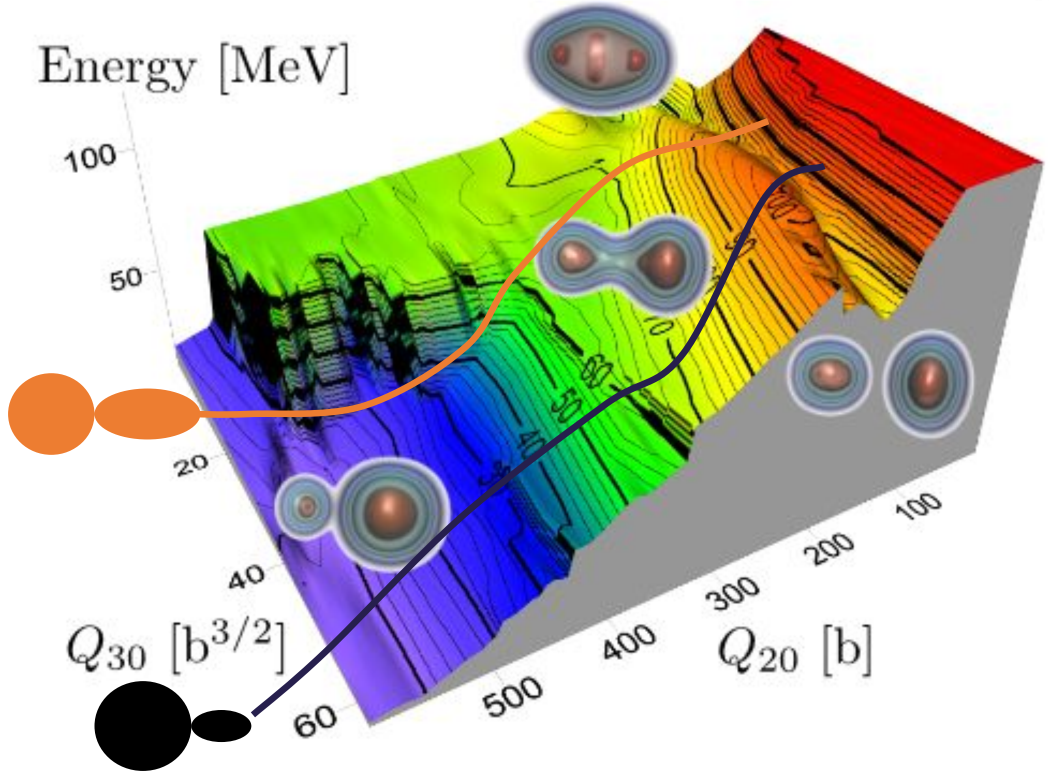

More **complex PES** can be calculated for **2, 3, etc. deformation parameters**

↓

The **possible paths** the system can have through the surface define the probabilities of the **final configurations of the fragments**

Fission observables: yields

The **probability of producing a fission fragment** with a given A, Z, N, etc. :

$$Y(Z, A) = 200 \cdot \frac{N(Z, A)}{\sum_{Z,A} N(Z, A)}$$

^{230}**Th elemental yields also** show this **evolution** as a function of **excitation energy**

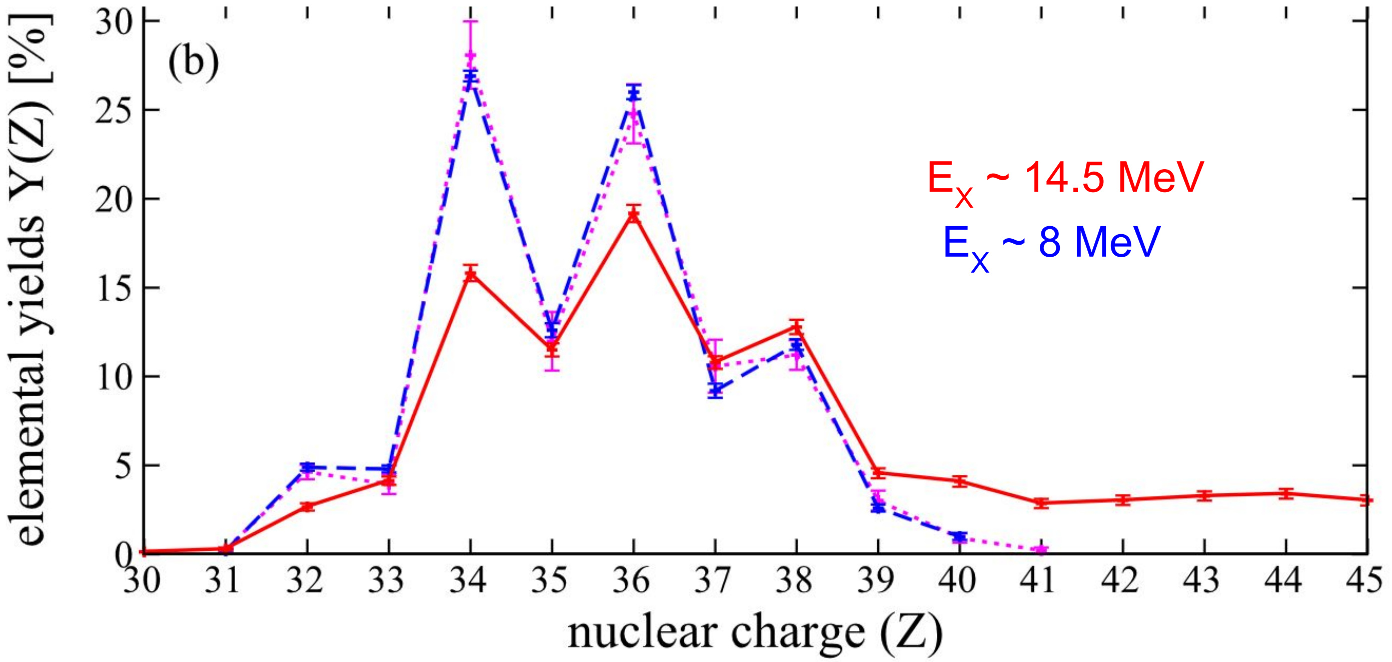

Chatillon, A., Taïeb, J., Alvarez-Pol, H., Audouin, L., Ayyad, Y., Bélier, G., ... & Weick, H. (2020). Evidence for a new compact symmetric fission mode in light thorium isotopes. Physical Review Letters, 124(20), 202502.

Fission observables: yields

The **probability of producing a fission fragment** with a given A, Z, N, etc. :

$$Y(Z,A) = 200 \cdot \frac{N(Z,A)}{\sum_{Z,A} N(Z,A)}$$

^{232}**Th elemental yields also** show this **evolution** as a function of **excitation energy**

THORIUM ANOMALY (2)

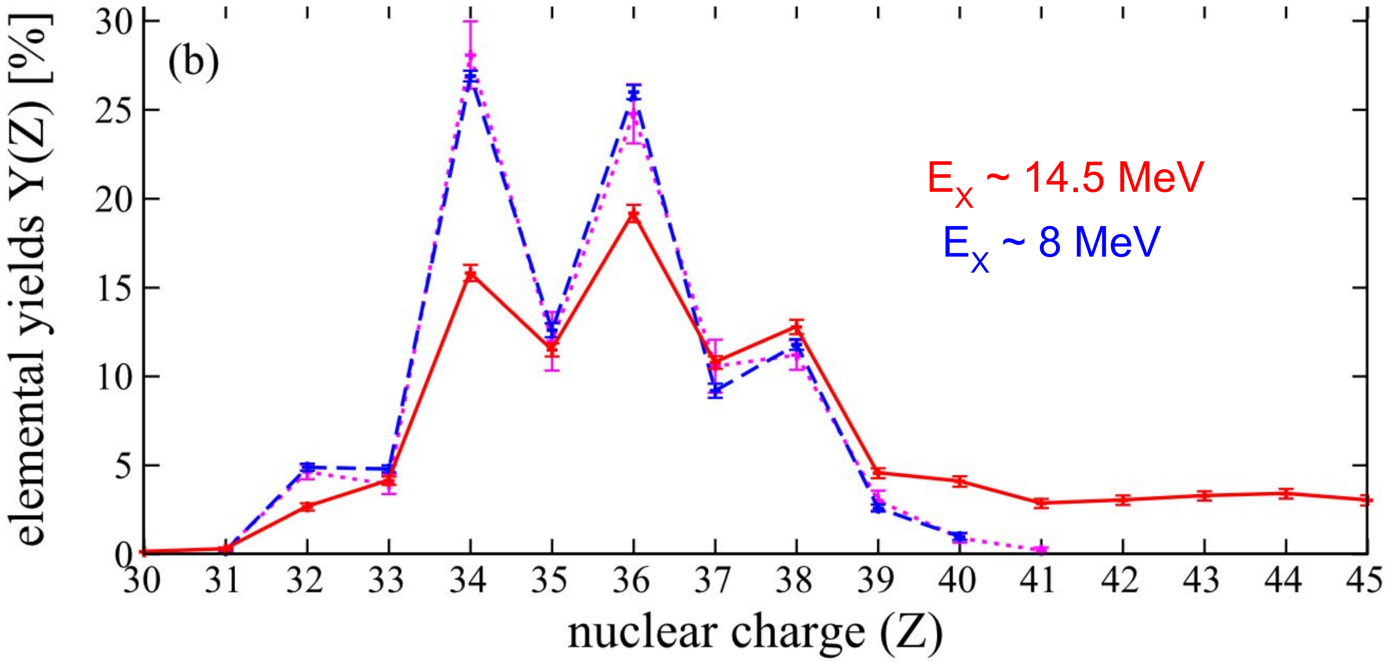

Chatillon, A., Taïeb, J., Alvarez-Pol, H., Audouin, L., Ayyad, Y., Bélier, G., ... & Weick, H. (2020). Evidence for a new compact symmetric fission mode in light thorium isotopes. *Physical Review Letters, 124(20), 202502.*

Neutron excess @ 7 ± 1 MeV

GANIL

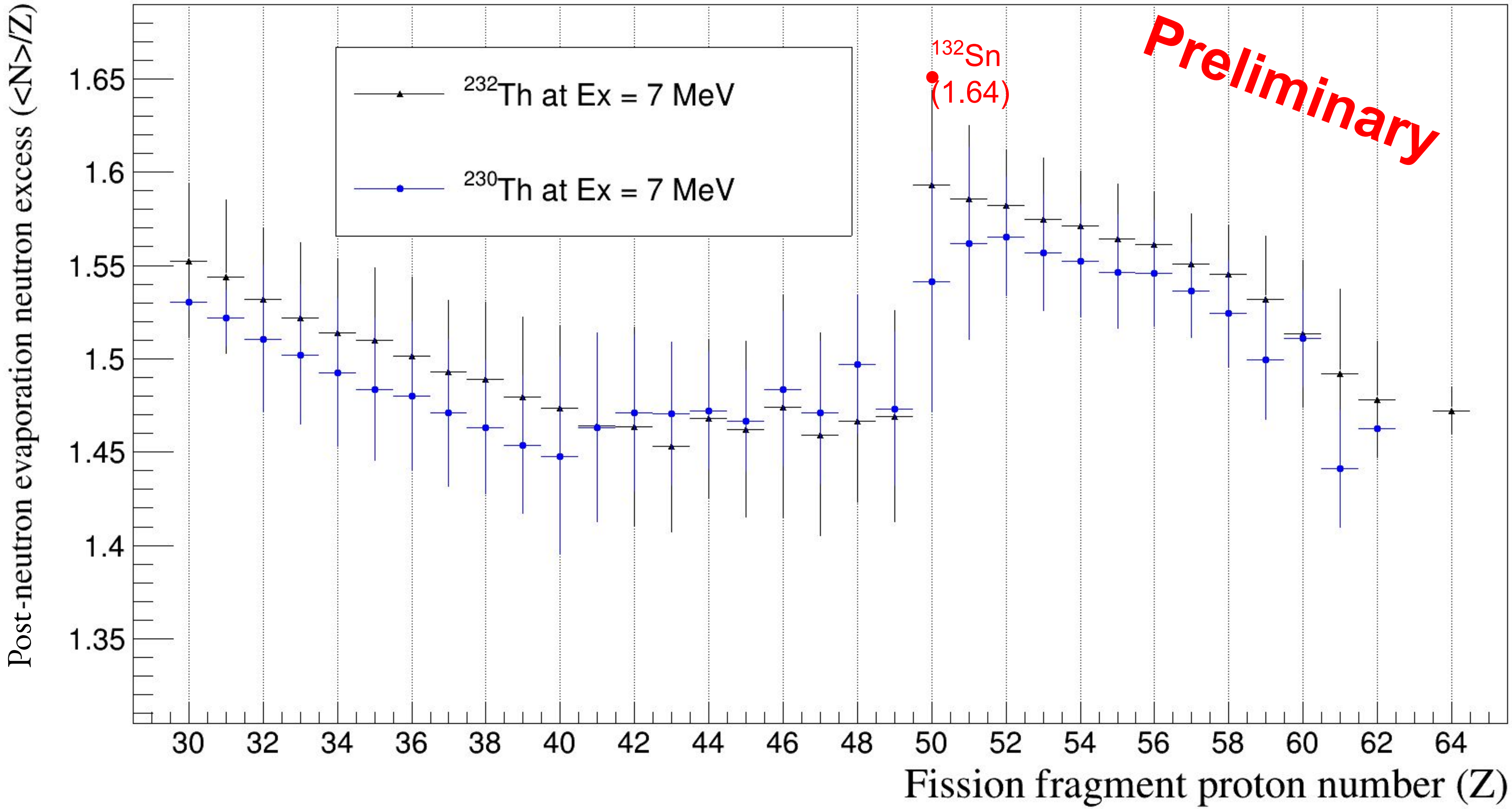

Elemental yields of ^{234}U

Yield: $Y(Z,A) = 200 * N(Z,A) / \sum_i N(Z_i, A_i)$

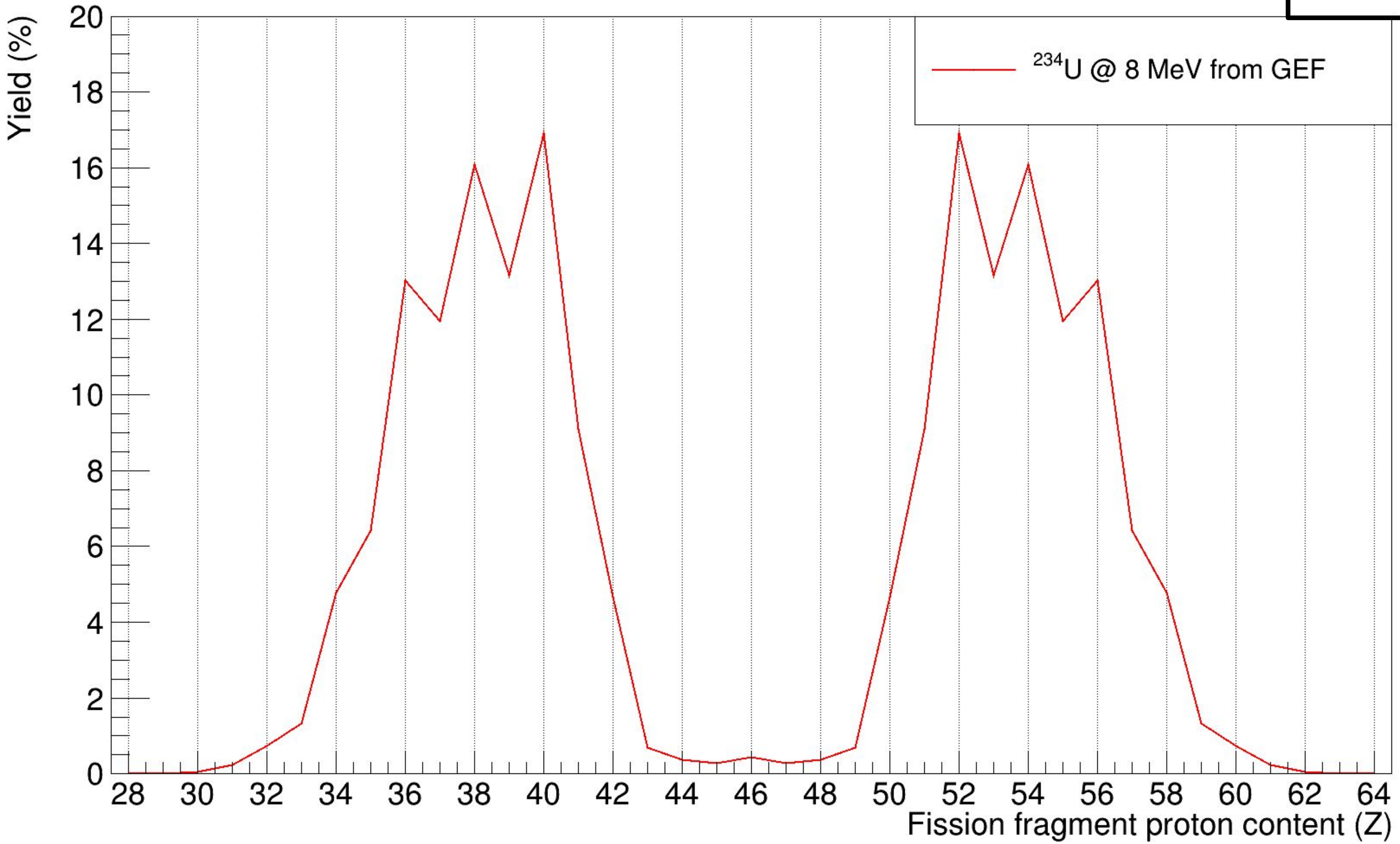

1. Choose your fissioning system
2. **Get the Z from VAMOS**

Elemental yields of ^{234}U

Yield: $Y(Z,A) = 200 * N(Z,A) / \sum_i N(Z_i, A_i)$

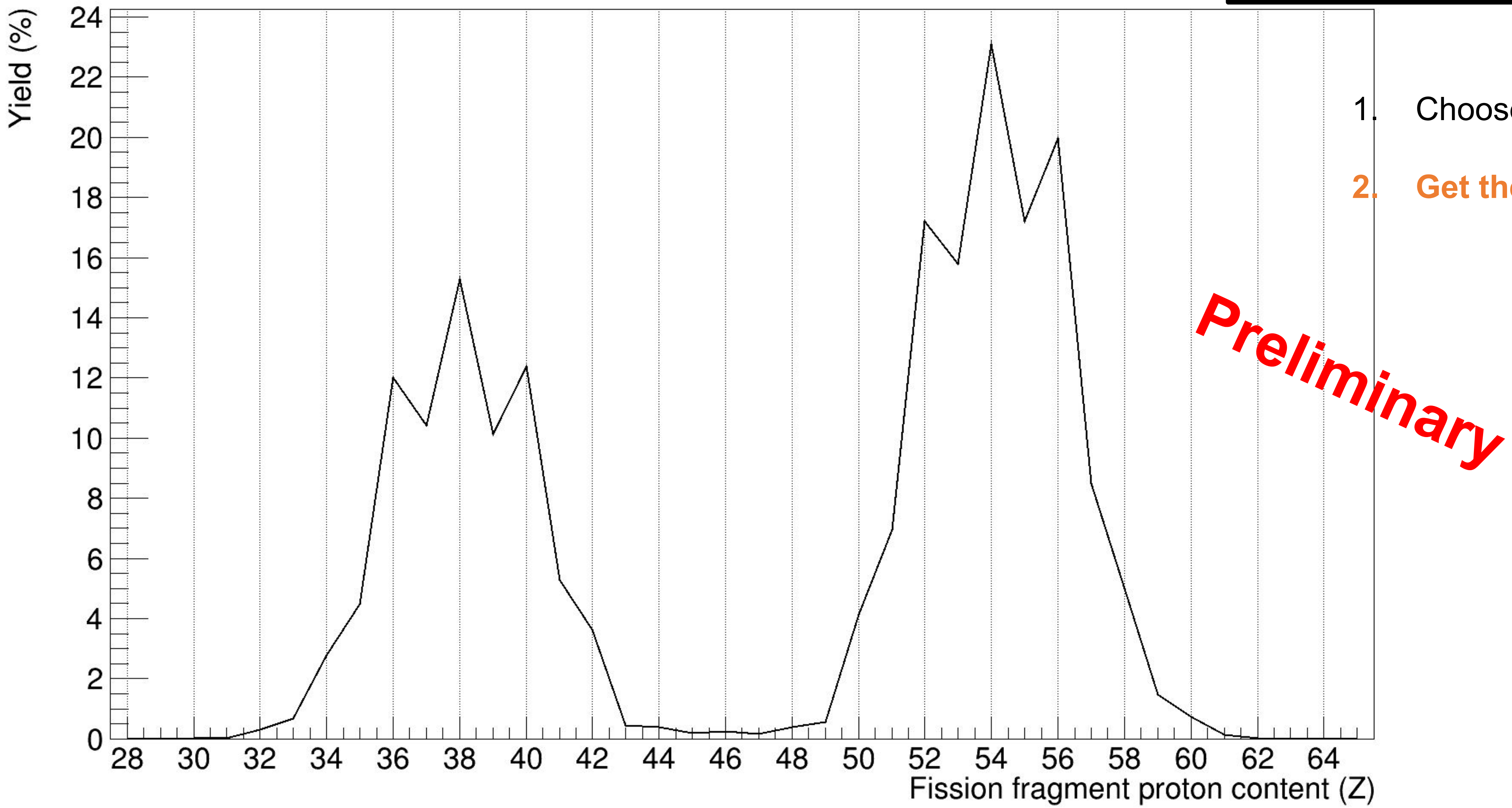

1. Choose your fissioning system
2. **Get the Z from VAMOS**

Elemental yields of ^{234}U

Yield: $Y(Z,A) = 200 * N(Z,A) / \sum_i N(Z_i, A_i)$

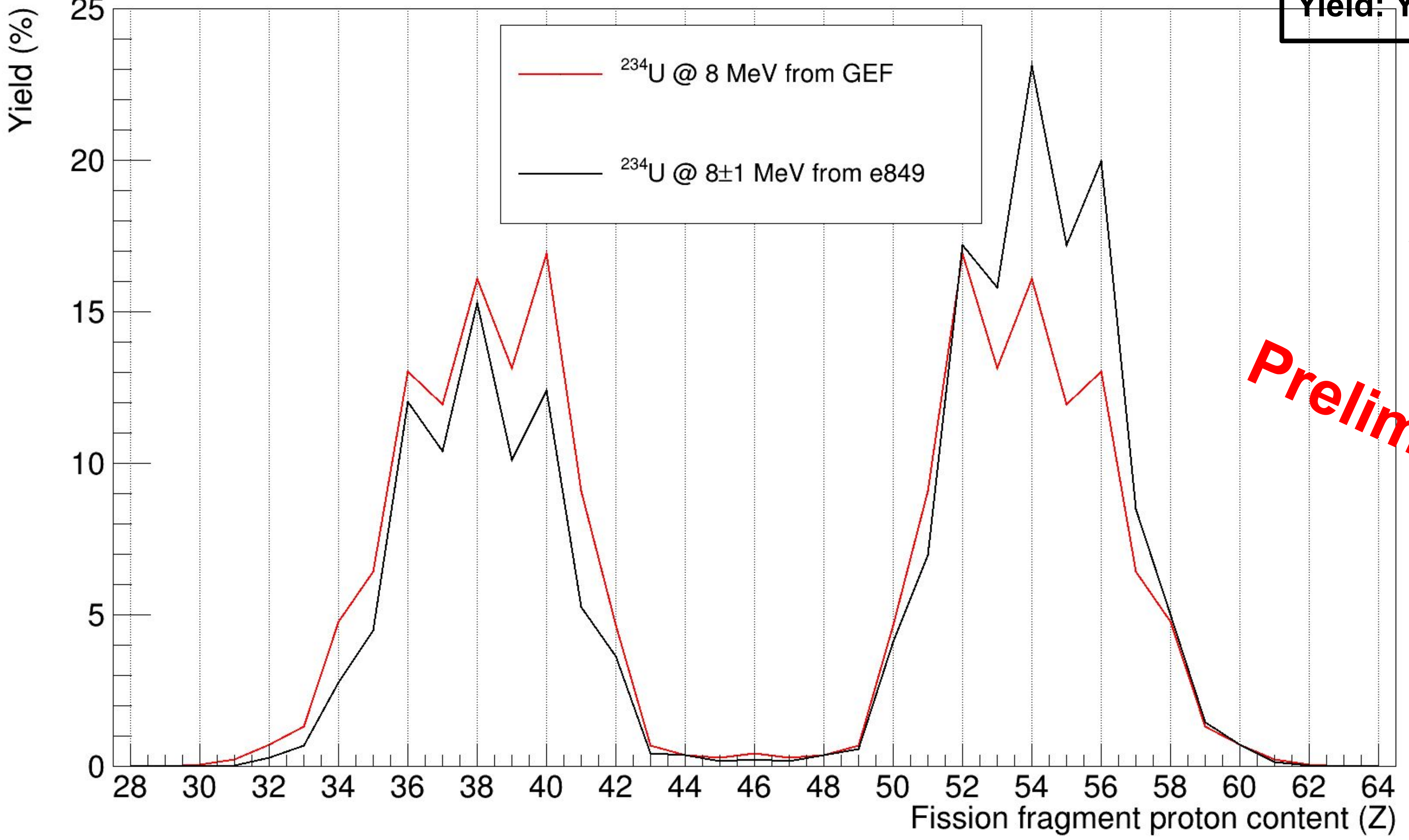

1. Choose your fissioning system
2. Get the Z from VAMOS
3. **Compare with data/model**

Elemental yields of ^{234}U

Yield: $Y(Z,A) = 200 * N(Z,A) / \sum_i N(Z_i, A_i)$

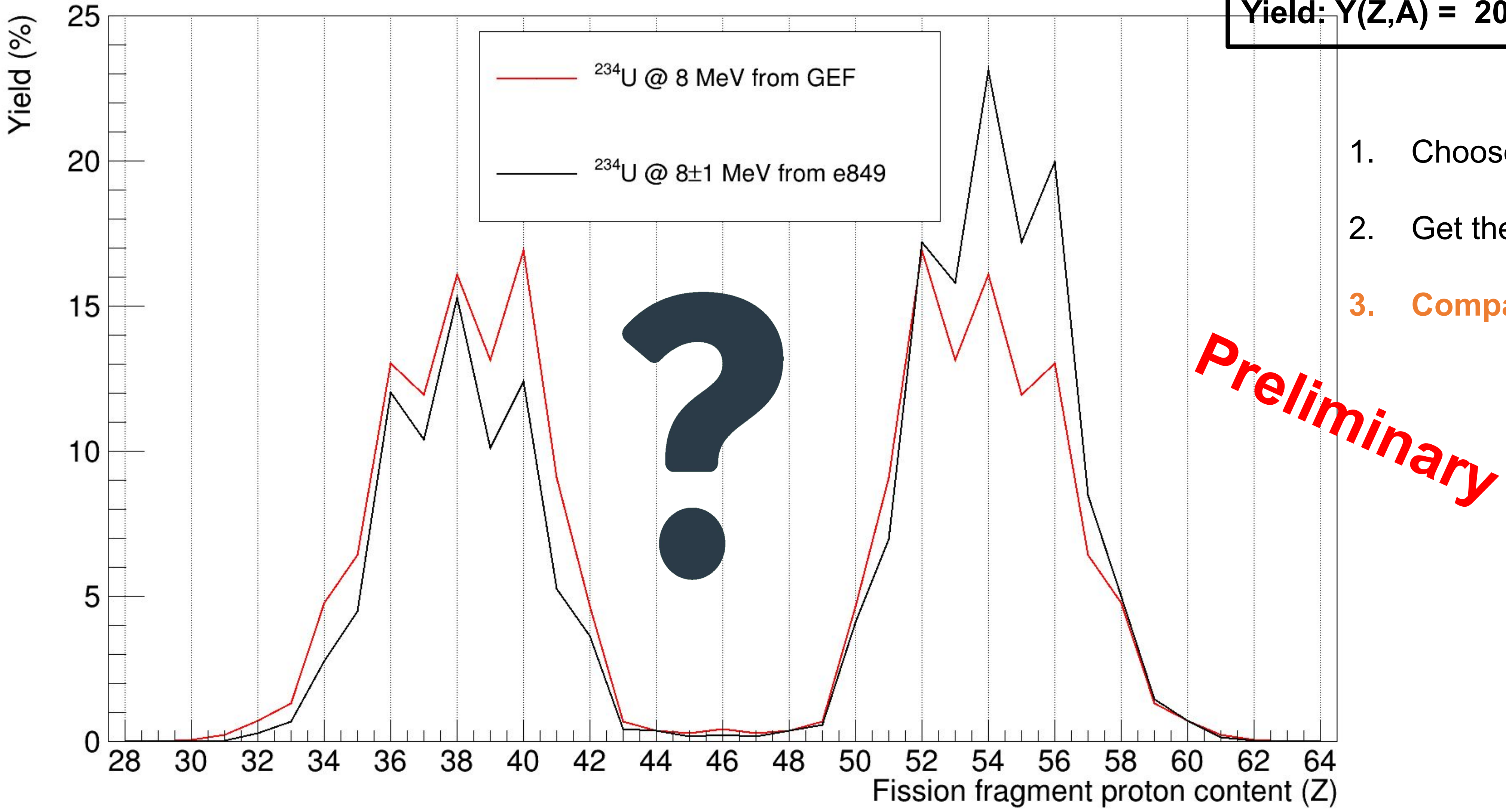

1. Choose your fissioning system
2. Get the Z from VAMOS
3. **Compare with data/model**

Spectrometer acceptance

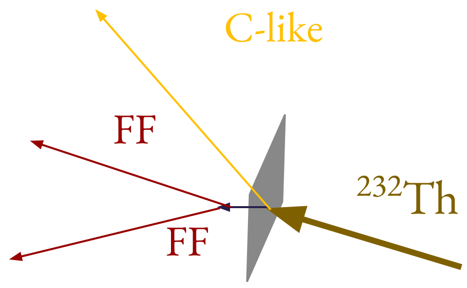

Spectrometer acceptance

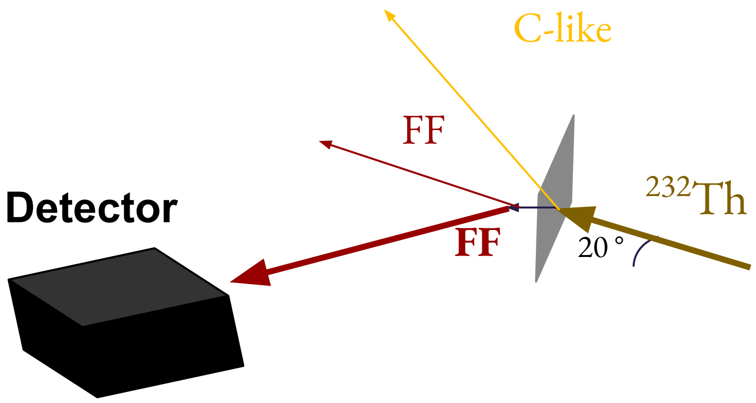

Direct measurement

Spectrometer acceptance

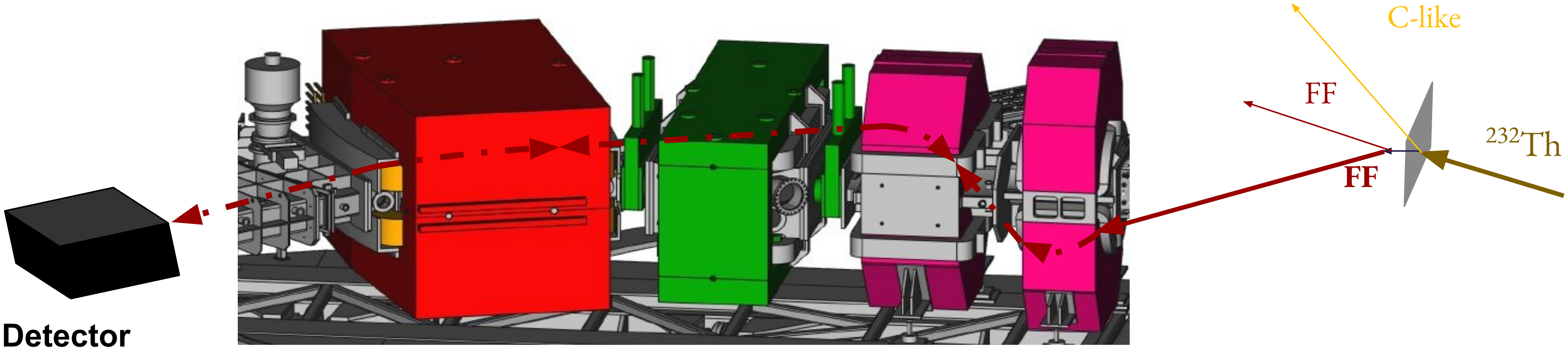

Spectrometer acceptance

We need to account for the trajectories that were not measured due to the different kinematics of the particle

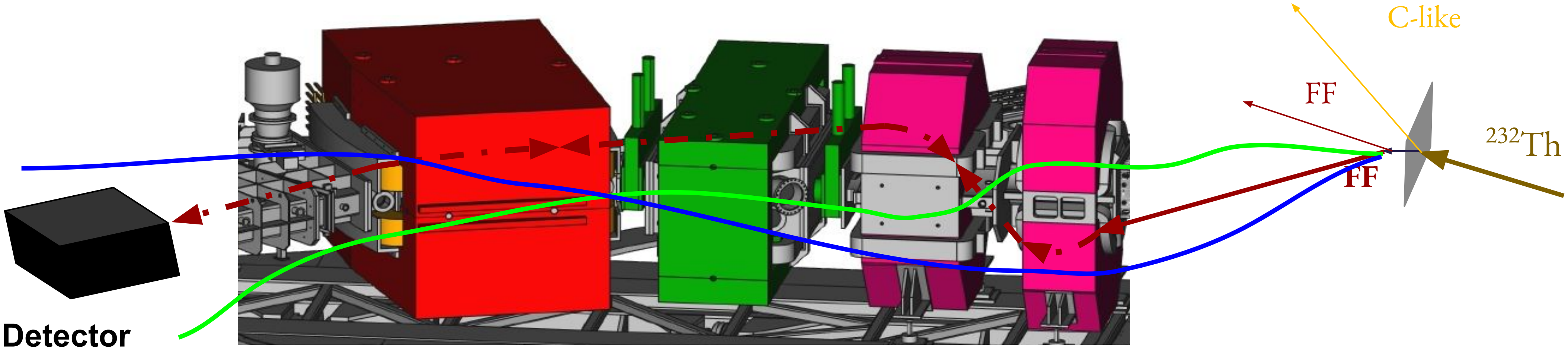

From identification to acceptance: ϕ range

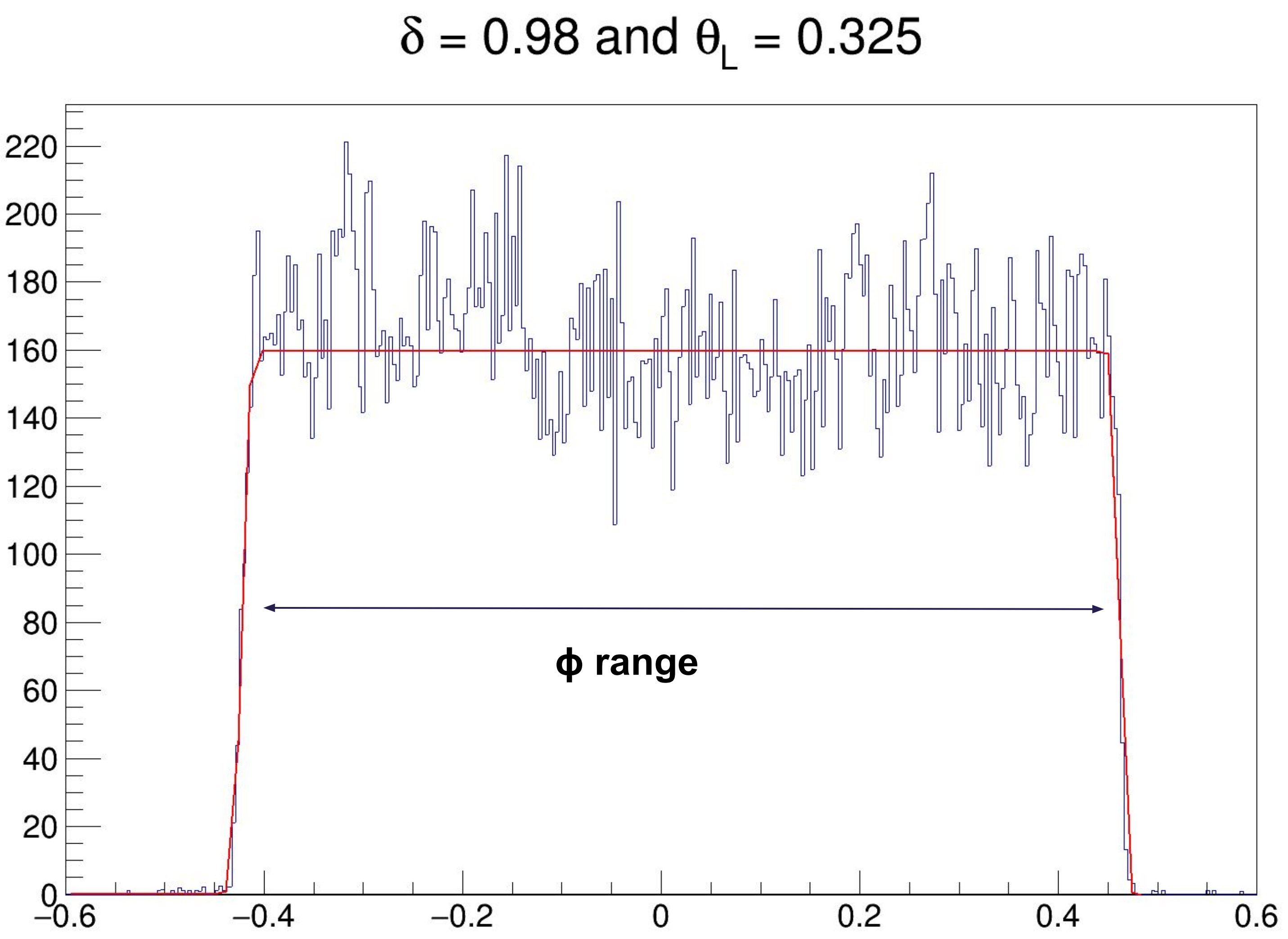

δ : Relative magnetic rigidity with respect to the central value

θ_L : polar angle in the laboratory frame

Get the ϕ range for a given δ ($B\varrho/B\varrho_{REF}$)

Fission fragments are emitted isotropically:
f_ϕ = 2π /(ϕ range)

From identification to acceptance: ϕ range

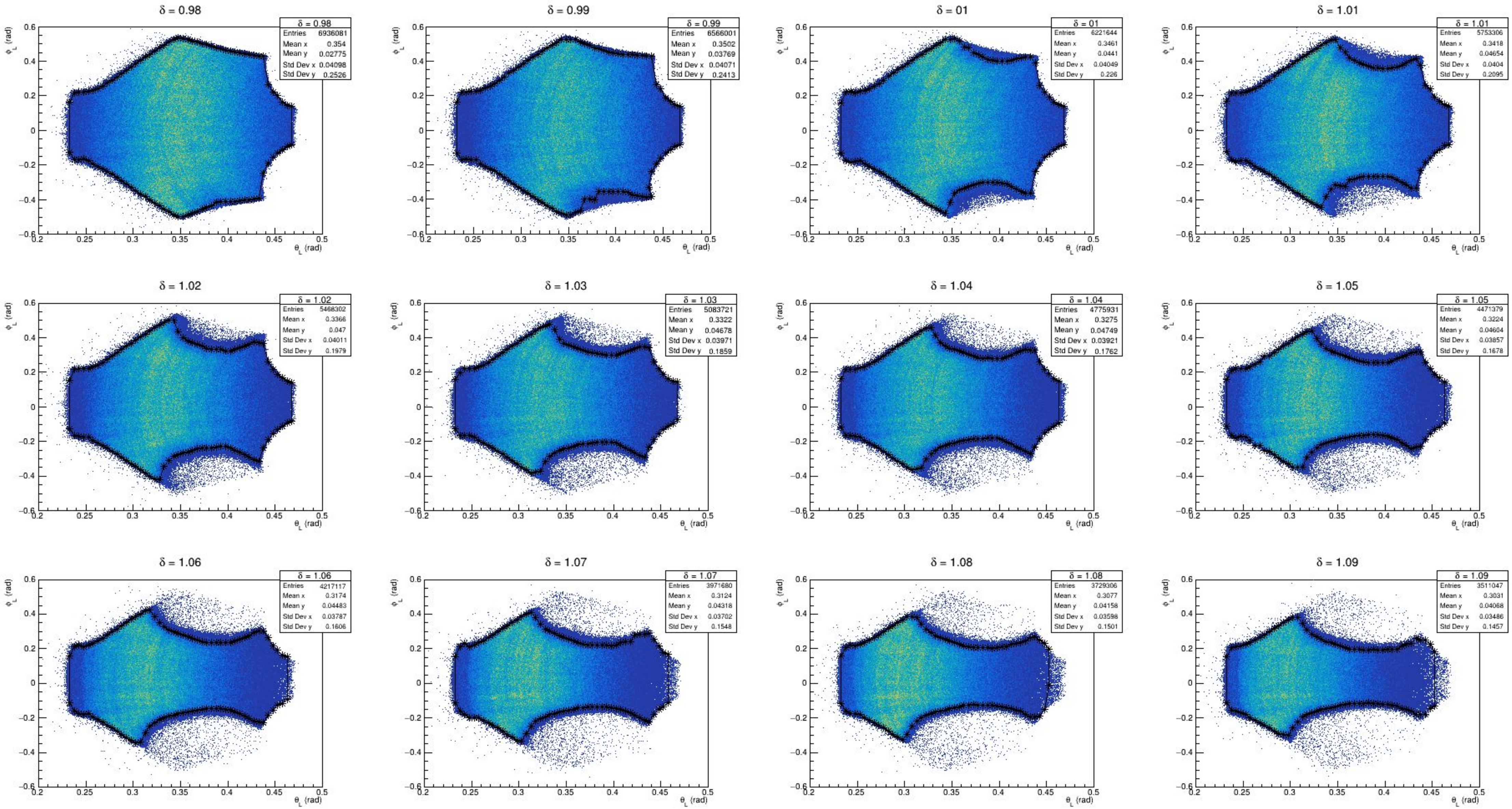

From identification to acceptance: ϕ range

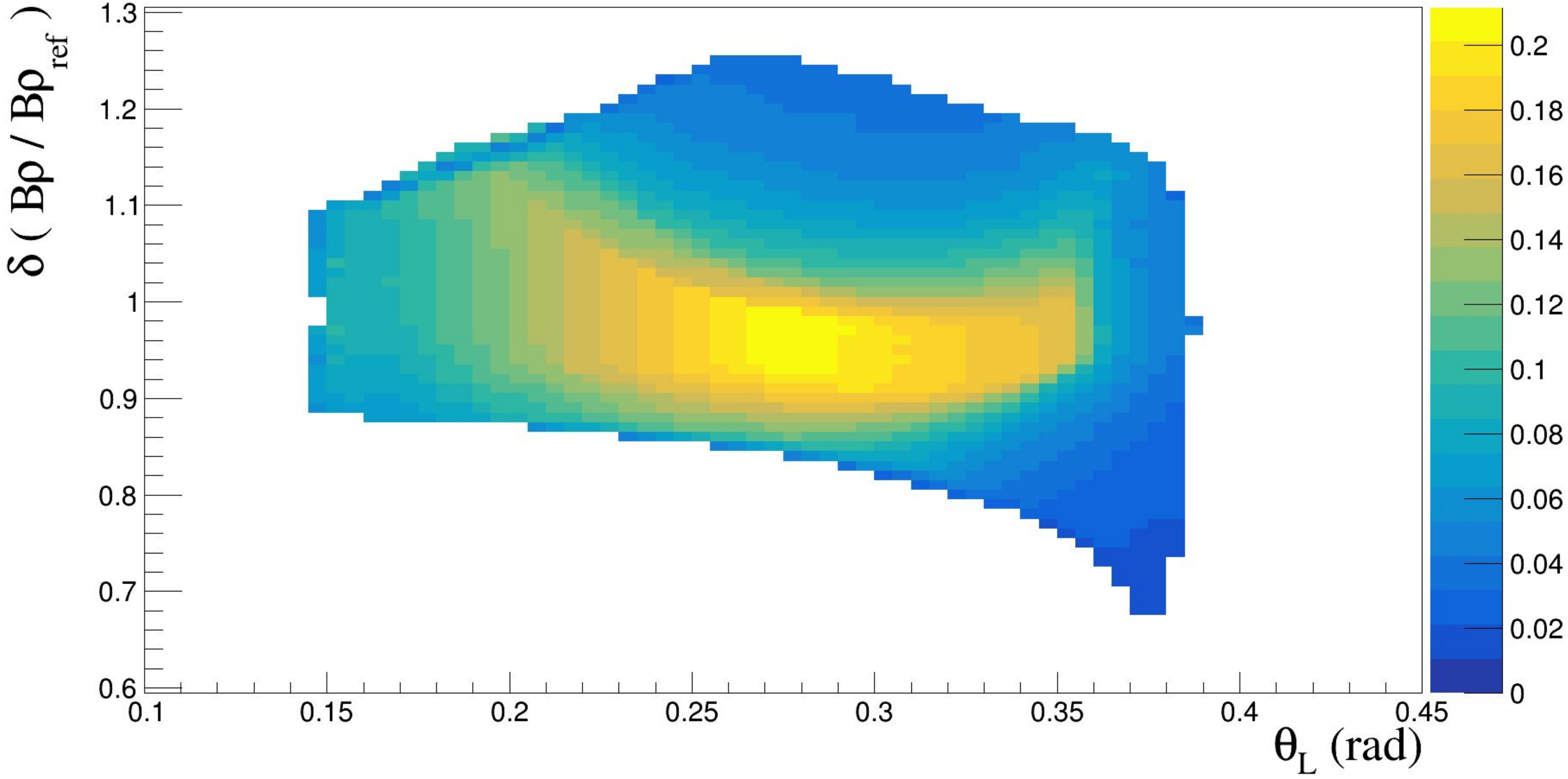

From identification to acceptance: cos(ϑ_{CM})range

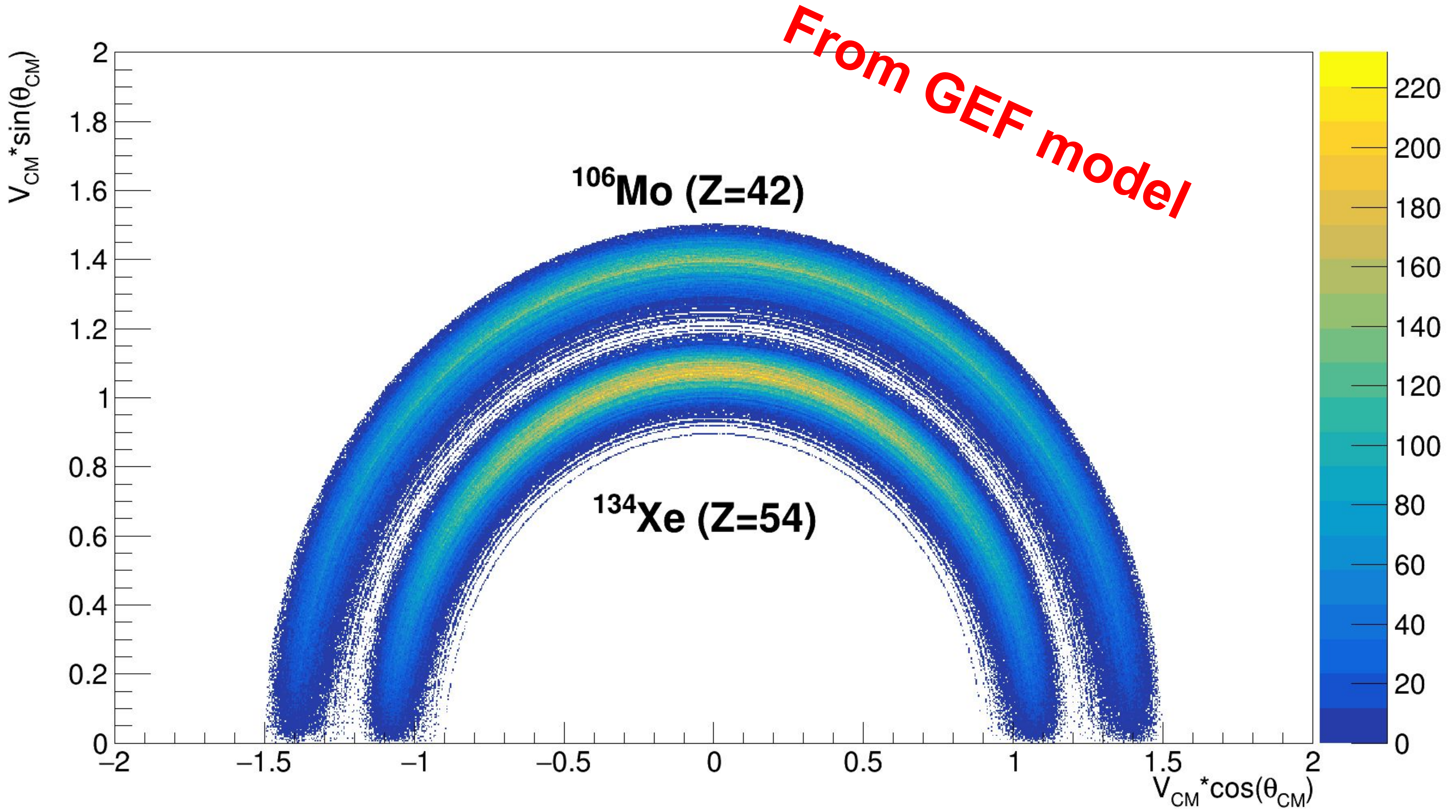

From identification to acceptance: cos(ϑ_{CM})range

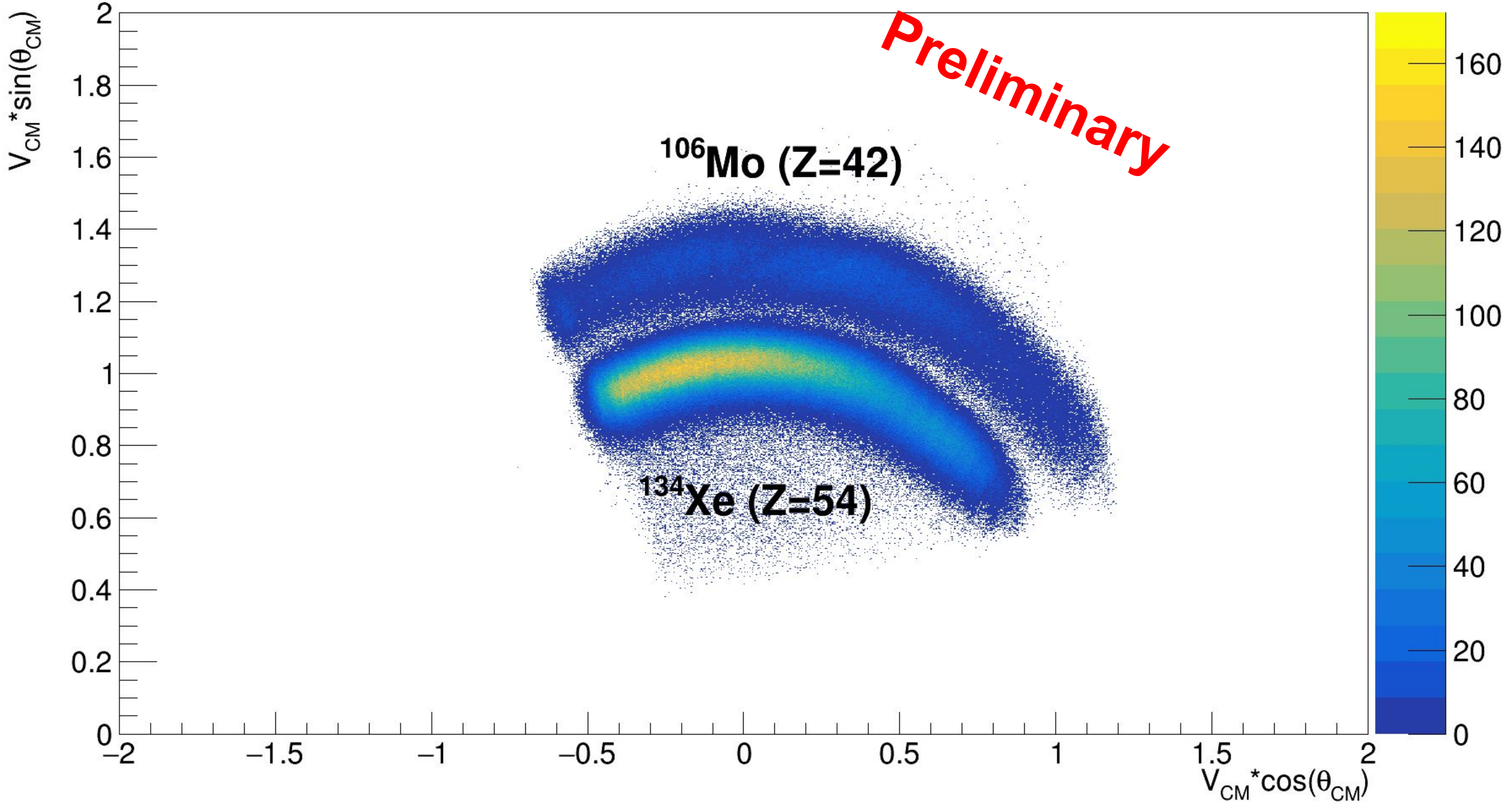

From identification to acceptance: cos(ϑ_{CM})range